PLACE IN RETURN BOX to remove this checkout from your record.

TO AVOID FINES return on or before date due.

MAY BE RECALLED with earlier due date if requested.

| DATE DUE | DATE DUE | DATE DUE |
|----------|----------|----------|
|          |          |          |
|          |          |          |
|          |          |          |
|          |          |          |
|          |          |          |
|          |          |          |

1/98 c/CIRC/DateDue.p65-p.14

# TRANSCRIPTIONAL REGULATION OF IgM EXPRESSION BY 2,3,7,8-TETRACHLORODIBENZO-p-DIOXIN AND THE AhR/DRE SIGNALING PATHWAY

Ву

Courtney E. W. Sulentic

### **A DISSERTATION**

Submitted to
Michigan State University
in partial fulfillment of the requirements
for the degree of

**DOCTOR OF PHILOSOPHY** 

Department of Pharmacology and Toxicology

1999

#### **ABSTRACT**

# TRANSCRIPTIONAL REGULATION OF IgM EXPRESSION BY 2,3,7,8-TETRACHLORODIBENZO-p-DIOXIN AND THE AhR/DRE SIGNALING PATHWAY

By

# Courtney E. W. Sulentic

Suppression of the humoral immune response by 2,3,7,8-tetrachlorodibenzo-p-dioxin (TCDD) is well established in a number of mouse models, including the B6C3F1 mouse, with several studies identifying the B-cell as a primary target of TCDD. The actual molecular mechanism responsible for the TCDD-mediated effects on B-cell function is unclear; however, many of the biological effects produced by TCDD are thought to be mediated by the aryl hydrocarbon receptor (AhR). The AhR signaling cascade involves TCDD binding to the AhR followed by nuclear translocation, dimerization with the AhR nuclear translocator (ARNT) and binding of the AhR nuclear complex to dioxin responsive elements (DRE) within the promoter regions of genes sensitive to TCDD. Although well characterized with the induction of metabolic enzymes, such as CYP1A1, this mechanism had not been directly linked to the effects of TCDD on B-cell function. The objectives of this investigation were four-fold. The first was to determine if the AhR and ARNT are functionally expressed in B6C3F1 mouse splenocytes. Northern and Western blot analysis of mRNA and whole cell lysate, respectively, isolated from mouse splenocytes identified message and protein for both the AhR and ARNT. Additionally, TCDD induces binding of these proteins to the DRE as detected by an electrophoretic mobility shift assay (EMSA). The second objective was to characterize the CH12.LX and BCL-1 murine B-cell lines as potential models in determining the relationship between TCDD-induced alteration of B-cell function and events mediated by an AhR/ARNT-DRE mechanism. Initial screening by Western analysis demonstrated a marked expression of the AhR protein in the CH12.LX cell line but not in the BCL-1 cell line which was confirmed at the transcriptional level by reverse transcription-polymerase chain reaction (RT-PCR). ARNT mRNA and protein are highly expressed in both cell lines. In addition, the AhR and ARNT protein are functional in CH12.LX cells as demonstrated by TCDD-induced Cyplal induction. TCDD did not induce Cyplal induction in the BCL-1 cells. Furthermore, TCDD treatment resulted in a concentrationdependent suppression of LPS-induced IgM secretion in CH12.LX cells which was not observed in the AhR-deficient BCL-1 cells. The third objective was to further investigate the role of the AhR in TCDD-induced inhibition of IgM secretion through a characterization of the structure activity relationship (SAR) between inhibition of both immunoglobulin (Ig) secretion and Ig heavy chain transcription and AhR-mediated enzyme induction in CH12.LX cells. The effects of several polychlorinated dibenzo-pdioxin (PCDD) congeners on each endpoint followed a SAR. Among the three endpoints, there was also a general concordance between the EC<sub>50</sub> and IC<sub>50</sub>'s for a particular congener. In addition, the PCDD congeners had no effect on IgM secretion,  $\mu$ expression or Cyplal expression in the AhR-deficient BCL-1 cells. The final objective was to determine if the AhR nuclear complex can bind to two DRE-like sites identified within the Ig heavy chain  $3'\alpha$  enhancer. EMSA-western analysis with the CH12.LX cells demonstrated TCDD-induced binding of the AhR nuclear complex to both DRE-like sites as well as TCDD-induced binding of several NF-kB/Rel proteins to a kB site which overlaps one of the DRE-like sites. Interestingly, kB binding in the BCL-1 cells was induced by TCDD demonstrating an AhR-independent effect on kB binding. However, taken together, the results of this investigation are consistent with an AhR-mediated inhibition of IgM expression which may result from an altered regulation of the Ig heavy chain gene perhaps due to TCDD-induced binding of the AhR-nuclear complex to DRElike sites within the  $3'\alpha$  enhancer.

#### **DEDICATION**

To my husband, Jon, whose unwavering support, friendship and love have formed the foundation for this work.

To my unborn daughter, who has already brought a great deal of joy and perspective to my life.

To my parents, William and Joan, for their many years of support and guidance and for teaching me the value of education and hard work.

To my sister, Heather, for always being my best friend.

#### **ACKNOWLEDGMENTS**

There are many people I wish to acknowledge. First and foremost is my advisor, Dr. Norbert Kaminski, for his support and guidance and for providing a challenging and comfortable learning environment. Dr. Michael Holsapple, who first sparked my interest in immunotoxicology and initiated the funding for this project, has been a valuable contributor as both a coauthor and committee member. The rest of my committee members, Dr. Kathryn Brooks, Dr. Margarita Contreras and Dr. Lawrence Fischer, contributed very lively discussions and many helpful suggestions during, as well as outside of, scheduled committee meetings. The whole Kaminski lab, past and present, have been invaluable for their constructive criticism in lab meetings, entertaining lab discussions and comic relief. I should especially thank Robert Crawford and Robin Condie for their vast scientific knowledge and for their patience with a beginner's endless questions. I also wish to acknowledge Dr. Richard Pollenz, Dr. Gregory Fink, Dr. Ronald Johnson and Dr. Kurunthacha Kannan who have offered valuable advice, help and/or reagents critical to my project.

# TABLE OF CONTENTS

|             |        | Page  |
|-------------|--------|---|
| LIST OF TAE | BLES   | x   |
| LIST OF FIG | URES   | xi  |
| LIST OF ABI | BREVIA | ATIONSxiii  |
| INTRODUCT   | TION   |   |
| LITERATUR   | E REV  | EW 3  |
| I.          | B-cell | activation and differentiation                            |
|             | A.     | B-cells and the immune system                             |
|             | B.     | B-cell activation4  |
|             | C.     | Regulation of immunoglobulin expression7                  |
|             | D.     | Regulators of the immunoglobulin heavy chain 3'α enhancer |
|             |        | 1. The B-cell-specific activator protein                  |
|             |        | •   |
|             |        | 2. The NF-κB/Rel protein family12                         |
| II.         | Toxic  | effects of TCDD14   |
|             | A.     | General toxicity of TCDD14                                |
|             | B.     | Immunotoxicity of TCDD16                                  |
| III.        |        | of the AhR in TCDD-mediated immune ession                 |
|             | A.     | The AhR signaling pathway18                               |
|             | В.     | The AhR and TCDD-mediated immunotoxicity21                |
|             | C.     | The AhR, BSAP and inhibition of CD19 expression23         |
| MATERIALS   | S AND  | METHODS25   |
| I.          | Chemi  | icals25   |
| II.         | Anima  | ds25  |

|   | III.  | Cell L  | ines  | .25 |
|---|-------|---------|---|-----|
|   | IV.   | Northe  | ern Blot Analysis   | .26 |
|   |       | A.      | RNA Isolation and Analysis                                      | .26 |
|   |       | B.      | cDNA Probes   | .27 |
|   | V.    | Revers  | se Transcription-Polymerase Chain Reaction                      | .27 |
|   |       | A.      | RNA Isolation   | .27 |
|   |       | В.      | Qualitative RT-PCR Analysis                                     | 28  |
|   |       | C.      | Quantitative RT-PCR Analysis                                    | 29  |
|   | VI.   | Enzyn   | ne-Linked Immunosorbent Assay for IgM                           | .30 |
|   | VII.  | Whole   | Cell Lysate Protein Preparation                                 | .30 |
|   | VIII. | Weste   | rn Blot Analysis  | .31 |
|   | IX.   | Slot B  | lot Analysis  | .32 |
|   | X.    | Nuclea  | ar Protein Preparation  | 32  |
|   | XI.   | Electro | ophoretic Mobility Shift Assay                                  | .33 |
|   |       | A.      | Analysis of Protein-DNA Complexes                               | .33 |
|   |       | B.      | Synthetic DRE Oligonucleotides                                  | .34 |
|   | XII.  | EMSA    | A-Western Analysis  | 34  |
|   | XIII. | Statist | ical Analysis of Data   | 35  |
| EXPE  | RIMEN | TAL R   | ESULTS  | 36  |
| I. Identification of AhR and ARNT in B6C3F1 mouse splenocytes |       |         | cytes   | 36  |
|   |       | A.      | Northern blot analysis of mouse splenocytes                     | .36 |
|   |       | В.      | Western blot analysis of mouse splenocytes                      | .36 |
|   |       | C.      | Slot blot and quantitative RT-PCR analysis of mouse splenocytes | .40 |
|   |       | D.      | EMSA analysis of mouse splenocytes                              | .40 |
|   | П.    |         | cterization of the AhR and ARNT in the CH12.LX and B-cell lines | .43 |
|   |       | A.      | AhR and ARNT expression in two B-cell lines                     | 43  |

|            | В.           | AhR and ARNT regulate gene transcription in the CH12.LX B-cell line  | 48 |
|------------|--------------|--|----|
|            | C.           | TCDD alters immune function in CH12.LX B-cells but not in AhR-deficient BCL-1 B-cells  | 48 |
|            | D.           | Differential expression of AhR in LPS-differentiated CH12.LX B-cells   | 51 |
|            | E.           | TCDD does not alter Ahr expression in naive or LPS-stimulated CH12.LX cells  | 51 |
|            | F.           | Ahr upregulation does not enhance the sensitivity of activated CH12.LX cells to TCDD   | 60 |
| III.       | The Sabindin | AR of several PCDD-mediated endpoints and AhR ag affinity  | 64 |
|            | A.           | PCDD-mediated inhibition of LPS-induced IgM secretion in CH12.LX B-cells follows an SAR which is concordant with AhR ligand binding affinity and Cyplal induction. | 64 |
|            | В.           | Specific PCDD congeners have no affect on Cyplal expression or LPS-induced IgM secretion from the AhR-deficient BCL-1 B-cells                                      | 68 |
|            | C.           | LPS-induced $\mu$ expression in CH12.LX cells is inhibited by PCDD congeners and follows an SAR for AhR binding  | 68 |
|            | D.           | Inhibition of IgM protein secretion and $\mu$ expression is AhR-dependent  | 72 |
| IV.        |              | tion of protein binding at the 3'α Ig heavy chain enhancer   | 74 |
|            | A.           | TCDD induces binding to a DRE-like site located within the 3'αE(hs1,2) and 3'α-hs4 enhancers   | 74 |
|            | В.           | TCDD induces binding to a κB site located within the 3'α-hs4 enhancer  | 81 |
| DISCUSSION | V            |  |    |
| I.         | Functi       | ional AhR and ARNT in murine splenocytes   | 88 |
| П.         | AhR-cactiva  | dependent suppression by TCDD of IgM secretion in ted B-cells  | 92 |
| III.       | Trans        | criptional regulation of IgM expression by TCDD and nR/DRE signaling pathway   |    |
|            |              |  |    |

| LITERATURE CITED10 | 02 |
|--------------------|----|
|--------------------|----|

# LIST OF TABLES

| Table |   | Page |
|-------|---|------|
| 1.    | Quantitative analysis of Ahr and Arnt mRNA as determined by RT-PCR  | 42   |
| 2.    | Congener specific IC <sub>50</sub> for inhibition of LPS-induced $\mu$ expression and protein secretion or EC <sub>50</sub> for induction of Cypla1 | 66   |

# **LIST OF FIGURES**

| Figure |  | Page |
|--------|--|------|
| 1.     | The $3'\alpha$ enhancer of the mouse Ig heavy chain gene                               | 9    |
| 2.     | The AhR signaling pathway  | 19   |
| 3.     | Northern blot analysis of Ahr and Arnt mRNA expression in splenocytes and liver.       | 37   |
| 4.     | Western blot analysis of the AhR and ARNT in splenocytes and liver                     | 39   |
| 5.     | Slot blot analysis of the AhR and ARNT in splenocytes and liver                        | 41   |
| 6.     | Binding of Hepa 1c1c7 or splenocyte nuclear proteins to a DRE                          | 44   |
| 7.     | Western blot analysis for the AhR and ARNT protein in the CH12.LX and BCL-1 cell lines | 46   |
| 8.     | Basal expression of Ahr and Arnt transcripts in the CH12.LX and BCL-1 cell lines       | 47   |
| 9.     | Dose response and time course of TCDD-induced Cyp1a1 induction in CH12.LX cells        | 49   |
| 10.    | Effect of TCDD on Cyplal induction in BCL-1 cells                                      | 50   |
| 11.    | Effect of TCDD on LPS-induced IgM secretion in CH12.LX cells                           | 52   |
| 12.    | Effect of TCDD on LPS-induced IgM secretion in BCL-1 cells                             | 53   |
| 13.    | Effect of LPS-induced differentiation on Ahr expression in the CH12.LX cells           | 54   |
| 14.    | Ahr expression in LPS-stimulated CH12.LX and BCL-1 cells                               | 55   |
| 15.    | AhR protein expression in LPS-stimulated CH12.LX cells                                 | 56   |
| 16.    | Arnt expression in LPS-stimulated CH12.LX cells  | 57   |
| 17.    | Effect of TCDD on Ahr expression in the CH12.LX cells                                  | 58   |
| 18.    | Effect of TCDD on LPS-induced Ahr expression in the CH12.LX cells                      | 59   |
| 19.    | Time course of Cyplal induction in CH12.LX cells cotreated with LPS and TCDD           | 61   |

| 20. | Effect of a 24 hr LPS cotreatment on TCDD-induced Cyplal induction in CH12.LX cells  | 62  |
|-----|--|-----|
| 21. | TCDD-induced Cyplal induction in LPS pretreated CH12.LX cells  | 63  |
| 22. | Concentration-dependent effect of selected chlorinated dibenzo-p-dioxin congeners on Cyplal expression in CH12.LX cells                        | 65  |
| 23. | Concentration-dependent effect of selected chlorinated dibenzo-p-dioxin congeners on LPS-induced IgM secretion from CH12.LX cells              | 67  |
| 24. | Effect of selected chlorinated dibenzo-p-dioxin congeners on Cyplal expression in BCL-1 cells  | .69 |
| 25. | Effect of selected chlorinated dibenzo-p-dioxin congeners on LPS-induced μ expression and IgM secretion in BCL-1 cells                         | .70 |
| 26. | Concentration-dependent effect of a 24 hr incubation with selected chlorinated dibenzo-p-dioxin congeners on $\mu$ expression in CH12.LX cells | 71  |
| 27. | Concentration-dependent effect of a 48 hr incubation with selected chlorinated dibenzo-p-dioxin congeners on $\mu$ expression in CH12.LX cells | 73  |
| 28. | Oligomers derived from the 3'\alpha enhancer used in the EMSA analysis   | .75 |
| 29. | TCDD-induced binding to a DRE-like site within the 3'αE(hs1,2) enhancer  | 76  |
| 30. | TCDD-induced binding to a DRE-like site within the 3'α-hs4 enhancer  | 78  |
| 31. | TCDD-induced binding of NF-κB/Rel proteins from CH12.LX cells to a κB binding site within the 3'α-hs4 enhancer                                 | 82  |
| 32. | TCDD-induced binding of NF-κB/Rel proteins from BCL-1 cells to a κB binding site within the 3'α-hs4 enhancer                                   | 85  |

#### LIST OF ABBREVIATIONS

2,4-dichlorophenoxyacetic acid

2,4,5-T 2,4,5-trichlorophenoxyacetic acid

 $3'\alpha E(hs1,2)$   $3'\alpha$  enhancer, hypersensitive site 1 and 2

 $3'\alpha$ -hs4  $3'\alpha$  enhancer, hypersensitive site 4

AFC antibody forming cell

AhR aryl hydrocarbon receptor

 $Ahr^{bb}$  high-responsive Ahr allele

Ahrdd low-responsive Ahr allele

AIP AhR-interacting protein

ARNT AhR nuclear translocator

BCA bicinchoninic acid

B-cell bursal or bone marrow derived cell

bHLH basic helix-loop-helix

BSA bovine serum albumin

BSAP B-cell -specific activator protein

BCR B-cell receptor

C $\alpha$ 3'E 3' $\alpha$  enhancer, 5' of hs(1,2), 3 and 4

CAT chloramphenicol acetyl transferase

CD cluster of differentiation

cDNA complimentary DNA

C<sub>H</sub> heavy chain constant region

CMI cell-mediated immunity

CYP1A1 cytochrome P-4501A1

D Ig diversity region

DCDD 2,7-dichlorodibenzo-p-dioxin

DMSO dimethyl sulfoxide

DNA deoxyribonucleic acid

DNP-Ficoll dinitrophenyl haptenated ficoll

DRE dioxin responsive element

 $E\mu$   $\mu$  heavy chain enhancer

ELISA enzyme-linked immunosorbent assay

EMSA electrophoretic mobility shift assay

ER estrogen receptor

EROD 7-ethoxyresorufin O-deethylase

GC/MS gas chromatography/mass spectrophotometry

HAH halogenated aromatic hydrocarbons

HI humoral immunity

HPLC high performance liquid chromatography

hs3 3'α enhancer, hypersensitive site 3

hsp heat shock protein

HxCDD 1,2,3,4,7,8-hexachlorodibenzo-p-dioxin

Ig immunoglobulin

IgH Ig heavy chain

IκB inhibitory κB

IKK IkB kinase

IL Interleukin

IFN-γ interferon-γ

IS internal standard

J Ig joining region

LBP LPS-binding protein

LPS lipopolysaccharide

μ heavy chain gene for IgM

MHC major histocompatibility complex

MCDD 1-monochlorodibenzo-p-dioxin

mlcls molecules

mRNA messenger RNA

NF-κB nuclear factor-κ light chain of B-cells

OD optical density

PAGE polyacrylamide gel electrophoresis

PBS phosphate-buffered saline

PCDD polychlorinated dibenzo-p-dioxins

PEST proline-glutamine-serine-threonine

PLC phospholipase C

RNA ribonucleic acid

RT-PCR reverse transcription-polymerase chain reaction

SAR structure activity relationship

SDS sodium dodecyl sulfate

sRBC sheep red blood cell

TBS tris-buffered saline

TCDD 2,3,7,8-tetrachlorodibenzo-p-dioxin

T-cell thymic derived cell

TD T-dependent

TI T-independent

TNP-LPS trinitrophenyl haptenated LPS

TriCDD 2,3,7-trichlorodibenzo-p-dioxin

tRNA transfer RNA

V Ig variable region

V<sub>H</sub> heavy chain variable region

VH vehicle

#### INTRODUCTION

Alterations in immune function are among the earliest and most sensitive responses to 2,3,7,8-tetrachlorodibenzo-p-dioxin (TCDD) exposure in most animal models. Previous cell separation-reconstitution experiments have identified the B-cell as a primary target of TCDD. In addition to immune suppression, TCDD has been shown to mediate a variety of toxic effects in a broad range of tissues, the best characterized of which is the liver. In the liver, TCDD acts as a tumor promoter as well as an inducer of the drug metabolizing isozyme, cytochrome P-4501A1 (CYP1A1). Induction of CYP1A1 by TCDD is mediated through the binding of TCDD to the cytosolic aryl hydrocarbon receptor (AhR). Once bound by TCDD, the ligand-receptor complex translocates to the nucleus where it forms a heterodimer with the AhR nuclear translocator (ARNT). The TCDD/AhR-ARNT protein complex is capable of functioning as a transcriptional regulator through direct binding to DNA at the dioxin-responsive enhancer (DRE). There is evidence for an AhR-dependency of TCDD-mediated immune suppression based on earlier studies which utilized: a) Ah high-responsive  $(Ah^{bb})$  and Ah low-responsive  $(Ah^{dd})$  mouse strains (1); b) congenic mice at the Ah locus (2); and c) structure activity relationships between various AhR ligands and inhibition of the antibody forming cell (AFC) response (3, 4). However, these findings were tempered by the fact that: (a) although present in lymphoid tissues, the AhR and ARNT had not been demonstrated in immunocompetent cells; (b) using rat and guinea pig spleen extracts, TCDD did not induce binding of the AhR/ARNT heterodimer to the DRE (5); (c) the low affinity AhR ligand, 2,7-dichlorodibenzo-p-dioxin (DCDD) and TCDD produce comparable inhibition of the anti-sheep red blood cell (sRBC) IgM AFC response following subchronic treatment of mice in vivo and following direct addition to naive splenocytes in vitro (6); and (d) subchronic TCDD treatment produces a marked immunosuppression in both DBA/2 (Ah low-responsive) and B6C3F1 (Ah highresponsive) mice (7). From these results, it is unclear whether the AhR is a mediator of the immunotoxic effects of TCDD. The purpose of this investigation was to test the following hypothesis: TCDD acts directly on B-cells to suppress immunoglobulin secretion; this suppression is mediated by the AhR which adversely regulates immunologically relevant genes possessing DREs in their 5' regulatory regions. Initial experiments focused on identifying functional components of the AhR signaling pathway in B6C3F1 mouse splenocytes which has been the historical model of our laboratory for studying the effects of TCDD on immune competence. To more efficiently test our hypothesis, subsequent experiments focused on developing and characterizing a B-cell line model which has provided considerable insight into the mechanism of TCDD-induced alteration of B-cell function.

#### LITERATURE REVIEW

#### I. B-cell activation and differentiation

## A. B-cells and the immune system

A functional immune system plays a central role in maintenance of health. Its ability to maintain protection from infectious diseases is dependent on distinguishing foreign or "nonself" antigens from "self" antigens and then to neutralize and/or eliminate the foreign antigen. The immune system is not confined to a single site in the body unlike most organ systems. It is composed of numerous lymphoid organs and cells. Immune cells circulate through the blood and lymph and are capable of migrating to virtually any location in the body. Primary lymphoid organs provide a microenvironment capable of supporting the production or maturation of immunocompetent cells. For example, all leukocytes and platelets are produced in the bone marrow. Maturation of these cells, except T-cells, occurs in the bone marrow as well; T-cells mature in the thymus. The site of antigen contact with virgin lymphocytes (T- and B-cells) occurs in secondary lymphoid organs such as the spleen and lymph nodes which filter the blood and the fluid surrounding the tissues, respectively, for antigens. Antigen recognition results in lymphocyte activation, proliferation and differentiation into effector or memory cells.

There are two functional divisions of mammalian immunity, innate and acquired immunity. Innate immunity encompasses the intrinsic, nonspecific host defenses and involves anatomic, physiologic, endocytic and phagocytic, and inflammatory defense mechanisms. Acquired immunity is mediated by lymphocytes following exposure to antigen and exhibits specificity, diversity, memory, and self/nonself recognition. Acquired immunity is further divided into cell-mediated immunity (CMI) and humoral immunity (HI). CMI defends the host against intracellular bacteria, viruses, and cancer. This

immunity is mediated by antigen-specific T-cells which mature in the thymus and by various nonspecific cells of the immune system. HI defends the host against extracellular bacteria, parasites, and foreign macromolecules and is mediated by soluble antibodies which are secreted from differentiated B-cells (plasma cells or AFCs). Secreted antibodies coat a specific antigen and facilitate antigen clearance by recruiting complement components and nonspecific immune cells which destroy and remove the antigen. Antibodies or immunoglobulins (Ig) are composed of two identical heavy chains and two identical light chains. There are five distinct classes of Ig which possess a characteristic type of heavy chain. For example, the heavy chains for IgM, IgG, IgA, IgE and IgD are encoded, respectively, by  $\mu$ ,  $\gamma$ ,  $\alpha$ ,  $\epsilon$ , and  $\delta$  heavy chain genes. Each class of Ig appears to have unique biological properties. For example, IgM is pentameric or hexameric resulting in high antigen valence, has relatively low affinity for antigen and is the major Ig involved in a primary antibody response. IgG is monomeric, has high affinity for antigen, can cross the placental barrier and is the hallmark of a secondary antibody response. IgE is also monomeric and is involved in allergic and anti-parasitic responses. IgA is monomeric or dimeric, is very efficient at bacterial lysis and is the main secretory antibody. IgD is monomeric, is a major surface component on many B-cells and has unknown biological properties. In vivo and in vitro antigen activation of B-cells leading to differentiated AFCs requires the coordinated interaction of several different immune cells, such as macrophages, T-cells, and B-cells for the T-dependent antigen, sRBC; macrophages and B-cells for the T-independent antigen, dinitrophenyl (DNP)-ficoll; and only B-cells for the polyclonal activator, lipopolysaccharide (LPS).

## B. B-cell activation

As alluded to above, B-cells can be activated in a T-dependent or -independent manner. Antibody responses to most protein antigens are dependent on T-helper cells since

most of these responses are not elicited in athymic mice (8). In a T-dependent (TD) response, naive B-cells circulate through blood and lymph until they contact a specific antigen which usually occurs in the spleen or lymph nodes. Antigen recognized by the Bcell receptor (BCR) is internalized, processed and presented on the B-cell surface in association with major histocompatibility complex (MHC) class II molecules. The same antigen is phagocytosed by other antigen presenting cells (macrophages and/or dendritic cells), processed and presented to T-cells, again, in the context of MHC class II molecules. T-cells that recognize the processed antigen are activated to search for B-cells presenting the same processed antigen. T- and B-cells with the same antigen specificity form a stable association through an interaction of surface ligands and receptors on either cell. This association allows the T-cell to provide the B-cell with activation and differentiation signals. These signals initiate from membrane-bound molecules and soluble cytokines and interact with surface molecules on B-cells. T-cell signals induce B-cells to proliferate and terminally differentiate into plasma cells. It should be noted that a T-cell can provide differentiation signals to a B-cell in an antigen nonspecific manner. Though both cells are initially activated by different antigens, they are still capable of associating through cellsurface molecules. This association results in B-cell differentiation and secretion of antibodies specific for the antigen that originally activated the B-cell, not the T-cell. Though this type of humoral response is generally very weak, it may be associated with background antibody titers as well as certain autoimmune reactions.

An initial response or primary response to a TD antigen results in a burst of IgM production at the site of B-cell activation; however, some B-cells, prior to differentiation, migrate into the follicular region of secondary lymphoid organs and initiate germinal centers. Activated B-cells forming germinal centers undergo rapid proliferation along with rapid somatic mutation of their Ig genes. Following somatic mutation, germinal center B-cells experience positive selection for high affinity membrane-bound Ig. Ig class switching which is independent from affinity maturation (somatic mutation and selection) also occurs

in germinal center B-cells (9). Positively selected B-cells will either terminally differentiate to plasma cells or to quiescent memory cells. Most plasma cells live for only a few days before programmed cell death; however, these cells may migrate to the gut or bone marrow, where they secrete antibody and may live for more than 20 days (8). The second and subsequent responses to a particular antigen are more rapid and of a longer duration than a primary antibody response. In addition, the antibody titer is greater in a secondary response and consists primarily of IgG as opposed to IgM from the primary response. This enhanced secondary antibody response is due to immunologic memory.

T-independent (TI) antigens have been classified as TI-1 or TI-2 based on mechanistic differences in antibody responses to these antigens. TI-1 antigens such as LPS, are generally polyclonal B-cell activators; whereas, TI-2 antigens such as viral particles, are usually repeating polymers that are not polyclonal activators of B-cells (8). LPS is the best studied of the bacterial components; however more progress has been made on how macrophages recognize LPS as opposed to B-cells. Macrophages respond to lower concentrations of LPS (1 ng/ml) as compared to those concentrations (10 µg/ml) required to initiate a B-cell polyclonal response. This greater sensitivity of macrophages to LPS is due to expression of the cluster of differentiation 14 (CD14). CD14, a glycosylphosphatidylinositol-linked protein, has no transmembrane or cytoskeletal domains and therefore, has no signaling capacity. CD14 has high affinity for LPS which is generally transferred to CD14 from the LPS-binding protein (LBP) (10). Macrophages lacking CD14 still respond to LPS but like B-cells, require higher concentrations. This has led to the theory that macrophages and B-cells express similar low affinity LPS receptors and that at high concentrations LPS can directly bind to this receptor and stimulate both macrophages and B-cells (10). Most B-cells are stimulated by LPS to proliferate and differentiate resulting in the polyclonal B-cell activator phenomenon. LPS at low concentrations only stimulates macrophages and B-cells if another receptor (i.e., CD14 for macrophages and BCR with LPS specificity for B-cells) is present. This second receptor has high affinity for LPS allowing the adjacent low affinity LPS signaling receptor to bind LPS and induce biological responses in macrophages (production of cytokines and other mediators) and B-cells (proliferation and differentiation). This is only a model of LPS activation and little is known about the existence of an LPS signaling receptor or about the molecular details of LPS activation (8, 10).

The strength of an antibody response varies among antigens; some antigens are more efficient than others at inducing BCR signaling. For example, a soluble antigen triggers a moderate antibody response but requires additional signals from accessory cells (macrophages and T-cells). A cell-bound antigen produces a strong antibody response due to the polyvalent nature of the antigen and to cell-cell adhesion. A polysaccharide antigen elicits a very strong antibody response through crosslinking of many BCRs. This response has the least requirement for additional signals from T-helper cells and macrophages. Bacterial cell walls contain both repetitious polysaccharides and polyclonal B-cell activators. These antigens are thus potent stimulators of B-cell activation due to a combination of strong signaling via the BCR of antigen specific B-cells (TI-2 response) with the nonspecific induction of B-cell terminal differentiation by polyclonal activators (TI-1 response) (8).

# C. Regulation of immunoglobulin expression

The transcriptional  $\mu$  heavy chain enhancer,  $E\mu$ , lies between the variable ( $V_H$ ) and constant ( $C_H$ ) regions of an assembled  $\mu$  heavy chain and was identified by its effects on immunoglobulin heavy chain (IgH) gene transcription and has been shown to enhance the variable (V)-diversity (D)-joining (I) recombination process (11, 12). Although  $E\mu$ , in conjuction with a IgH promoter, can result in tissue-specific expression of an Ig gene, they are not sufficient for high level IgH gene expression in vivo (13-15). This observation and the identification of several Ig-secreting cells that function normally in the absence of  $E\mu$ ,

suggested the existence of additional IgH locus enhancers (16-19). A DNA segment with transcriptional enhancer activity was identified at the 3'-end of the murine IgH locus (20, 21). This enhancer,  $3'\alpha E(hs1,2)$  [3' $\alpha$  enhancer, hypersensitive sites (hs) 1 and 2], lies 13 kb downstream of the  $\alpha$  gene and has been implicated in the induction of germline transcripts and class switching to most downstream  $C_H$  genes (22). It was soon discovered that the  $3'\alpha E(hs1,2)$  enhancer was one of four enhancers contained within an approximately 50 kb DNA segment (23-25). These enhancers [ $C\alpha 3'E$ ,  $3'\alpha E(hs1,2)$ , hs3 and  $3'\alpha$ -hs4], collectively referred to as the  $3'\alpha$  enhancer, are thought to form a locus control region and have been divided into two separate structural and functional units (21, 26) (see Figure 1).

Unit I is approximately 25 kb and includes the  $C\alpha 3'E$ ,  $3'\alpha E(hs1,2)$ , and hs3 enhancers. This unit has extensive dyad symmetry with 1067 bp of Ca3'E and hs3 being virtually identical (26, 27). All three enhancers of Unit I are DNase I hypersensitive late in B-cell differentiation (activated B-cells or plasma cells) (20, 26, 28). The 3'αE(hs1,2) enhancer has transcriptional activity only in B-cells and plasma cells as determined by transfert transfection assays (20, 29-33) and studies with transgenic mice (13). In contrast,  $C\alpha 3$ 'E and hs3, individually, have no activity in pre-B-cells (immature B-cells), B-cells or plasma cells (23, 25, 26, 33); however each enhancer in duplicate or paired together has substantial activity in plasma cells (25, 26). Interestingly, a chloramphenicol acetyl transferase (CAT) construct containing Ca3'E and Eµ had greater activity than Eµ alone in a plasma cell line. Synergy between these two regulatory domains did not occur in a pre-B- or B-cell line (33). Synergy also occurs with the enhancers of Unit I since addition of all three enhancers results in greater activity in a B-cell and plasma cell line than with 3'αE(hs1,2) alone (33). Addition of Eμ to a construct containing Unit I dramatically increases enhancer activity in a plasma cell line; again this synergy did not occur in a pre-Bor B-cell line (33).

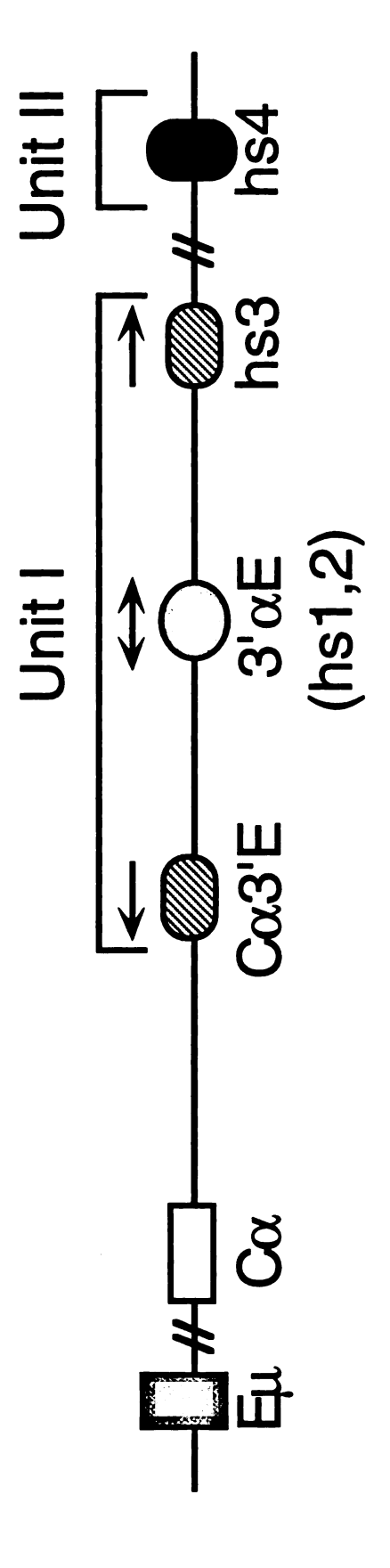


Figure 1. The 3'\alpha enhancer of the mouse Ig heavy chain gene. The 3'\alpha enhancer is composed of two functional units. Unit I contains the  $C\alpha 3'E$ ,  $3'\alpha E(hs1,2)$  and hs3 enhancers. Unit II contains the  $3'\alpha$ -hs4 enhancer. A DRE-like site is located within the  $3'\alpha E(hs1,2)$ and 3'α-hs4 enhancers.

Unit II of the 3' $\alpha$  enhancer contains a single enhancer, hs4, which is DNase I hypersensitive at both the pre-B and plasma cell stage (24, 28). This enhancer is transcriptionally active in a pre-B- and B-cell line but lacks activity in a plasma cell line (33). Interestingly, addition of E $\mu$  does not enhance the activity of hs4 and in a pre-B-cell line the combined activity is less than E $\mu$  alone (33).

The intact 3' $\alpha$  enhancer (Unit I and II) has greater activity in a pre-B-cell, B-cell or plasma cell line than any of the individual enhancers alone or in combination (33). This activity was also greater than E $\mu$  alone in the B-cell and plasma cell line but equal to E $\mu$  in the pre-B-cell line (33). Addition of E $\mu$  greatly enhanced activity of the 3' $\alpha$  enhancer in a pre-B- and B-cell line but not in a plasma cell line (33).

The interplay between the individual enhancers appears to be complex, stage specific and not fully understood. In general, synergy of the entire 3'α enhancer with Eμ appears to be more important in pre-B- and B-cell lines. The hs4 enhancer appears to be more active in pre-B- and B-cell lines as compared to plasma cells whereas Ca3'E, 3'αE(hs1,2) and hs3 seem to be more active in B-cell and plasma cell lines. It has been proposed that hs4 may have distinct functions at the pre-B cell stage, perhaps to facilitate early stages of development (e.g. V(D)J recombination), and that at the B-cell and plasma cell stage the 3'\alpha enhancers may function cooperatively to control events such as Ig transcription and class switching (34, 35). In fact, a variant of a plasmacytoma which expresses very low levels of IgA has a complete deletion of the 3'α enhancer (24, 36). Replacement of the 3'\(\alpha E(\hs1,2)\) with a neo gene in a plasma cell line results in decreased IgH gene expression (37). A similar experiment in mice resulted in deficient class switching to certain isotypes; secretion of IgM, IgG1 and IgA was normal (22). However, an approximately 2-fold increase or decrease in  $\mu$  expression has been observed following activation or repression, respectively, of the 3'\(\alpha E(\text{hs1,2})\) enhancer (13, 20, 38). Addition of the other enhancer domains might result in a more profound effect on  $\mu$  expression as was seen with  $\alpha$  expression following a complete deletion of the 3' $\alpha$  enhancer (24, 36). The specific regulation of the 3'α enhancer has not been elucidated; however, several DNA binding proteins, including BSAP, NF-κB, Oct proteins and a G-rich DNA binding protein have been shown to affect 3'αE(hs1,2) and hs4 enhancer activity at various B-cell stages (31, 32, 34, 39). Interestingly, LPS activates the 3'αE(hs1,2) enhancer (13) and LPS will induce a class switch to IgG3 and IgG2b isotypes (40). Conversely, the aforementioned isotypes are significantly decreased in 3'αE(hs1,2) knockout mice (22).

# D. Regulators of the immunoglobulin heavy chain $3'\alpha$ enhancer

# 1. The B-cell-specific activator protein

The B-cell-specific activator protein (BSAP) is encoded by the Pax5 gene and is a member of the highly conserved *Pax*-gene family of transcription factors (41). Within the hematopoietic system, BSAP expression and DNA binding activity are restricted to the B-cell lineage and are initiated in pro-B cells continuing throughout the B-cell maturation pathway until the cells terminally differentiate into plasma cells in which BSAP is no longer expressed (42). Various binding sites for BSAP have been identified in the promoter regions of B-cell specific genes such as genes encoding CD19 (43), Blk (44), lambda 5, and VpreB1 (45). These genes play important roles in early B-cell development (lambda 5 and VpreB1) and surface Ig signaling (CD19 and Blk). In addition BSAP appears to positively regulate promoters of these genes implying an important role of BSAP in immature B-cell development. This implication was confirmed by the demonstration that *Pax5*-knockout mice failed to produce small pre-B-, B-, and plasma cells (46).

BSAP binding sites have also been identified 5' to and within the switch regions of Ig heavy chain genes (47-49). Wakatsuki and coworkers (50) demonstrated an inhibition of isotype switching induced by various stimuli, most notably, LPS plus interleukin-4 (IL-4), after downregulation of BSAP by antisense oligonucleotides. However, the authors

caution that this effect may be a more general effect on cell proliferation since proliferation has been shown to be a prerequisite of isotype switching.

In addition to these positive effects of BSAP on gene regulation, BSAP has been shown to negatively regulate the murine Ig heavy chain  $3'\alpha E(hs1,2)$  enhancer in B-cells (31, 32, 34). Suppression of this enhancer by BSAP may lead to downregulation of Ig gene transcription and would explain the lack of BSAP expression in plasma cells whose main function is high-rate Ig gene transcription (50). Studies utilizing the CH12.LX B-cell lymphoma demonstrated that BSAP negatively regulates the  $3'\alpha E$  (hs1,2) by suppressing the downstream binding of a 40-kDa protein (NF- $\alpha$ P) that positively affects enhancer activity and Ig gene transcription (31). BSAP also regulates another  $3'\alpha$  enhancer,  $3'\alpha$ -hs4. In contrast to  $3'\alpha E(hs1,2)$ , BSAP has been shown to positively regulate  $3'\alpha$ -hs4 in the A-20 B-cell line, implying distinct functions of these  $3'\alpha$  enhancers which are dependent on the maturation state of the B-cell (34). Opposite effects of BSAP at these two enhancers is probably due to a difference in protein-protein interaction rather than differences in BSAP binding.

# 2. The NF-κB/Rel protein family

The NF-κB/Rel protein family has been divided into two groups based on structure, function and mode of synthesis (51, 52). The p50 (NF-κB1) and p52 (NF-κB2) proteins which are synthesized as precursor proteins of 105 and 100 kDa, respectively, comprise the first group, while the second group consists of p65 (RelA), c-Rel (Rel) and RelB which are not synthesized as precursors. Both groups possess the Rel homology domain which is responsible for protein dimerization, nuclear localization and DNA binding. In addition to the Rel homology domain, p65, c-Rel and RelB, unlike p50 and p52, also have one or more transcriptional activation domains. Inactive NF-κB/Rel proteins are anchored in the cytoplasm as homo- or heterodimers bound to a member of the

IKB protein family (IKB- $\alpha$ , IKB- $\beta$ , IKB- $\gamma$ , IKB- $\epsilon$ ) or as heterodimers of a processed NFκB/Rel protein and an unprocessed NF-κB/Rel precursor (53, 54). The IκB protein family contain an ankyrin repeat motif important for an interaction between NF-kB/Rel proteins and a C-terminal PEST sequence which may be involved in protein degradation (55). NFκB/Rel inducers such as, phorbol esters, calcium ionophores, inflammatory cytokines, bacterial LPS, antigen receptor cross-linking of T- and B-cells, oxidative and physical stress and viral infection, appear to activate NF-kB/Rel proteins via several different signal transduction pathways that converge at phosphorylation of IkB and of NF-kB/Rel precursors (51, 54-57). IkB is phosphorylated by an IkB kinase (IKK) which is a large molecular weight complex (500-900 kDa) composed of several polypeptides, two of which hold the kinase activity (IKK\alpha and IKK\beta) (54, 58). Phosphorylation of I\beta and of NFkB/Rel precursors appears to result in ubiquitination and subsequent proteosome processing and release of NF-kB/Rel which translocates to the nucleus and activates target genes (59, 60). A wide variety of genes are targeted by NF-KB/Rel proteins including genes encoding viruses, immunoreceptors, cell adhesion molecules, cytokines, hematopoietic growth factors, acute phase proteins and transcription factors (51).

In B-cells, NF-κB/Rel proteins are involved in cellular activation and Ig gene expression. In fact, NF-κB was first identified by its binding to a specific DNA site within the Ig κ light chain intronic enhancer (61). Interestingly, in pre-B cell lines NF-κB must be activated by PMA or LPS; whereas in B-cell and plasma cell lines, NF-κB is a constitutively active nuclear protein complex (51, 59). The constitutive form of NF-κB is primarily composed of c-Rel-p50 heterodimers; p65-p50 heterodimers are inactive and are at normal levels in the cytosol (62, 63). Constitutive nuclear levels of c-Rel-p50 may be due to an increased instability of IκBα and by increased transcription of the c-Rel gene (63). In addition, proliferative responses as well as Ig production to certain stimuli was impaired in B-cells from both p50 and c-Rel knockout mice (64-66). These specific effects were not observed with p65 and RelB knockout mice (67-69). In agreement with these

results, Michaelson and coworkers (34) have demonstrated  $\kappa B$  binding sites within the  $3'\alpha E(hs1,2)$  and  $3'\alpha$ -hs4 domains of the Ig heavy chain  $3'\alpha$  enhancer. NF- $\kappa B/Rel$  proteins bind to both of these  $\kappa B$  sites (34). In a B-cell line, c-Rel and p50 bind to the  $3'\alpha E(hs1,2)$   $\kappa B$  site and RelB, p50 and p52 bind to the  $3'\alpha$ -hs4  $\kappa B$  site. As homodimers or heterodimers with each other, p50 and p52 are negative regulators of gene transcription. The protein composition for the  $3'\alpha E(hs1,2)$   $\kappa B$  site is slightly altered in a plasma cell line in that RelB, in addition to c-Rel and p50 was identified. Protein binding to the  $3'\alpha$ -hs4  $\kappa B$  site in plasma cells was not assessed. Interestingly, NF- $\kappa B/Rel$  proteins negatively regulate, in conjunction with BSAP,  $3'\alpha E(hs1,2)$  activity in two B-cell lines but positively regulate this enhancer in a plasma cell line as determined by transient transfection assays (34). In contrast, NF- $\kappa B/Rel$  proteins positively regulate the  $3'\alpha$ -hs4 activity in the two B-cell lines as well as in the plasma cell line (34). In addition, octamer binding to sites within the  $3'\alpha E(hs1,2)$  and  $3'\alpha$ -hs4 enhancers results in the same regulation profile as NF- $\kappa B/Rel$  proteins except that octamer binding had no effect on  $3'\alpha$ -hs4 activity in a plasma cell line (31, 34, 39).

#### II. Toxic effects of TCDD

#### A. General toxicity of TCDD

Halogenated aromatic hydrocarbons (HAH) such as the polychlorinated dibenzo-p-dioxins (PCDD), dibenzofurans and biphenyls are persistent environmental toxins. TCDD has been considered the prototype of HAHs because of its biological potency in experimental animals. TCDD is a true contaminant that is produced during the combustion of organic materials in the presence of chlorine and for example, is formed during the production of the herbicides 2,4-dichlorophenoxyacetic acid (2,4-D) and 2,4,5-trichlorophenoxyacetic acid (2,4,5-T) which are the main components of Agent Orange (a

1:1 mixture of 2,4-D and 2,4,5-T). TCDD contamination of Agent Orange has led to the exposure of soldiers and civilians to TCDD during and after the Vietnam war (70). In addition, residents of Alsea, Oregon (70); Times Beach, Missouri (71, 72); and Seveso, Italy (73, 74) have been exposed to TCDD during defoliation of forests with 2,4,5-T; spraying of dirt roads for dust control with TCDD-contaminated chemical wastes; and accidental release of TCDD contaminated chemicals from an industrial plant, respectively. These highly publicized incidents of human exposure have generated considerable public concern toward this contaminant. TCDD is also formed during combustion of municipal and industrial wastes, wood pulp and paper bleaching, wood and coal burning, and metal recycling.

The toxic effects of TCDD on humans remains unclear and presently only sufficient evidence exists for a causal relationship between TCDD exposure and the development of soft tissue sarcoma, chloracne and porphyria cutanea (70). A causal relationship between TCDD exposure and the development of various cancers, teratogenicity, neurotoxicity and immunotoxicity remains uncertain (70). However, a wide range of toxic responses have been observed in most animal models after exposure to TCDD and these include death, generalized wasting syndrome, lymphoid involution (especially of the thymus), hepatotoxicity, teratogenicity, developmental toxicity, carcinogenesis, neurotoxicity and immunotoxicity (reviewed in references 75 and 76). In addition to these toxic effects, TCDD causes oxidative stress, hormonal alterations, changes in phosphorylation patterns, and alteration of gene expression such as induction of metabolic enzymes, most notably specific isozymes of cytochrome P450 such as CYP1A1 (75, 77-81). There has been considerable effort directed towards characterizing the mechanism by which TCDD causes induction of metabolic enzymes; however, no causal relationship has been demonstrated between this induction and the toxic effects of TCDD.

Notable variation in the effects of TCDD within and between species has been observed. In terms of LD<sub>50</sub>, the guinea pig is the most sensitive species to TCDD whereas

the hamster is the least sensitive (75). Within species variation has been best characterized with different strains and F1 crosses of mice (82-84). For example, C57Bl/6 and B6C3F1 mice are on the average 10- to 20-fold more sensitive to TCDD than DBA/2 and AKR mice (1, 85). Although there is considerable debate over the actual sensitivity of humans to the toxic effects of TCDD, the persistence of this contaminant in the environment in addition to its potent toxicity in laboratory animals has resulted in continued public concern regarding the potential health effects of human exposure to TCDD.

## B. Immunotoxicity of TCDD

Alteration of immune function is among the earliest and most sensitive responses to TCDD exposure in most animal models and occurs at doses which do not produce overt organ toxicity. TCDD has been shown to alter both innate and acquired immunity (reviewed in 86). Because of the marked thymic involution observed in most species after exposure to TCDD, early immunotoxicological studies focused on TCDD-induced alteration of CMI. Initial studies demonstrated an almost complete loss of cortical derived thymocytes in rats and mice after peri- and post-natal exposure to TCDD (87, 88). However, Greenlee and coworkers (89) later demonstrated that TCDD treatment of the thymus directly induces terminal differentiation of the thymic epithelial cells which plays a major role in thymocyte maturation. These authors conclude that terminal differentiation of the thymic epithelial cells may result in a loss of their ability to support thymocyte maturation. In contrast, Staples and coworkers (90) through irradiation and reconstitution experiments, have identified hemopoietic components which give rise to macrophages and dendritic cells as opposed to stromal components as the primary mediator of thymic atrophy. In addition several laboratories have observed a significant suppression of B-cell function (TD antibody response) to acute TCDD exposure at concentrations minimally affecting both thymic weight (1, 91-93) and T-cell function (proliferative response, graft versus host reaction and cytotoxic T lymphocyte response) (94, 95) suggesting a greater sensitivity of HI to TCDD-induced immune alteration. Interestingly, time of addition studies demonstrate that TCDD must be added to splenocyte cultures within 24 hr of antigen stimulation to produce a significant and potent inhibition of the plaque forming cell response to sRBC (93). Since this TD antibody response requires both macrophages and T-cells as accessory cells for the production of antigen-specific antibody, a series of studies aimed at characterizing the specific cellular target(s) of TCDD were initiated. Separation/reconstitution studies and characterization of in vitro responses to various defined antigens requiring differential cellular cooperativity identified the B-cell as a cellular target for TCDD-mediated humoral suppression (96-98). In these studies the polyclonal response to LPS, the TI responses to trinitrophenyl (TNP)-LPS (96), and DNP-Ficoll and the TD response to sRBC were all comparably suppressed by TCDD (97); notably, only the B-cell is required for all three types of these responses. Results from separation/reconstitution studies in which splenocytes from mice exposed to vehicle or TCDD were separated into various cell populations (macrophages, T-cells and B-cells) and reconstituted in various combinations in cell culture, demonstrated that a significant suppression of the sRBC immune response required TCDD exposed B-cells (97). These findings further supported the conclusion that the B-cell is a cellular target of TCDD. In addition, an increase in protein phosphorylation (99, 100) and Ca<sup>2+</sup> influx (101, 102) occur following TCDD-treatment of primary B-cells; these cellular changes have been implicated in TCDD-induced suppression of the antibody response. Because of the above results, our laboratory has focused primarily on elucidating the mechanism responsible for TCDDmediated B-cell dysfunction. However, it should be recognized that TCDD does have effects on other leukocyte populations and that these effects may also contribute to an alteration in B-cell function. For instance, Shepherd and Kerkvliet (103) have recently identified decreased levels of T-cell derived cytokines as well as IL-12 in TCDD-treated mice. IL-12 drives T-cell differentiation and is produced by antigen presenting cells. From this and previous results, the authors have hypothesized that the effect of TCDD on T-cell function is a consequence of dysfunctional antigen presenting cells resulting in decreased T helper cell differentiation (103, 104). However, cell separation/reconstitution experiments suggest that TCDD has no effect on the ability of macrophages to support the plaque forming cell response to sRBC and has only a modest effect on T-cell accessory function (97).

# III. Role of the AhR in TCDD-mediated immune suppression

# A. The AhR signaling pathway

The putative mechanism of action for TCDD and structurally related compounds is believed to involve the cytosolic AhR and its binding partner, ARNT (75, 76, 105-107) (Figure 2). This mechanism has been primarily elucidated by studying HAH-induced upregulation of drug metabolizing enzymes, such as CYP1A1, in liver and liver-derived cell-lines. The AhR is a 95-110 kDa basic helix-loop-helix (bHLH) type of liganddependent transcription factor (105, 106). In the absence of ligand, the AhR is primarily located in the cytoplasm and is complexed with heat shock protein (hsp) 90, c-src and the AhR-interacting protein (AIP) (108-112). Binding of TCDD to the AhR results in disassociation of the cytoplasmic complex and translocation of the liganded AhR into the nucleus where it forms a heterodimer with a structurally related 87 kDa bHLH protein called ARNT (111, 113-119). Recent results suggest that hsp90 translocates with the AhR into the nucleus where it is displaced by ARNT (Pollenz, personal communication 1999). The AIP and c-src proteins are localized in the cytosol and presumably disassociate from the AhR following ligand binding (109, 110). It has been suggested that c-src is activated following release from the AhR which is consistent with the increase in c-src activity and in protein phosphorylation identified by several laboratories following TCDD treatment (81,

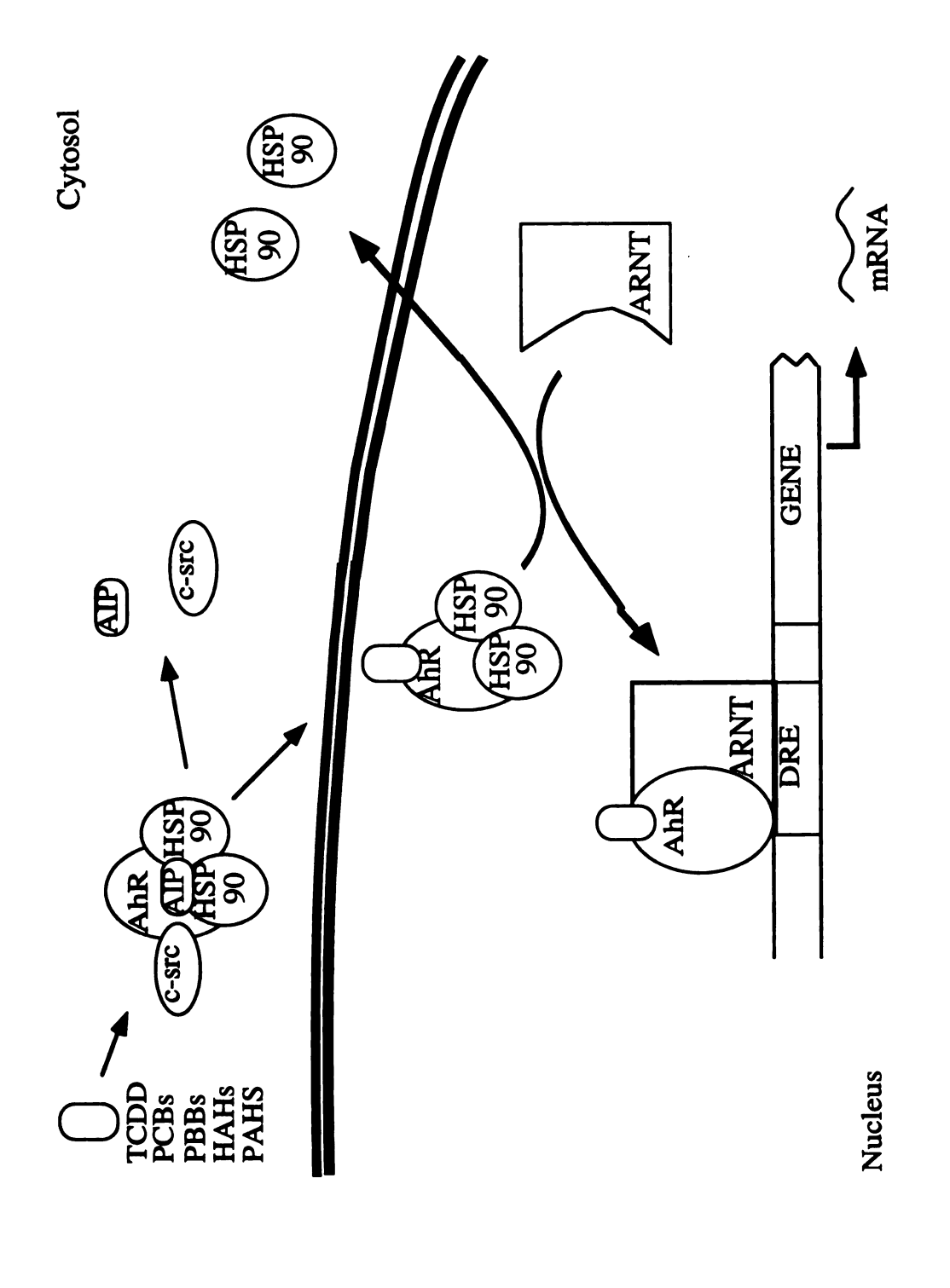


Figure 2. The AhR signaling pathway.

99, 100, 120, 121). The other AhR cytosolic partner, AIP, has homology with the FK506-binding protein family and is thought to have a positive influence on AhR-mediated signaling (110). In any case, the ligand-AhR/ARNT complex can act as a transcription factor by binding to DNA at the DRE in the promoter region of sensitive genes such as CYP1A1, glutathione S-transferase, and menadione oxidoreductase (75, 76, 113, 122-126). This mechanism has only been characterized with the induction of metabolic enzymes and as previously mentioned, this upregulation has not been directly correlated with the toxicity of TCDD. In fact, the most TCDD-susceptible species based on the LD<sub>50</sub> concentration is the guinea pig which does not exhibit a notable induction of CYP1A1 activity with TCDD treatment (127). In contrast, the least TCDD-susceptible species, the hamster, shows a marked induction of CYP1A1 activity with TCDD treatment (81). Indeed, several other genes such as those encoding plasminogen activator inhibitor-2, interleukin-1 $\beta$ , transforming growth factor- $\alpha$  and - $\beta$ , epidermal growth factor receptor, estrogen receptor, c-fos, c-jun, and recombination activating gene have been shown to be upregulated or downregulated following TCDD treatment (128-133). The modulation of non-metabolic genes such as those above, may account, in varying degrees, for the various toxicities observed in animals treated with TCDD. In addition, DRE-like sites have been found in the promoter regions of several of these genes supporting the possibility for transcriptional regulation through the AhR which would be mechanistically analogous to CYP1A1 induction (134). Furthermore, several laboratories have demonstrated novel protein-protein associations involving the AhR and several other proteins some of which are NF-κB, Sp1, transcription factor IIB, retinoblastoma protein and as mentioned above, the Src family kinase, c-src (109, 135-138). This suggests a possible interaction of the AhR with different signaling pathways and thus, a potential for DRE-independent mediation of some of TCDD's effects.

Four different allelic forms of the murine AhR have been identified and may account for strain differences in sensitivity to TCDD (139). These alleles are separated into

two groups based on ligand binding affinity. There are three high affinity alleles,  $Ah^{b-1}$  (95 kDa),  $Ah^{b-2}$  (104 kDa) and  $Ah^{b-3}$  (105 kDa) as well as one low affinity allele,  $Ah^d$  (104 kDa). Marked species variability in biochemical responses to TCDD may also be a result of differences in the AhR across species. The most extensively studied group of ligands for the AhR have been the HAHs which are xenobiotics. The actual endogenous ligand for the AhR is unknown; however, the endogenous metabolite bilirubin has been shown to directly regulate CYP1A1 gene expression in an AhR-dependent manner (140). Dietary and therapeutic AhR ligands such as indolocarbazoles, tryptophan metabolites and omeprazole have also been identified (141-143). It has been suggested that indolocarbazoles may be physiological AhR ligands due to their prevalence in the diet and to a virtually equal potency in activating the AhR as TCDD (142). The biological consequences of indolocarbazole and AhR interactions is unknown.

#### B. The AhR and TCDD-mediated immunotoxicity

Despite a lack of direct evidence, there is a wide spread belief among researchers in this area that most if not all of the effects produced by TCDD are mediated through binding of the ligand-bound AhR/ARNT complex to DRE motifs present in the 5' regulatory regions of target genes. This belief has been supported by the generally observed parallel relationship between CYP1A1 induction and toxic responses induced by HAH exposure (75, 144, 145). In terms of TCDD-induced immunotoxicity there is evidence for and against the involvement of an AhR/ARNT-DRE-mediated mechanism. Structure-activity relationship (SAR) studies have demonstrated that with few exceptions, high affinity AhR ligands are more immunosuppressive than low affinity ligands (3). Immune suppression following acute exposure to TCDD was shown to segregate with the AhR using mouse strains susceptible (Ah high-responsive) or resistant (Ah low-responsive) to enzyme induction. Ah high-responsive C57BL/6 and C3H/HeN strains were highly sensitive to the

immunosuppressive effects of TCDD; whereas, Ah low-responsive DBA/2 and AKR strains were less sensitive to immunosuppression (1, 2, 146). Additional studies using congenic mice at the Ah locus demonstrated that B6 mice expressing the wild-type phenotype Ahbb allele are more sensitive to TCDD-induced suppression of the antibody response than congenic B6 Ahdd mice (2). The Ahbb allele encodes for an AhR with high affinity for ligand, while the Ahdd allele which is the wild-type phenotype for the DBA/2 mouse strain encodes for an AhR with low affinity for ligand (83). In addition Lorenzen and coworkers (147) identified nuclear [3H]-TCDD by sucrose density gradient centrifugation in human tonsilar cells, thus suggesting the translocation of the AhR-TCDD complex to the nucleus. However, these findings were tempered by the fact that although identified in lymphoid tissues, the AhR and ARNT had not been directly demonstrated in immunocompetent cells. This was an important distinction because of previous results by Greenlee and coworkers (89) demonstrating that the thymic epithelial cells express significantly more binding of [3H]-TCDD as compared to thymocytes and were directly targeted by TCDD. In addition, a study by Neumann and coworkers (148) demonstrated comparable binding of [3H]-TCDD between the splenic capsule and isolated splenocytes. In contrast to SARs observed between AhR binding and immunotoxicity, the low affinity AhR ligand, DCDD, and TCDD produced comparable inhibition of the TD antibody forming cell response following subchronic treatment of mice in vivo and following direct addition to naive splenocytes in vitro (6, 149). The condition of TCDD exposure appears to be a factor in segregation of the immunotoxicity with the AhR in that, subchronic TCDD treatment produced a marked immunosuppression in DBA/2, B6C3F1, and congenic Ahdd mice (7, 149) indicating a loss of the resistance seen in DBA/2 mice after acute TCDD exposure (1, 2, 146). In addition, binding of the AhR/ARNT heterodimer to the DRE following TCDD-treatment has not been detected in spleen using an electrophoretic mobility shift assay (EMSA) which measures the ability of a DNA regulatory protein to bind a specific DNA motif (5); again, questioning if the AhR and ARNT are present and functional in immunocompetent cells. Furthermore, increased protein phosphorylation that did not segregate with the AhR (99) and an increase in Ca<sup>2+</sup> influx which may be AhR-independent (101, 102, 132) occur in primary B-cells following TCDD treatment. In light of the above observations, it was unclear what role the AhR plays in mediating the immunotoxicity of TCDD.

#### C. The AhR, BSAP and inhibition of *CD19* expression

Masten and Shiverick (150) have identified a DRE core motif within a BSAP binding site that is located in the CD19 promoter region. CD19 is a signal transducing protein that is expressed through the early stages of B-cell development but is lost upon Bcell differentiation to a plasma cell (151). Masten and Shiverick (150) have also demonstrated a TCDD-induced suppression of CD19 mRNA expression in a human B-cell line. They have proposed that this inhibition is a result of the AhR nuclear complex interfering with the binding of BSAP to a common DNA binding site in the CD19 promoter region. This speculation was supported by EMSA analysis and competition experiments in which unlabeled oligonucleotide corresponding to the BSAP binding site in the CD19 promoter region partially inhibits the formation of an AhR/ARNT-DRE complex and is effective at high concentrations in competing with the DRE for binding of the AhR nuclear complex. These results suggest that the AhR nuclear complex is capable of binding the BSAP binding motif with weak affinity in comparison to DRE binding. However, this interaction between BSAP and the AhR is limited to the human CD19 promoter and to a moderate affinity BSAP site which may not play a prominent role in CD19 expression (43). Therefore, the inhibition of CD19 expression seen by Masten and Shiverick (150) is probably not due to an interaction between BSAP and the AhR. In addition, this particular DRE-containing BSAP site is not present in the mouse CD19 promoter (43); however, we have identified a DRE-like site within the transcription initiation region of both the mouse

and human *CD19* genes. It is unclear if these DRE sites mediate an affect on CD19 gene expression and will be a focus of future studies in our laboratory.

#### MATERIALS AND METHODS

#### I. Chemicals

TCDD, 1,2,3,4,,7,8-hexachlorodibenzo-p-dioxin (HxCDD), 2,3,7-trichloro-dibenzo-p-dioxin (TriCDD) and 1-monochlorodibenzo-p-dioxin (MCDD), in 100% DMSO, were purchased from AccuStandard Inc. (New Haven, CT). The certificate of product analysis stated the purity of TCDD, HxCDD, TriCDD and MCDD to be 99.1, 100, 99.6, 100% respectively, as determined by AccuStandard, using gas chromatography/mass spectrophotometry (GC/MS). DMSO and LPS were purchased from Sigma Chemicals (St. Louis, MO).

#### II. Animals

Virus-free female B6C3F1 (C57BL/6 x C3H) mice, 5-6 weeks of age were purchased from the Frederick Cancer Research Center (Frederick, MD). On arrival, mice were randomized, transferred to plastic cages containing a saw dust bedding (5 mice per cage) and quarantined for 1 week. Mice were provided with food (Purina Certified Laboratory Chow) and water *ad libitum*. Animal holding rooms were kept at 21-24°C and 40-60% relative humidity with a 12 hour light/dark cycle.

#### III. Cell Lines

The CH12.LX B-cell line derived from the murine CH12 B-cell lymphoma, which arose in B10.H-2<sup>a</sup>H-4<sup>b</sup>p/Wts mice (B10.A x B10.129), has been previously characterized (152) and was a generous gift of Dr. Geoffrey Haughton (University of North Carolina). The BCL-1 B-cell line was derived from a murine B-cell lymphoma that spontaneously

arose in a BALB/c mouse (153). This cell line has been previously characterized (154) and was generously provided by Dr. Kathryn H. Brooks (Michigan State University). CH12.LX and BCL-1 cell lines were grown in RPMI-1640 (Gibco BRL, Grand Island, NY) supplemented with heat-inactivated bovine calf serum (10% for CH12.LX cells and 5% for BCL-1 cells) (Hyclone, Logan, UT), 13.5 mM HEPES, 23.8 mM sodium bicarbonate, 100 U/ml penicillin, 100 µg/ml streptomycin, 2 mM L-glutamine, 0.1 mM non-essential amino acids, 1.0 mM sodium pyruvate, and 50 µM β-mercaptoethanol. The mouse hepatoma cell line, Hepa 1c1c7, was generously provided by Michael S. Denison (University of California, Davis). Hepa 1c1c7 cells were cultured in αMEM media supplemented with 13.5 mM HEPES, 23.8 mM sodium bicarbonate, 100 units/ml of penicillin, 100 µg/ml streptomycin, 2 mM L-glutamine, and 5% bovine calf serum. All cells were maintained at 37° C in atmosphere of 5% CO<sub>2</sub>.

# IV. Northern Blot Analysis

#### A. RNA Isolation and Analysis

Total RNA was isolated using a modified method of Chomczynski and Sacci (155). Briefly, mouse spleen and liver was homogenized in denaturing solution (4 M guanidium isothiocyanate, 25 mM sodium citrate, 0.5% sarcosyl, 100 mM 2-mercaptoethanol) and extracted twice with phenol:chloroform:isoamyl alcohol (1:1:24). Nucleic acids were precipitated and resuspended in water. Poly(A) RNA was purified by PolyATtract (Promega, Madison, WI), precipitated, resuspended in water, and quantitated spectrophotometrically. Poly(A) RNA was fractionated in a 1.2% agarose-formaldehyde gel, transferred to nylon membrane (Amersham, Arlington Heights, IL), and cross-linked to the membrane using a UV Stratalinker 1800 (Stratagene, LaJolla, CA). Blots were prehybridized for 2-6 hr and hybridized overnight at 42°C in hybridization solution [50%]

formamide, 5x SSPE (0.9 M NaCl<sub>2</sub>, 0.05 M NaH<sub>2</sub>PO<sub>4</sub> and 0.005 M EDTA), 10x Denhardt's solution, 2% SDS (sodium dodecyl sulfate), 7% dextran sulfate, yeast tRNA at 130 μg/ml, and labeled probe], then washed twice for 5 min in 2x SSPE with 0.5% SDS, twice for 15 min in 1x SSPE with 1% SDS, and twice for 15 min in 0.1x SSPE with 0.1% SDS if needed. Blots were then exposed to Reflection film (Dupont NEN, Boston, MA) at -80°C in the presence of intensifying screens.

Mouse spleen without capsule was prepared by carefully separating the splenic pulp from the splenic capsule. The spleen cells were homogenized in denaturing solution and mRNA was isolated as described above.

#### B. cDNA Probes

The plasmid pSportAhR (ATCC 63215) developed by Bradfield (106) contains a 3.12 kb insert of the cDNA for the mouse AhR gene which was cloned from the Hepa 1c1c7 cell line. The AhR cDNA probe was a 1.87 kb fragment cut with restriction enzymes Hind III and BamH I from pSportAhR and corresponds to the 3' end of the cloned AhR gene. The 75 base ARNT oligomer probe was synthesized using an Applied Biosystem DNA synthesizer and purified by HPLC (Macromolecular Structure Facility, MSU). This oligomer represents nucleotides 360 to 435 of the human ARNT cDNA clone sequenced by Hoffman *et al.*, (122).

# V. Reverse Transcription-Polymerase Chain Reaction

#### A. RNA Isolation

Total RNA for the reverse transcription-polymerase chain reaction (RT-PCR) was isolated using Tri Reagent (Molecular Research Center, Cincinnati, OH) as described by

Chomczynski (156, 157) or with the High Pure RNA Isolation system (Boehringer Mannheim Biochemicals, Indianapolis, IN). RNA samples were first analyzed for DNA contamination by PCR analysis without reverse transcriptase. RNA samples containing DNA were incubated with RNase-free DNase for 15 min at 37°C in 10mM MgCl<sub>2</sub>, 1mM DTT, 25 units RNasin, 10mM Tris, 1mM EDTA, then phenol:chloroform extracted, and precipitated in isopropanol.

## B. Qualitative RT-PCR Analysis

Primer sequences for RT-PCR analysis were chosen using GeneWorks, IntelliGenetics, Inc. (Real Mountain View, CA). No significant homology was detected when each sequence was searched in the Genebank database and the PCR products were observed as a single band of the expected size (Ahr 385 bp; Arnt 340 bp; Cyp1a1 228 bp; µ 404 bp) on an ethidium bromide-stained agarose gel. The forward and reverse primers were synthesized using an Applied Biosystems DNA synthesizer and purified by HPLC (Macromolecular Structure Facility, MSU) and were as follows: Ahr, TCATGGAGAGGT GCTTCAGG and GTCTTAATCATGCGGATGTGG; Arnt, TTCCGATTCCGATCTAAG ACC and TGTTCTGATCCTGCACTTGC; µ, TGAGCAACTGAACCTGAGG and TGCATACACAGAGCAACTG. Primers for the CYP1A1 gene were a generous gift of Dr. Dale Morris (J. D. Searle). For the cDNA reaction, known amounts of total RNA was reverse transcribed by RT into cDNA using oligo(dT)<sub>15</sub> primers. For the PCR amplification reaction, a PCR master mix consisting of PCR buffer, MgCl<sub>2</sub> (4 mM for the Ahr and Cyplal reactions and 2 mM for the Arnt and  $\mu$  reactions), 6 pmol each of the appropriate forward and reverse primer, and 2.5 units Tag DNA polymerase were added to the cDNA samples. For the Ahr and Arnt reactions, samples were then heated to 94°C for 4 min and cycled 32 times at 94°C for 15 sec (disassociation), 59°C for 30 sec (annealing), and 72°C for 30 sec (elongation) after which an additional extension step at 72°C for 5 min was included. The PCR reactions for Cyp1a1 and  $\mu$  were performed as described above except that the annealing temperature was 56°C for Cyp1a1 and 60°C for  $\mu$ . In addition, the  $\mu$  reaction was cycled 30 times. PCR products were electrophoresed in 1.5% agarose gels and visualized by ethidium bromide staining and assessed qualitatively. All RT-PCR reagents were purchased from Promega (Madison, WI) except the Taq DNA polymerase which was purchased from Perkin Elmer (Foster City, CA).

## C. Quantitative RT-PCR Analysis

Quantitative RT-PCR was performed as outlined in Gilliland et al. (158, 159), except that the recombinant RNA (rcRNA) was used as an internal standard (IS) instead of genomic DNA. Each IS was generated as previously described (160) and contain specific PCR primer sequences for Ahr, Arnt, Cyplal, or \(\mu\) (PCR product sizes: Ahr 385 bp; Ahr-IS 256 bp; Arnt 340 bp; Arnt-IS 255 bp; Cyp1a1 228 bp; Cyp1a1-IS 336 bp; μ 404 bp; μ-IS 309 bp). Briefly, known amounts of total RNA sample and IS rcRNA were reverse transcribed simultaneously, in the same reaction tube, into cDNA using oligo(dT)<sub>15</sub> as primers. PCR amplification of the IS and sample cDNA was performed as described above for qualitative RT-PCR. PCR products were electrophoresed in 3% NuSieve 3:1 gels (FMC Bioproducts, Rockland, ME) and visualized by ethidium bromide staining. Quantitation was performed by assessing the optical density for both of the DNA bands (i.e., IS versus target gene) using a Gel Doc 1000 video imaging system (Bio Rad, Hercules, CA). The number of transcripts was calculated from a standard curve generated by using the density ratio between the gene of interest and the different internal standard concentrations used (159). The point at which the ratio of IS to mRNA is equal to one signifies the "cross-over" point which represents the amount of Ahr, Arnt, Cyplal, or u molecules present in the initial RNA sample. At least two separate RNA isolations per experiment were analyzed for each of the tissues or cell lines.

## VI. Enzyme-Linked Immunosorbent Assay for IgM

Supernatants were harvested from naive or LPS (3 or 30 µg/ml)-stimulated CH12.LX or BCL-1 cells following a 72 hr incubation at 37°C in 5% CO<sub>2</sub> and were analyzed for IgM by sandwich enzyme-linked immunosorbent assay (ELISA). Briefly, 100 µl of supernatant or standard (mouse IgM, Sigma, St. Louis, MO) were added to wells of a 96-well microtiter plate coated with anti-mouse Ig capture antibody (Boehringer Mannheim, Indianapolis, IN), and then incubated at 37°C for 1.5 h. After the incubation period, the plate was washed with 0.05% Tween-20:phosphate-buffered saline (PBS) and H<sub>2</sub>0, followed by addition of a horseradish peroxidase anti-mouse IgM detection antibody (Sigma, St. Louis, MO) and another incubation at 37°C for 1.5 h. Unbound detection antibody was washed from the plate following the incubation period with 0.05% Tween-20 PBS then H<sub>2</sub>0. ABTS substrate (Boehringer Mannheim, Indianapolis, IN) was added and colorimetric detection was performed over a 1 hr period using an EL808 automated microplate reader with a 405 nm filter (BIO-TEK, Winooski, VT). The DeltaSoft 3 computer analysis program (BioMetallics, Princeton, NJ) calculated the concentration of IgM in each sample from a standard curve generated from the absorbance readings of known IgM concentrations.

#### VII. Whole Cell Lysate Protein Preparation

Livers were perfused with HEDGM (25 mM HEPES (pH 7.5), 1 mM EDTA, 2 mM DTT, 10% (v/v) glycerol, 20 mM sodium molybdate), through the portal vein, isolated, pooled, and minced in buffer. The last wash was passed through a cheesecloth and 1.5 (w/v) of HEDGM/LAP (HEDGM with 100 μM leupeptin, 40 U/ml aprotinin, and 200 μM PMSF) was added. The sample was homogenized and centrifuged at 21,000 x g; supernatant was collected and then centrifuged at 105,000 x g. Single spleen cell

suspensions without red blood cells were prepared as previously described (161). Briefly, splenocytes were carefully removed from the splenic capsule, washed once with complete media (10% BCS) and treated with Gey's solution (5 ml Gey's per 1x10<sup>8</sup> cells) for 3 minutes on ice to lyse the RBCs. Gey's solution was then removed by diluting with complete media (10% BCS) and centrifuging at 200 x g for 10 min at 4°C. Cells were then washed once more in complete media (10% BCS). After the last wash, one cell volume of HEDM/LAP was added and the cells were homogenized with a tight fitting pestle. An equal volume of HED2GM/LAP (HEDM/LAP with 20% glycerol) was added and centrifuged at 105,000 x g for 1 hr at 4°C.

Whole cell lysates from CH12.LX, BCL-1 and Hepa 1c1c7 cells were prepared in HEDGM/LAP, homogenized and centrifuged as above. Hepa 1c1c7 cells were first removed from tissue culture flasks with 0.5 M EDTA in PBS. The supernatant was aliquoted and stored at -80°C prior to use in the western and slot blot analysis. Protein concentrations were determined by the bicinchoninic acid (BCA) protein assay (Sigma, St. Louis, MO).

#### VIII. Western Blot Analysis

Cell lysate proteins were resolved by denaturing SDS-polyacrylamide gel electrophoresis (PAGE) with 7.5% polyacrylamide (National Diagnostics, Atlanta, GA). The electrophoresed proteins were transferred to nitrocellulose (Amersham, Arlington Heights, IL). Protein blots were blocked in BLOTTO buffer [5% low fat dry milk in 0.1% Tween-20:tris-buffered saline (TBS)] for 1-2 hr at 22°C. Primary antibodies to the AhR (17-10B) and ARNT protein (20-9B), previously characterized by Pollenz *et al.*, (111), were a generous gift of Dr. Richard S. Pollenz (Medical University of South Carolina). Immunochemical staining was carried out as previously described (111). The AhR antibody and the ARNT antibody were diluted to 1 μg/ml in antibody dilution buffer [0.1%

ficoll, 0.1% polyvinylpyrrolidone, 0.05% gelatin, 0.1% Nonidet p-40, and 0.5% bovine serum albumin (BSA) in borate buffered saline]. Detection was performed using the ECL method (Amersham, Arlington Heights, IL). The relative intensity for the protein of interest was measured by densitometry using a model 700 imaging system (Bio Rad) and was derived from the adjusted volume [optical density (OD) times the area].

## IX. Slot Blot Analysis

Varying amounts of whole cell protein lysates were directly filtered onto nitrocellulose membranes using a Bio-Dot SF microfiltration apparatus (Bio-Rad, Hercules, CA). The same procedures used in the Western blot analysis were employed for the detection of AhR and ARNT proteins in the slot blots. The negative control consisted of cell lysates which were incubated with the secondary antibody but not with the primary antibody. Slot blots were analyzed by densitometry as described above.

#### X. Nuclear Protein Preparation

Single spleen cell suspensions without red blood cells were prepared as described above. Splenocytes, Hepa1c1c7 cells, CH12.LX cells or BCL-1 cells were incubated with DMSO (0.01%) or 30 nM TCDD in DMSO for 1 hr at 37°C then harvested by centrifugation at 1,200 rpm for 10 min. Hepa1c1c7 cells were first removed from culture flasks with 0.5 M EDTA in PBS. Following centrifugation, the cells were washed once with 1x PBS, then incubated in 10 mM HEPES (pH 7.5) for 5 min on ice, and centrifuged at 1,200 rpm for 5 min. One ml of MDH/LAP (3 mM MgCl<sub>2</sub>, 1 mM DTT, 25 mM HEPES, 100 μM leupeptin, 40 U/ml aprotinin, and 200 μM PMSF) was added to the cell pellet and homogenized with a tight fitting pestle. Nuclei were pelleted by centrifuging at 1000 X g for 5 min, washed twice with MDHK/LAP (3 mM MgCl<sub>2</sub>, 1 mM DTT, 25 mM

HEPES, 100 mM KCL, 100 μM leupeptin, 40 U/ml aprotinin, and 200 μM PMSF), then resuspended in 100 μl of HEDGK/LAP (25 mM HEPES, 1 mM EDTA, 1 mM DTT, 10% glycerol, 400 mM KCl, 100 μM leupeptin, 40 U/ml aprotinin, and 200 μM PMSF), incubated on ice with agitation for 40 min and centrifuged at 14,000 X g for 15 min. The supernatant was aliquoted and stored at -80°C prior to use in the EMSA. Protein concentrations were determined using the BCA protein determination assay (Sigma, St. Louis, MO).

## XI. Electrophoretic Mobility Shift Assay

## A. Analysis of Protein-DNA Complexes

Nuclear protein preparations were used in the EMSA as previously described (113, 119) with a few modifications. Briefly, nuclear extracts (6 μg of protein for the Hepa 1c1c7 and splenocyte experiments and 10 ug of protein for the CH12.LX and BCL-1 experiments) were incubated with poly(dI-dC) (Boehringer Mannheim Biochemicals, Indianapolis, IN) at room temperature for 15 min. Radiolabeled DRE3, 3'αE(hs1,2) or 3'α-hs4 oligomer was added (80,000 cpm for the Hepa 1c1c7 and splenocyte experiments and 40,000 cpm for the CH12.LX and BCL-1 experiments) and incubated at room temperature for another 30 min. Final reaction concentrations for the Hepa 1c1c7 cells were as follows 25 mM HEPES (pH 7.5), 1 mM EDTA, 2 mM DTT, 10% glycerol, 110 mM KCl, and 1.8 μg poly(dI-dC). The splenocyte reaction mixture was identical to that used for the Hepa1c1c7 cells with the exception of the poly (dI-dC) concentration (0.4 μg). The CH12.LX and BCL-1 reaction mixtures were also identical to that used for the Hepa1c1c7 cells with the exception of the KCL concentration (108 mM) and the poly (dI-dC) concentration (1.0 μg). Where indicated, 50- to 100- fold excess of unlabeled DRE3, 3'αE(hs1,2) or 3'α-hs4 oligomer was added to the reaction. Binding of protein to the

DNA was resolved by a 4.0% nondenaturing PAGE gel, dried on 3MM filter paper (Whattman, Hillsboro, OR) and autoradiographed.

#### B. Synthetic DRE Oligonucleotides

Complementary pairs of synthetic DNA fragments corresponding to the AhR/ARNT binding site of mouse DRE3 (162), to two putative DRE sites in the mouse Ig 3'α enhancer, 3'αE(hs1,2) (TAGGGGTCTATTAACTCACCACGCTAGGCCATC ATGGAGAG; positions 1096-1136) (GenBank accession No. X62778, 20) and 3'α-hs4 (AGCAGAGGGGGGGACTG GCGTGGAAAGCCCCATTCACCCAT; position 319-360) (GenBank accession No. L39932, 24) and to the κB site from the 3'α-hs4 enhancer (hs4-κB; GATCTCTCTGGAAAGCCCCTCTGA) were synthesized using an Applied Biosystems DNA synthesizer and purified by HPLC (Macromolecular Structure Facility, MSU). The DRE oligonucleotides were annealed by heating equal concentrations of the sense and antisense strands at 88°C for 5 min and allowing the mixture to cool slowly at room temperature. The double-stranded oligomer was then end labeled using T4 polynucleotide kinase (Boehringer Mannheim Biochemicals, Indianapolis, IN) and [γ-32P]ATP (Dupont NEN, Boston, MA).

## XII. EMSA-Western Analysis

EMSA analysis was conducted as described above but included samples containing 10 pmol of cold DRE3, 3'αE(hs1,2) or 3'α-hs4 instead of radiolabeled oligomers. The nonradiolabeled portion of the EMSA gel was separated from the radiolabeled portion and transferred to nitrocellulose (Amersham, Arlington Heights, IL). Protein blots were blocked in BLOTTO buffer (1% low fat dry milk in 0.1% Tween-20 TBS) for 1-2 hr at 22°C. Primary antibody to the AhR (17-10B), previously characterized by Pollenz et al.

(111), was a generous gift of Dr. Richard S. Pollenz (Medical University of South Carolina). The ARNT antibody (NB 100-110) was purchased from Novus Biological (Littleton, CO). RelA (p65), p50 (NF-kB1), RelB, and c-rel antibodies were purchased from Santa Cruz Biotechnology (Santa Cruz, CA). Immunochemical staining was performed as described above for the Western analysis. Optical density for the protein of interest was measured by densitometry using a model 700 imaging system (Bio Rad).

## XIII. Statistical Analysis of Data

The mean  $\pm$  S.E.M. was determined for each treatment group of a given experiment. Where indicated, the statistical difference between treatment groups and the vehicle controls was determined by Dunnett's two-tailed *t*-test. For EC<sub>50</sub> and IC<sub>50</sub> generation, a complete concentration-response curve for TCDD, HxCDD, and TriCDD was obtained for a given endpoint. Concentration-response curves were fit by a four parameter logistic concentration-response equation given as  $Y=[A_1-A_2)/[1+(X-X_0)^P]]+A_2$ . The derived parameter, EC<sub>50</sub> or IC<sub>50</sub> (X<sub>0</sub>; concentration generating half-maximal response) was expressed as nM (mean  $\pm$  S.E.M). Statistical difference between EC<sub>50</sub> and IC<sub>50</sub> means was determined by a 1-way ANOVA followed by a least significant difference test. P<0.05 was considered statistically significant.

#### **EXPERIMENTAL RESULTS**

## I. Identification of AhR and ARNT in B6C3F1 mouse splenocytes

## A. Northern blot analysis of mouse splenocytes

Transcripts for the *Ahr* and *Arnt* have been identified in rat spleen by ribonuclease protection analysis (163). The purpose of the following studies was to determine if *Ahr* and *Arnt* were also expressed in splenic RNA isolated from B6C3F1 mice. Liver RNA from the same mouse strain was isolated as a comparative control since the AhR and its putative mechanism of action have been primarily studied using hepatic tissue and hepatic cell lines. Northern analysis for the AhR using a 1.87 kb mouse cDNA probe identified a transcript of approximately 6.6 kb in mouse spleen and liver (Figure 3A). Splenocytes devoid of connective tissue were examined by Northern analysis for the AhR to address the possibility that the transcripts observed from the spleen may have originated primarily from the connective tissue encapsulating the spleen. Transcripts detected in the splenocytes matched the liver control (Figure 3B). Northern analysis using a radiolabeled 75 base oligomer synthesized from human cDNA for ARNT (122) revealed three transcripts of approximately 5.6 kb, 2.0 kb and 1.1 kb in both the spleen and liver (Figure 3C).

## B. Western blot analysis of mouse splenocytes

Based on the identification of transcripts for both the Ahr and Arnt in mouse splenocytes, Western blot analysis was conducted on whole cell lysates prepared from splenocytes devoid of connective tissue and red blood cells. Antibodies to the AhR revealed two major proteins of approximately 95 kDa and 104 kDa in splenocytes and liver (Figure 4A). These two sizes correspond, respectively, to the codominant expression of

Figure 3. Northern blot analysis of Ahr and Arnt mRNA expression in splenocytes and liver. Using a guanidium isothiocyanate method, total RNA was extracted from the whole spleen, spleen without splenic capsule and liver. Poly(A) RNA was isolated from the total RNA using the PolyATtract mRNA isolation system. Poly(A) RNA from the spleen (6  $\mu$ g, A and C), the spleen without capsule (6  $\mu$ g, B), and liver (2  $\mu$ g, A, B and C) was loaded onto a 1.0% formaldehyde gel and electrophoresed at 100 volts for 4 hr. The gel was blotted onto a nylon membrane and hybridized with either a  $^{32}$ P-labeled 1.87 kb fragment from the cloned mouse Ahr (A and B) or a  $^{32}$ P-labeled 75 base oligomer synthesized from human cDNA for Arnt (C). These figures are representative of at least two separate experiments.

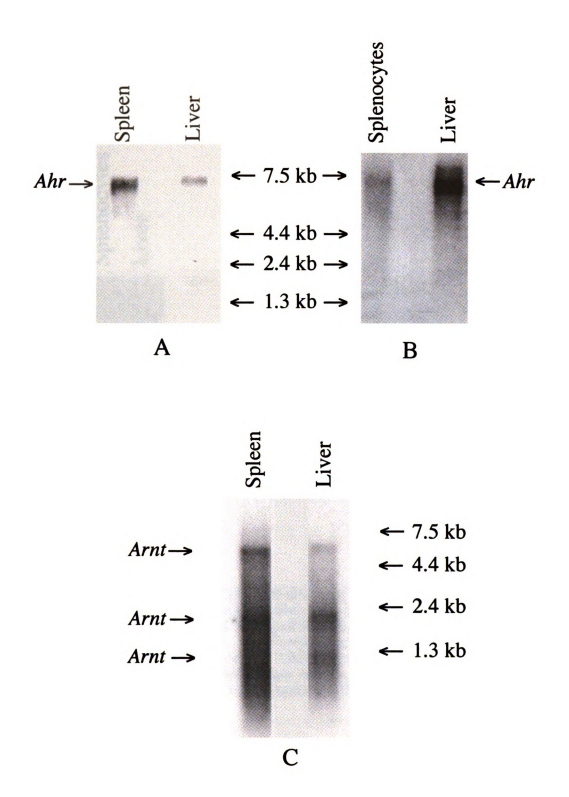


Figure 3. Northern blot analysis of Ahr and Arnt mRNA expression in splenocytes and liver.

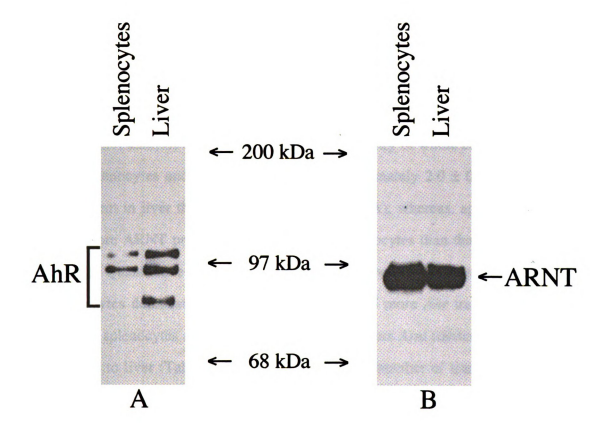


Figure 4. Western blot analysis of the AhR and ARNT in splenocytes and liver. Protein was isolated from whole cell lysates of splenocytes (devoid of splenic capsule and red blood cells) or liver. One hundred micrograms of protein was loaded in each lane and resolved on 7.5% SDS-PAGE gels, transferred to nitrocellulose, and incubated with 2 µg/ml of anti-AhR, 17-10B (A) or anti-ARNT, 2-0-9B (B). Antibody binding was visualized by staining the blot with donkey anti-rabbit horseradish peroxidase-linked immunoglobulins. These figures are representative of more than three separate experiments.

the  $Ah^{b-1}$  (C57BL/6) and  $Ah^{b-2}$  (C3H) alleles in the B6C3F1 (C57BL/6 x C3H) mice (164). An approximately 70 kDa protein, previously identified as a proteolytic fragment of the 95 kDa AhR in C57BL/6 mice (165), was detected in lysates prepared from liver of the B6C3F1 mice. Antibodies to ARNT identified an approximately 87 kDa protein in both tissues (Figure 4B).

## C. Slot blot and quantitative RT-PCR analysis of mouse splenocytes

Slot blot analysis and quantitation by densitometry of whole cell lysates prepared from the splenocytes and liver demonstrated approximately  $2.0 \pm 0.5$ -fold more AhR protein present in liver than in splenocytes (Figure 5A); whereas, approximately  $2.4 \pm 0.05$ -fold more ARNT protein was identified in splenocytes than that observed in liver (Figure 5B). Quantitative comparisons by RT-PCR of the Ahr and Arnt transcripts in liver and splenocytes demonstrated approximately 2.3-fold more Ahr transcripts in liver as compared to splenocytes and approximately 3.2-fold more Arnt transcripts in splenocytes as compared to liver (Table 1). In addition, a greater number of transcripts for Arnt as compared to Ahr were identified in both the liver and splenocytes (Table 1).

## D. EMSA analysis of mouse splenocytes

With the identification of both the AhR and ARNT proteins in splenocytes, the functionality of these proteins was assessed by EMSA. Hepa 1c1c7 cells served as a comparative control since this cell line has been extensively characterized with respect to the induction by TCDD of AhR nuclear translocation, dimerization with ARNT and DRE binding of the ligand-AhR/ARNT nuclear complex. Following a 2 hr treatment of Hepa 1c1c7 cells or splenocytes with 30 nM TCDD, the AhR nuclear complex was confirmed to be functional in both nuclear preparations as demonstrated by its ability to bind to the DRE

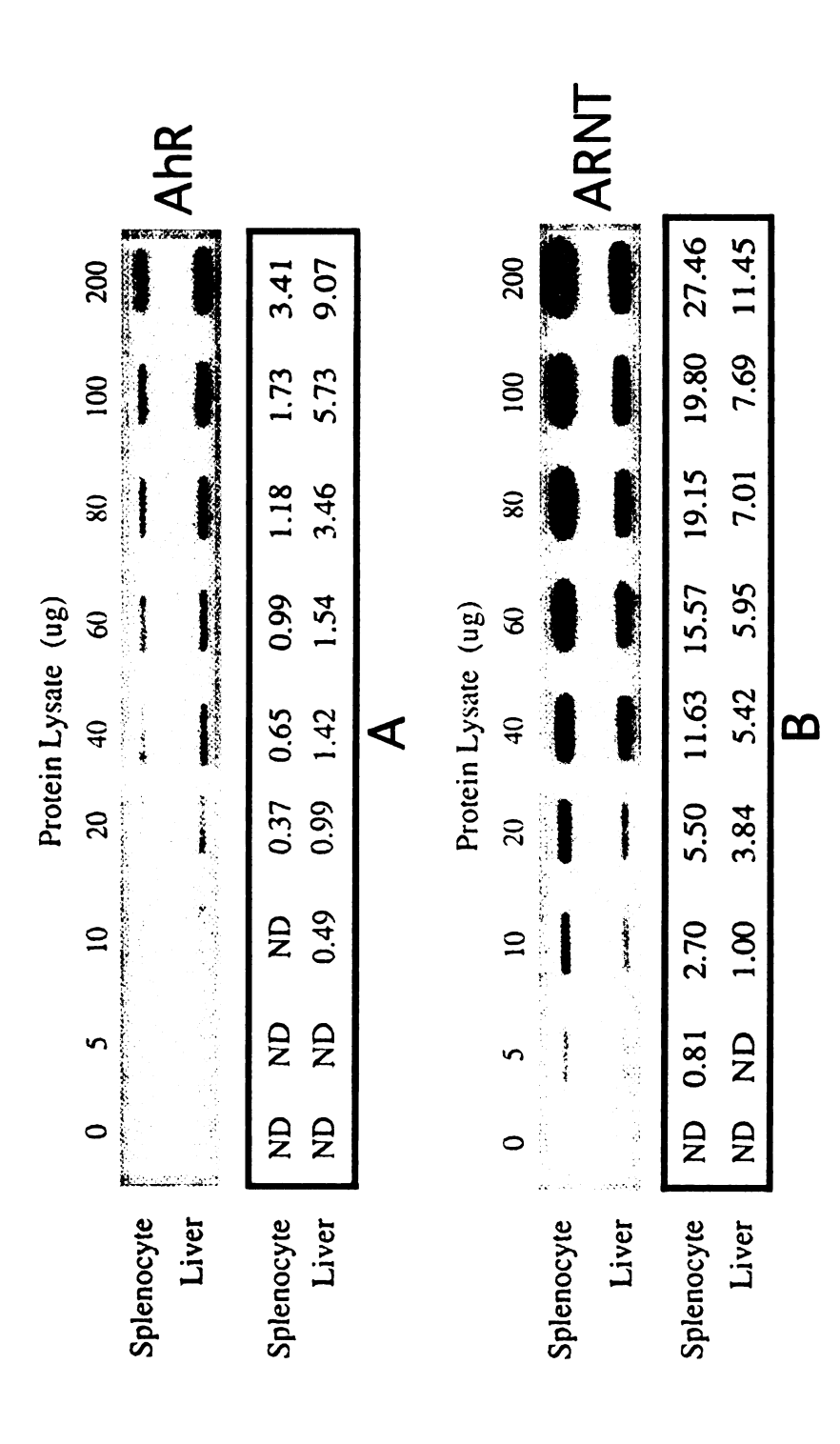


Figure 5. Slot blot analysis of the AhR and ARNT in splenocytes and liver. Increasing concentrations of protein from whole cell lysates ARNT, 20-9B (B). Antibody binding was visualized by staining the blot with donkey anti-rabbit horseradish peroxidase-linked immunoglobulins. Slot blots were analyzed using a densitometer. The table contains values derived from adjusted volume (O.D. x area) and reflect the relative intensity of each band. The regression coefficient was A) 0.996 and 0.957; and B) 0.955 and 0.987 for spleen were directly filtered onto a nitrocellulose membrane. The membrane was incubated with 2 ug/ml of anti-AhR, 17-10B (A) or antiand liver, respectively. These figures are representative of two separate experiments.

Table 1: Quantitative analysis of Ahr and Arnt mRNA as determined by RT-PCR.

<sup>a</sup>mean ± SE of molecules of target gene RNA/100 ng tissue RNA from three separate RNA isolations (n=3).

motif. This is shown in Figure 6, lane 3 for TCDD-treated Hepa 1c1c7 cells and in lane 5 for TCDD-treated splenocytes. Denison and Yao (162) have identified a constitutive protein-single-stranded DNA complex that migrates faster than the TCDD-inducible protein-DNA complex. We similarly observed this same constitutive complex in nuclear protein preparations from Hepa 1c1c7 cells and splenocytes (Figure 6, complex labeled C in lanes 2, 3, and 5). However, the gel retardation pattern observed with the TCDD-treated splenocytes was different from that observed with the Hepa 1c1c7 cells in that the TCDD-inducible protein-DNA complex resolved as a rather broad band in comparison to the complex formed in Hepa 1c1c7 cells (Figure 6, band labeled A and B in lane 5). Addition of excess unlabeled DRE abrogated the TCDD-induced mobility shift indicating binding specificity of the AhR nuclear complex for the DRE (Figure 6, lanes 6).

# II. Characterization of the AhR and ARNT in the CH12.LX and BCL-1 B-cell lines

## A. AhR and ARNT expression in two B-cell lines

Western analysis for the AhR and ARNT was performed using whole cell lysates from the CH12.LX and BCL-1 B-cell lines. Interestingly, an approximately 95 kDa AhR was markedly expressed in CH12.LX cells but was not detected in BCL-1 cells (Figure 7A). The 87 kDa ARNT protein was expressed in both B-cell lines (Figure 7B). To confirm a lack of AhR expression in BCL-1 cells, total RNA isolated from BCL-1 cells was analyzed by qualitative RT-PCR analysis, a more sensitive technique than Western analysis. In agreement with the above results, Ahr transcripts were not detected in BCL-1 RNA (Figure 8A). Quantitative RT-PCR analysis of basal Ahr and Arnt transcripts demonstrated a much greater expression of Arnt in CH12.LX cells as compared to Ahr

Figure 6. Binding of Hepa 1c1c7 or splenocyte nuclear proteins to a DRE. Six micrograms of nuclear protein from Hepa 1c1c7 cells (Hepa), vehicle (lane 2) or TCDD-treated (lane 3), or from B6C3F1 splenocytes, vehicle (lane 4) or TCDD-treated (lanes 5 and 6), were incubated with a <sup>32</sup>P-labeled, 26 bp DRE oligonucleotide. Protein-DNA complexes were resolved by EMSA. Unlabeled competitor DRE oligonucleotide was added at a 50-fold excess (lane 6) to show specific interaction of the proteins with the DRE oligonucleotide. Lane 1 is the labeled oligonucleotide without nuclear protein. Letters A and B identify TCDD-inducible protein-DNA complexes and letter C identifies constitutive protein-single-stranded DNA complexes. This figure is representative of more than three separate experiments.

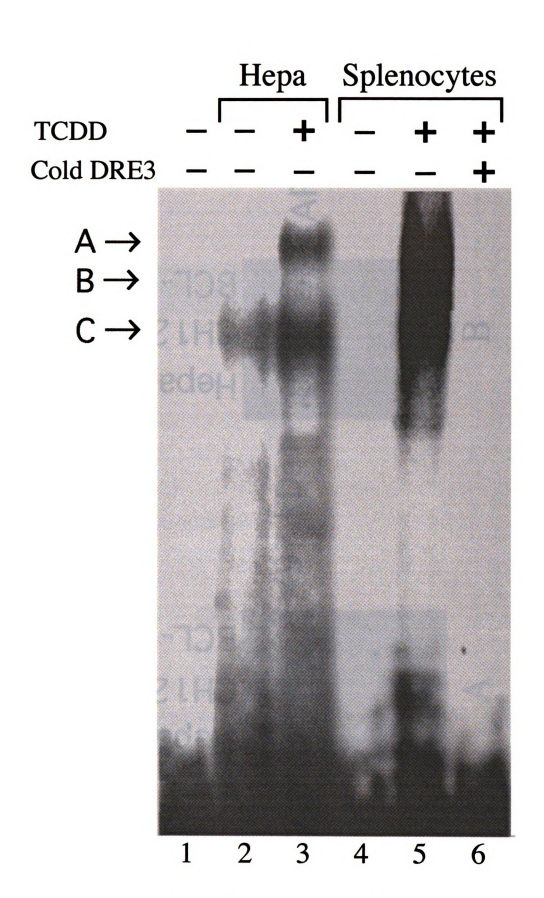
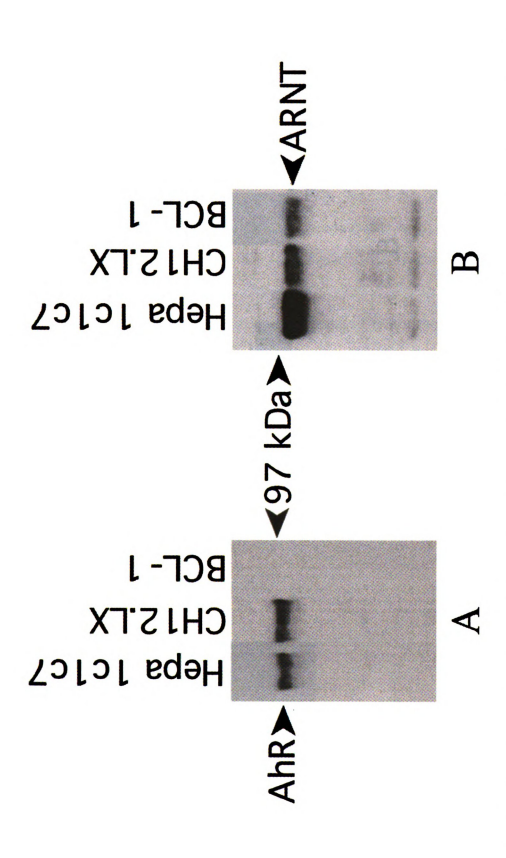


Figure 6. Binding of Hepa 1c1c7 or splenocyte nuclear proteins to a DRE.



control. Cell Iysate protein (70 µg) was loaded in each lane, resolved on a 7.5% SDS-PAGE gel and probed with (Å) I µg/ml anti-AhR antibody, and (B) I µg/ml anti-ARNT antibody. Results are representative of more than two separate experiments. Figure 7. Western blot analysis for the AhR and ARNT protein in the CH12.LX and BCL-1 cell lines. Whole cell lysate was isolated from untreated CH12.LX (5x10<sup>5</sup> cells/ml) and BCL-1 (5x10<sup>5</sup> cells/ml) cells. The Hepa 1c1c7 cells (5x10<sup>5</sup> cells/ml) served as a positive

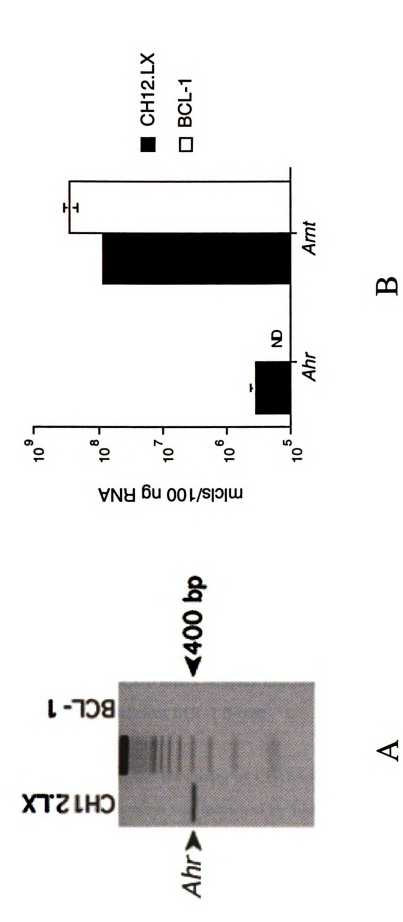


Figure 8. Basal expression of Ahr and Arnt transcripts in the CH12.LX and BCL-1 cell lines. Total RNA was extracted from untreated CH12.LX (5x105 cells/ml) and BCL-1 cells (5x105 cells/ml) and 100 ng of total RNA was analyzed by (A) qualitative RT-PCR analysis for Ahr or (B) quantitative RT-PCR analysis for Ahr and Arnt transcripts. Ahr and Arnt mRNA transcripts are represented on the y-axis as molecules (micls)/100 ng RNA. Samples in which transcripts were not detected were denoted ND. Each bar represents the mean and standard error for three separate RNA isolations (n=3). The results are representative of more than two separate experiments.

(Figure 8B). In addition, similar levels of *Arnt* transcripts were detected in BCL-1 cells as compared to CH12.LX cells (Figure 8B).

# B. AhR and ARNT regulate gene transcription in the CH12.LX B-cell line

"Functionality" of the AhR and ARNT was evaluated in CH12.LX cells by the ability of TCDD to induce Cyp1a1 expression. Unlike the EMSA, which is only an indicator of DRE binding, TCDD-induced upregulation of Cyp1a1 is an indicator of transcriptional regulation mediated by DRE binding, and thus is a more comprehensive indicator of AhR/ARNT function. Evaluation of Cyp1a1 gene expression by quantitative RT-PCR demonstrated a marked and rapid increase in Cyp1a1 transcripts following TCDD treatment. TCDD-induced Cyp1a1 expression occurred as early as 2 hr and was maximal by 8 h, remaining elevated throughout the time course (Figure 9A). Induction of Cyp1a1 in CH12.LX cells is also dose-dependent. An 8 hr treatment of TCDD at concentrations of 0.003, 0.03, 0.3 and 3.0 nM induced Cyp1a1 expression 14-, 38-, 44- and 120-fold, respectively, above the vehicle control (Figure 9B). BCL-1 cells were also analyzed for Cyp1a1 inducibility. As predicted because of the lack of AhR expression, Cyp1a1 transcripts were not detected by qualitative RT-PCR analysis in TCDD-treated BCL-1 cells (Figure 10).

# C. TCDD alters immune function in CH12.LX B-cells but not in AhR deficient BCL-1 B-cells

To assess the sensitivity of CH12.LX cells and BCL-1 cells to TCDD, LPS-induced IgM secretion was measured by ELISA. In primary B-cells TCDD has been previously shown to suppress IgM secretory responses to the polyclonal B-cell activator LPS (96-98, 149) and to soluble anti-IgM (101). LPS can induce CH12.LX and BCL-1

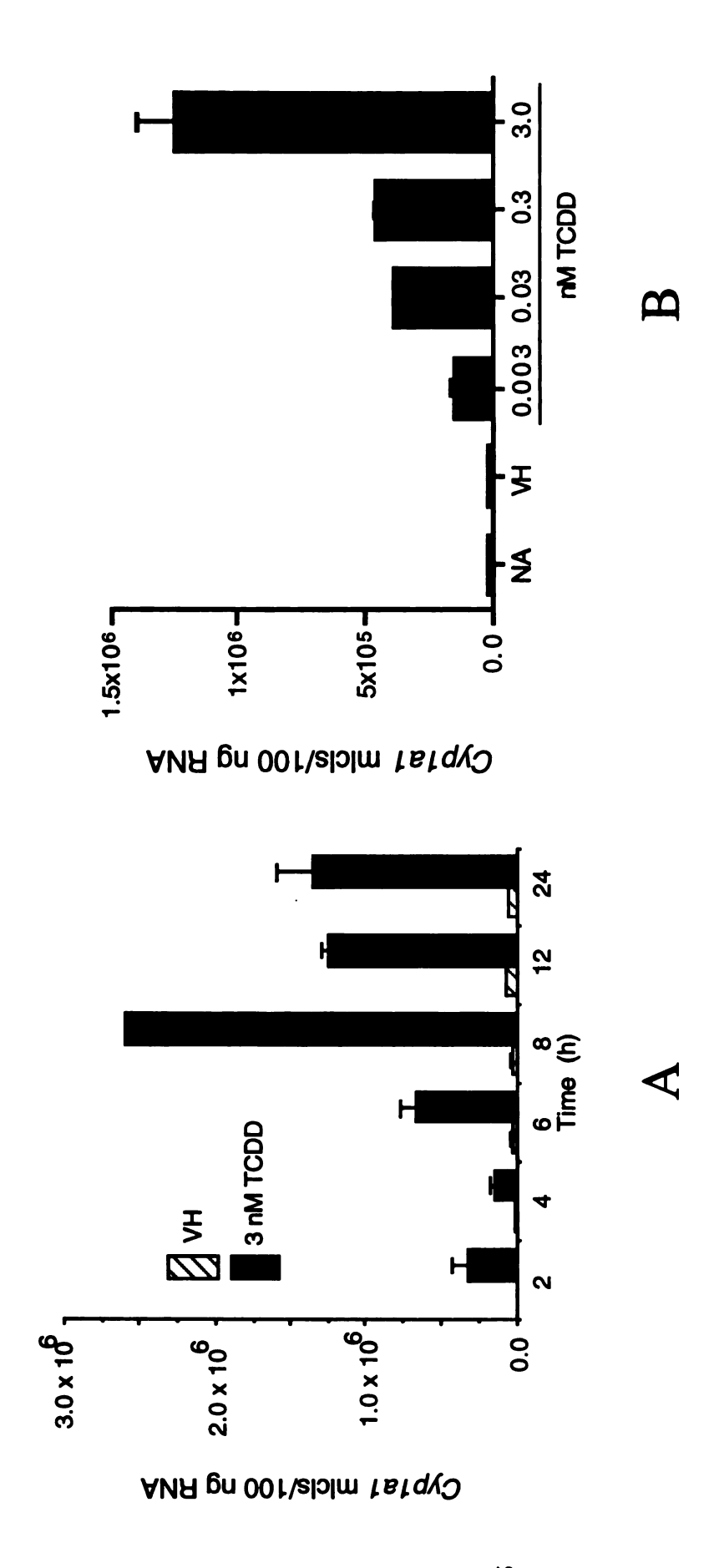


Figure 9. Dose response and time course of TCDD-induced Cyp1a1 induction in CH12.LX cells. CH12.LX cells (5x10<sup>5</sup> cells/ml) were treated with (A) 3.0 nM TCDD or vehicle (VH, 0.01% DMSO) for selected time points or (B) selected concentrations of TCDD or vehicle (0.01% DMSO) for 8 h. Quantitative RT-PCR analysis for Cyplal was performed on RNA extracted from each treatment group. Cyplal mRNA transcripts are represented on the y-axis as molecules (mlcls)/100 ng RNA. Bar, mean ± standard error for two separate RNA isolations (n=2). The results are representative of more than two separate experiments.

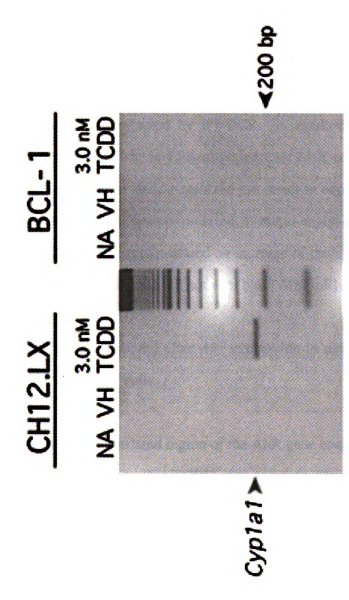


Figure 10. Effect of TCDD on Cyp1a1 induction in BCL-1 cells. BCL-1 (5x10<sup>5</sup> cells/ml) and CH12.LX (5x10<sup>5</sup> cells/ml) cells were treated with 3.0 ml TCDD or vehicle (VH, 0.0) is DMSO) for 24. Qualitative RT-PCR analysis for Cyp1a1 was performed on RNA extracted from each treatment group. Results are representative of more than two separate experiments.

cells to secrete IgM and treatment of CH12.LX cells with TCDD resulted in a marked inhibition of LPS-induced IgM secretion at concentrations as low as 0.03 nM TCDD (Figure 11). In contrast, LPS-induced IgM secretion in AhR-deficient BCL-1 cells was not inhibited at concentrations as high as 3.0 nM TCDD (Figure 12).

## D. Differential expression of AhR in LPS-differentiated CH12.LX B-cells

The effect of LPS-induced differentiation of the CH12.LX and BCL-1 cells on AhR gene expression was evaluated by RT-PCR. A marked upregulation of AhR gene expression occurred by 4 hr in LPS-activated CH12.LX cells (Figure 13). In contrast, LPS-induced activation of BCL-1 cells did not result in expression of the AhR gene (Fig 14). Consistent with AhR gene expression, Western analysis for the AhR protein in LPS activated CH12.LX cells demonstrated an increase in protein expression by 8 hr (Figure 15). In addition, LPS treatment did not alter basal *Arnt* mRNA expression (Figure 16).

# E. TCDD does not alter *Ahr* expression in naive or LPS-stimulated CH12.LX cells

Since the 5' untranslated region of the AhR gene contains a consensus DRE (166), we explored the possibility that TCDD may regulate Ahr expression. Naive and LPS-stimulated CH12.LX cells were evaluated by RT-PCR for Ahr expression. A 3.0 nM TCDD treatment did not alter Ahr expression in naive cells over a 24 hr time course (Figure 17). Likewise, TCDD did not alter the induction of AhR expression by LPS (Figure 18). It is notable that at the 6 and 8 hr timepoints there is an increase in Ahr expression in NA and LPS-stimulated CH12.LX cells which is more pronounced with the LPS stimulation and is not affected by TCDD treatment (Figures 17 and 18). This effect is probably related

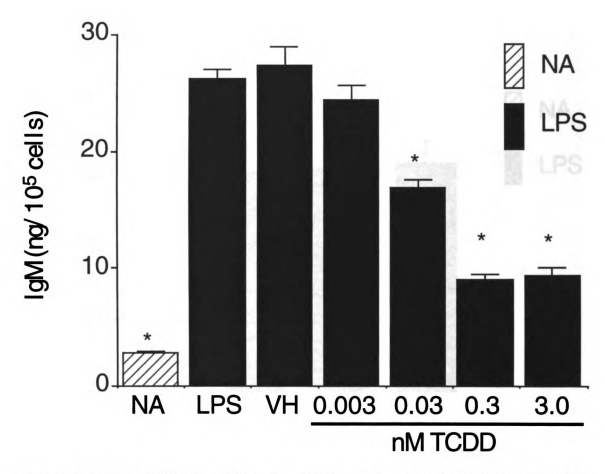


Figure 11. Effect of TCDD on LPS-induced IgM secretion in CH12.LX cell. CH12.LX cells (1x  $10^4$  cells/ml) were treated with LPS (30  $\mu$ g/ml) and selected concentrations of TCDD or vehicle (VH, 0.01% DMSO). Supernatants were harvested at 72 hr and analyzed for IgM by sandwich ELISA. Results from triplicate determinations are represented as mean IgM (ng/ $10^5$  cells)  $\pm$  standard error (n=3). These results were analyzed for statistical significance using Dunnett's two-tailed t-test. \*, values that are significantly different from the vehicle at P<0.05. The results are representative of more than three separate experiments.

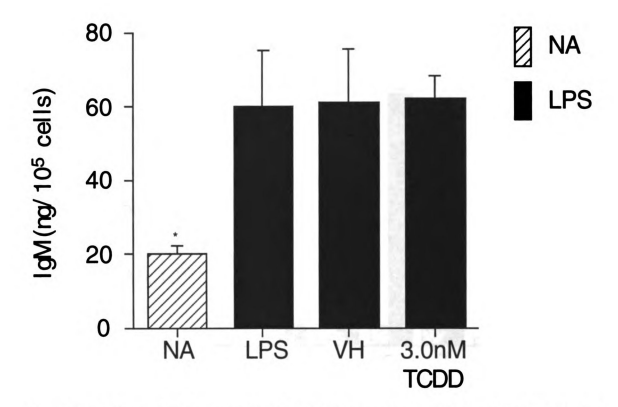


Figure 12. Effect of TCDD on LPS-induced IgM secretion in BCL-1 cells. BCL-1 cells  $(2x 10^4 \text{ cells/ml})$  were treated with LPS (30 μg/ml) and 3.0 nM TCDD or vehicle (VH, 0.01% DMSO). Supernatants were harvested at 72 hr and analyzed for IgM by sandwich ELISA. Results from triplicate determinations are represented as mean IgM  $(\text{ng/ml}) \pm \text{standard error } (n=3)$ . These results were analyzed for statistical significance using Dunnett's two-tailed t-test. \*, values that are significantly different from the vehicle at t-C0.05. The results are representative of more than three separate experiments.

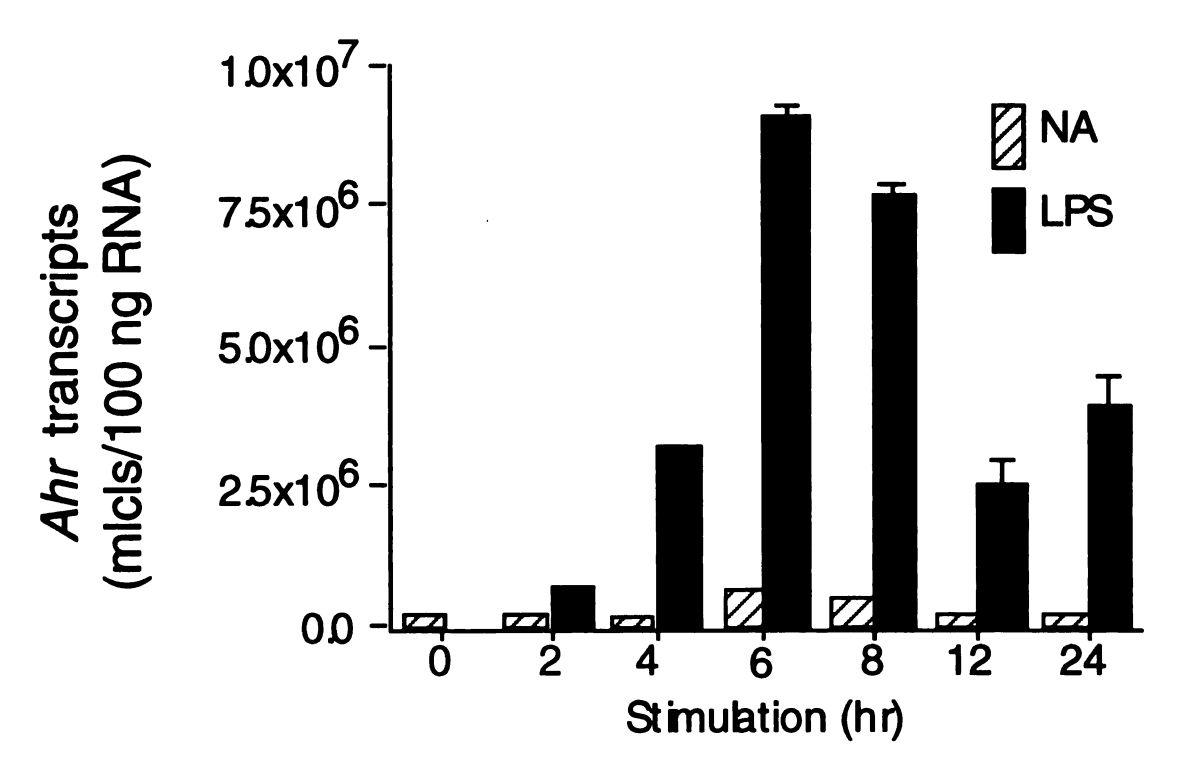


Figure 13. Effect of LPS-induced differentiation on Ahr expression in the CH12.LX cells. CH12.LX cells ( $5 \times 10^5$  cells/ml) were treated with LPS ( $30 \mu g/ml$ ) for selected time points. Quantitative RT-PCR analysis for Ahr was performed on RNA extracted from naive (NA) and LPS-stimulated cells at each time point. Ahr mRNA transcripts are represented on the y-axis as molecules(mlcls)/100 ng RNA. Bar, mean  $\pm$  standard error for two separate RNA isolations (n=2). The results are representative of more than two separate experiments.

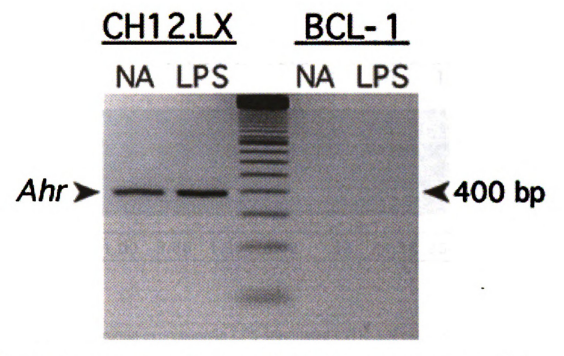


Figure 14. Ahr expression in LPS-stimulated CH12.LX and BCL-1 cells. CH12.LX  $(5x10^5 \text{ cells/ml})$  and BCL-1  $(5x10^5 \text{ cells/ml})$  cells were treated with LPS  $(30 \text{ }\mu\text{g/ml})$  for 6 hr. Qualitative RT-PCR analysis for Ahr was performed on RNA extracted from naive (NA) and LPS-stimulated cells. Results are representative of more than two separate experiments.

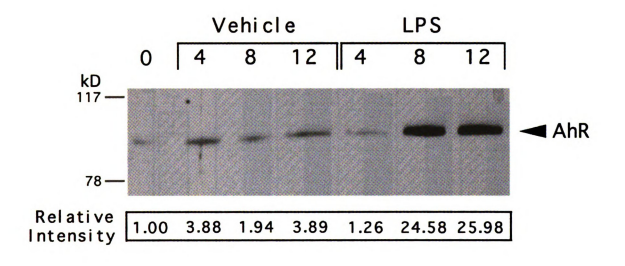


Figure 15. AhR protein expression in LPS-stimulated CH12.LX cells. CH12.LX cells  $(1x10^5 \text{ cells/ml})$  were treated with LPS  $(30 \, \mu g/\text{ml})$  for selected time points. Whole cell lysate was isolated from naive (NA) and LPS-stimulated cells at the selected time point. Cell lysate protein  $(12.5 \, \mu g)$  was loaded in each lane, resolved on a 7.5% SDS-PAGE gel and probed with 1  $\mu g/\text{ml}$  of the AhR antibody. The relative intensity for each band was derived from the adjusted volume  $(OD \, \text{times area})$ . Results are representative of more than two separate experiments.

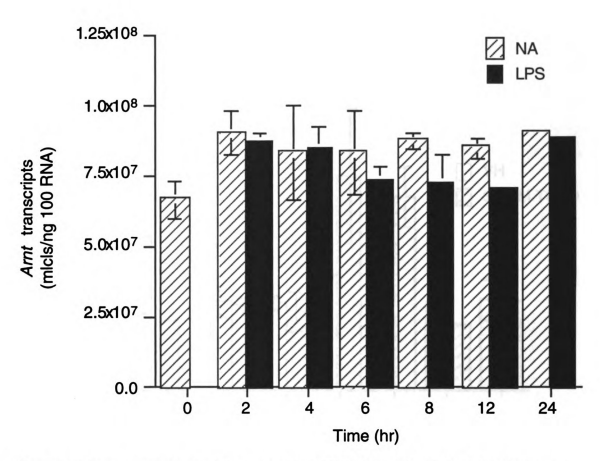


Figure 16. Arnt expression in LPS-stimulated CH12.LX cells. CH12.LX cells were treated with LPS (30 μg/ml) for selected time points. Quantitative RT-PCR analysis for Arnt was performed on RNA extracted from naive (NA) and LPS-stimulated cells (5x105 cells/ml) at each time point. Arnt mRNA transcripts are represented on the y-axis as molecules (mlc1)/100 ng RNA. Bar, mean ± standard error for two separate RNA isolations (n=2). The results are representative of more than two separate experiments.

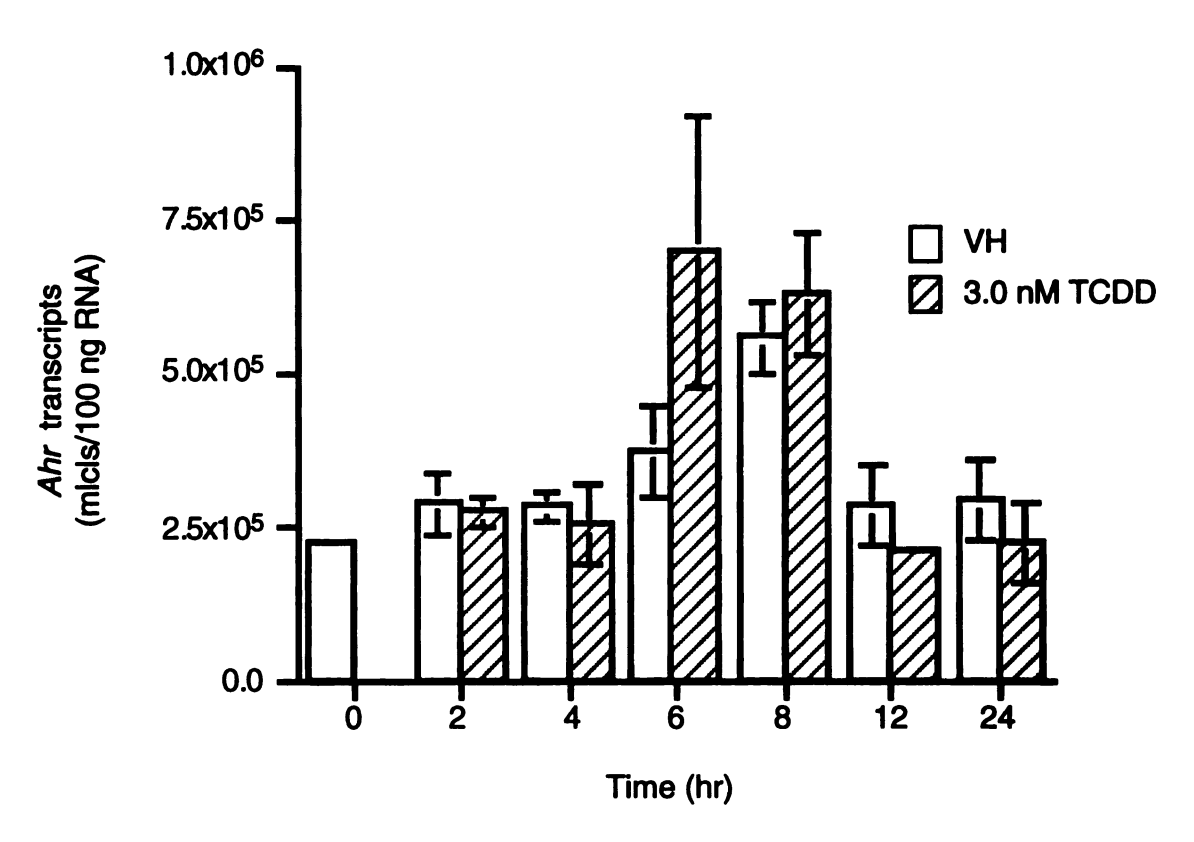


Figure 17. Effect of TCDD on Ahr expression in the CH12.LX cells. CH12.LX cells  $(5x10^5 \text{ cells/ml})$  were treated with 3.0 nM TCDD or vehicle (VH, 0.01% DMSO) for selected time points. Quantitative RT-PCR analysis for Ahr was performed on RNA extracted from each treatment group at each time point. Ahr mRNA transcripts are represented on the y-axis as molecules (mlcls)/100 ng RNA. Bar, mean  $\pm$  standard error for two separate RNA isolations. The results are representative of more than two separate experiments.

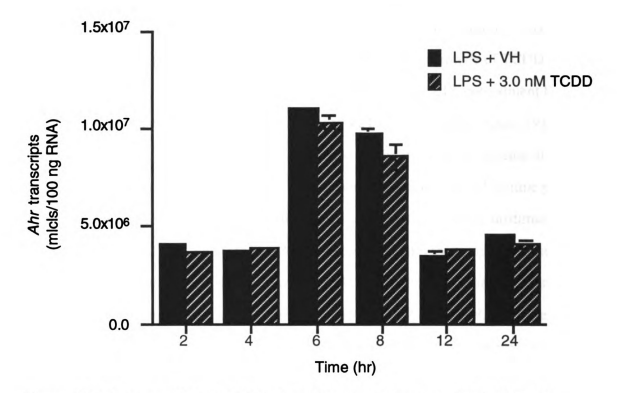


Figure 18. Effect of TCDD on LPS-induced Ahr expression in the CH12.LX cells. CH12.LX cells (5L05 cells/ml) were treated with LPS (30 µg/ml) and 3.0 nM TCDD or vehicle (VH, 0.01% DMSO) for selected time points. Quantitative RT-PCR analysis for Ahr was performed on RNA extracted from each treatment group at each time point. Ahr mRNA transcripts are represented on the y-axis as molecules (mlcls)/100 ng RNA. Bar, mean  $\pm$  standard error for two separate RNA isolations (n=2). The results are representative of more than two separate experiments.

to an initial lag period after cell seeding followed by normal progression through the cell cycle.

# F. Ahr upregulation does not enhance the sensitivity of activated CH12.LX cells to TCDD

If the AhR mediates the effects of TCDD, then perhaps an increase in AhR gene and protein expression following B-cell activation would enhance the sensitivity of B-cells to TCDD. To test this possibility, we evaluated the kinetics and magnitude of TCDD-induced Cyplal induction in naive and LPS-stimulated CH12.LX cells. LPS cotreatment had little effect on TCDD-induced Cyplal expression over a 24 hr time course (Figure 19). However, LPS-stimulation caused a slight decrease at 8 hr and a slight increase at 24 hr as compared to unstimulated cells (Figure 19). Further evaluation at the 24 hr time point demonstrated no difference in TCDD-induced Cyplal induction between unstimulated and LPS-stimulated CH12.LX cells (Figure 20). Since a 12 hr LPS treatment maximally increased AhR protein expression (Figure 15), CH12.LX cells were pretreated for 12 hr with LPS followed by an additional 12 hr treatment with 0.03 nM TCDD. A lower TCDD concentration (suboptimal for Cyplal induction) was used in this experiment to avoid the possibility that 3 nM TCDD might produce a maximum induction of Cyplal resulting in an inability to detect any additional LPS-induced changes. Again, no alteration in Cyp1a1 induction was observed above and beyond that produced by TCDD (Figure 21). However, it is notable that the fold-induction of Cyplal by 0.03 nM TCDD was much less than observed in previous experiments.

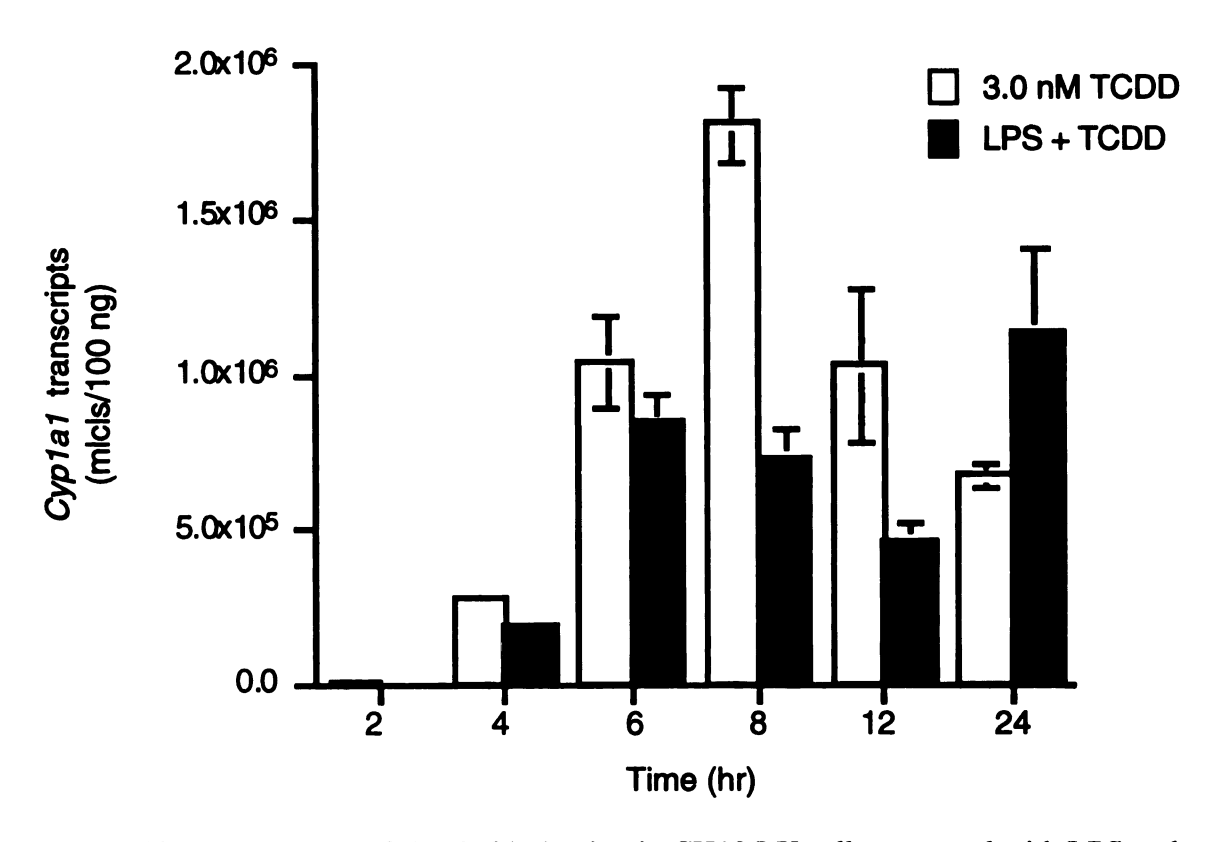


Figure 19. Time course of Cyp1a1 induction in CH12.LX cells cotreated with LPS and TCDD. CH12.LX cells  $(5x10^5 \text{ cells/ml})$  were treated with LPS  $(30 \mu g/\text{ml})$  and 3.0 nM TCDD or vehicle (VH, 0.01% DMSO) for selected time points. Quantitative RT-PCR analysis for Cyp1a1 was performed on RNA extracted from each treatment group at each time point. Cyp1a1 mRNA transcripts are represented on the y-axis as molecules (mlcls)/100 ng RNA. Bar, mean  $\pm$  standard error for two separate RNA isolations (n=2). The results are representative of more than two separate experiments.

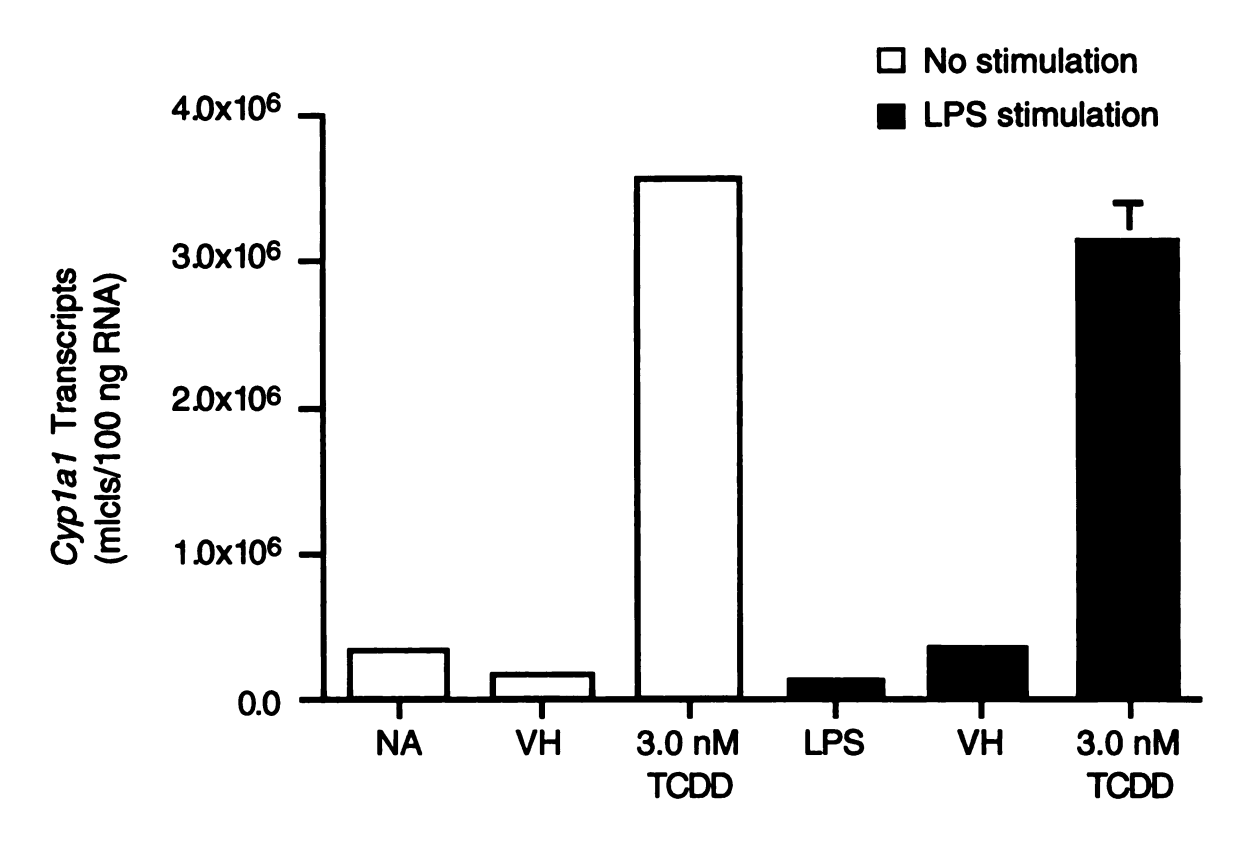


Figure 20. Effect of a 24 hr LPS cotreatment on TCDD-induced Cyp1a1 induction in CH12.LX cells. CH12.LX cells ( $5x10^5$  cells/ml) were treated with LPS ( $30 \mu g/ml$ ) and 3.0 nM TCDD or vehicle (VH, 0.01% DMSO) for 24 hr. Quantitative RT-PCR analysis for Cyp1a1 was performed on RNA extracted from each treatment group. Cyp1a1 mRNA transcripts are represented on the y-axis as molecules (mlcls)/100 ng RNA. Bar, mean  $\pm$  standard error for two separate RNA isolations (n=2). The results are representative of more than two separate experiments.

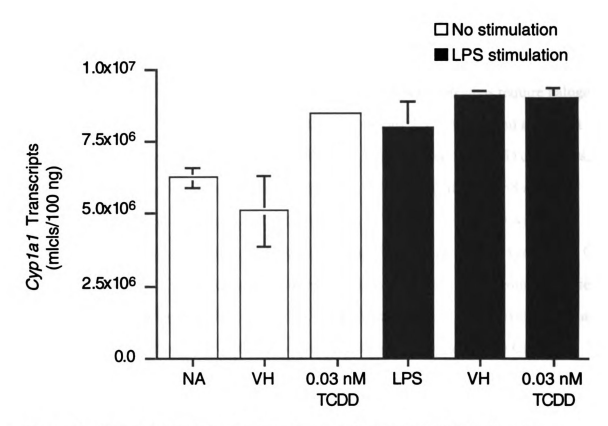


Figure 21. TCDD-induced Cyp1a1 induction in LPS pretreated CH12.LX cells. CH12.LX cells ( $5x10^5$  cells/ml) were pretreated for 12 hr with LPS (30 µg/ml) followed by an additional 12 hr incubation with 0.03 nM TCDD or vehicle (VH, 0.01% DMSO). Quantitative RT-PCR analysis for Cyp1a1 was performed on RNA extracted from each treatment group. Cyp1a1 mRNA transcripts are represented on the y-axis as molecules (mlcls)/100 ng RNA. Bar, mean  $\pm$  standard error for two separate RNA isolations (n=2). The results are representative of more than two separate experiments.

### III. The SAR of several PCDD-mediated endpoints and AhR binding affinity

A. PCDD-mediated inhibition of LPS-induced IgM secretion in CH12.LX B-cells follows a SAR which is concordant with AhR ligand binding affinity and Cypla1 induction

As discussed previously, transcriptional regulation through an AhR/DRE mechanism of TCDD-induced Cyplal expression is well established (76, 167-169). PCDD congeners that bind to the AhR and upregulate metabolic enzymes require halogen atoms in at least three of the lateral ring positions (positions 2,3,7, and 8) and require at least one unsubstituted ring position (170). For the following specific PCDD congeners, previous reports have determined the rank order for AhR binding affinity and AhRdependent induction of Cyplal, as TCDD > HxCDD > TriCDD >> MCDD with the MCDD congener having no affinity for the AhR and unable to induce 7-ethoxyresorufin Odeethylase (EROD) (171) which is a measure of CYP1A1 activity. The binding affinities (kd) for TCDD, HxCDD and TriCDD are 0.034, 0.77 and 1.92 nM, respectively (171 and personal communication, A. Poland). Likewise, induction of Cyplal in the CH12.LX cells following a 24 hr incubation with the PCDD congeners was concentration-dependent, as determined by quantitative RT-PCR, and correlated with AhR binding affinity (Figure 22). The rank order potency was TCDD > HxCDD > TriCDD >> MCDD; MCDD had no effect on Cyp1a1 expression (Table 2). To further characterize the AhR-dependency of TCDD-induced IgM secretion, the effect of these congeners on LPS-induced IgM protein secretion from the CH12.LX B-cell line was examined by ELISA. Inhibition of IgM secretion was concentration-dependent and correlated with AhR binding affinity (Figure 23). Similar to the results for Cyplal induction, the rank order potency was TCDD > HxCDD > TriCDD >> MCDD; again, MCDD had no affect on IgM secretion (Table 2).

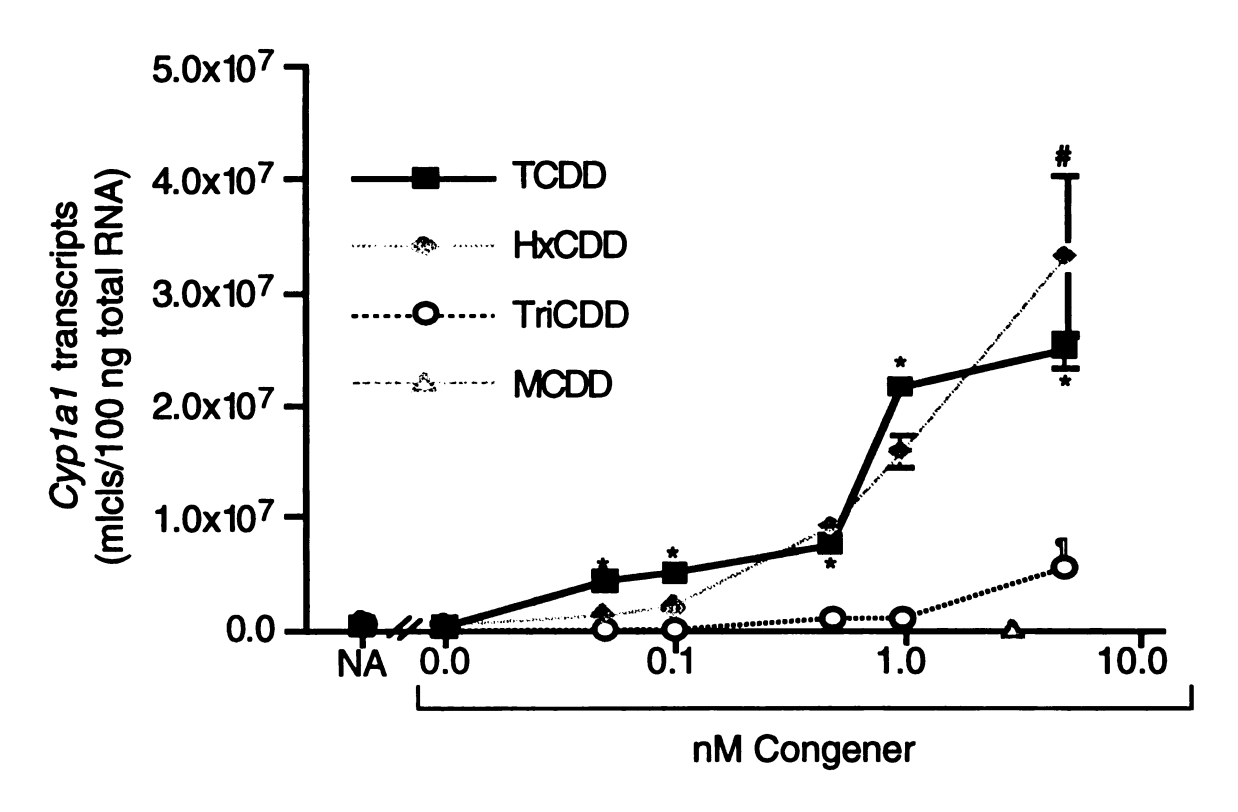


Figure 22. Concentration-dependent effect of selected chlorinated dibenzo-p-dioxin congeners on Cyplal expression in CH12.LX cells. CH12.LX cells ( $1x10^5$  cells/ml) were treated with TCDD, HxCDD, TriCDD and MCDD at various concentrations. The vehicle control (0.0 nM congener) was 0.01% DMSO. Quantitative RT-PCR analysis for Cyplal was performed on RNA extracted at 24 hr from each treatment group. Cyplal mRNA transcripts are represented on the y-axis as molecules (mlcls)/100 ng RNA. Symbol, mean  $\pm$  standard error for three separate RNA isolations (n=3). These results were analyzed for statistical significance using Dunnett's two-tailed t-test. \*, # and ¶, values that are significantly different from the VH control within the TCDD, HxCDD and TriCDD experiments, respectively, at P<0.05. The results are representative of more than two separate experiments.

Table 2: Congener specific IC<sub>50</sub> for inhibition of LPS-induced μ expression and protein secretion or EC<sub>50</sub> for induction of Cyplal.

| IgM secretion    | (n=4)       | (n=4) \$    | (n=4) ‡     |
|------------------|-------------|-------------|-------------|
| IC <sub>50</sub> | 0.065±0.021 | 0.343±0.090 | 1.263±0.261 |
| μ/48hr           | (n=5)       | (n=6)       | (n=5) #\$   |
| IC50             | 0.194±0.082 | 0.488±0.067 | 3.046±0.775 |
| μ/24hr           | (n=5) *     | (n=3)       | N. D.       |
| IC50             | 0.536±0.139 | 0.617±0.432 |             |
| Cyplal           | (n=4) a     | (n=4) ¶     | (n=3) ¶     |
| ECso             | 0.072±0.014 |             | 0.983±0.082 |
| Congener         | TCDD        | HxCDD       | TriCDD      |

determined by a 1-way ANOVA followed by a least significant difference test. P<0.05 was considered statistically significant. N. D. denotes <sup>a</sup>EC<sub>50</sub>'s and IC<sub>50</sub>'s (concentration generating half-maximal response) are represented as nM (Mean±SEM) and were generated from extensive concentration response curves that were fitted by a four parameter logistic curve. Statistical difference between EC<sub>50</sub> and IC<sub>50</sub> means was "not detected".

<sup>\*</sup>Significance compared to all other endpoints for TCDD.

<sup>#</sup>Significance compared to Cyplal EC<sub>50</sub> for TriCDD.

Significance compared to the Cyplal EC<sub>50</sub> for TCDD.

Significance compared to µ/48hr IC<sub>50</sub> for TCDD and HxCDD.

<sup>&</sup>lt;sup>‡</sup>Significance compared to IgM IC<sub>50</sub> for TCDD and HxCDD.

Significance compared to IgM IC<sub>50</sub> for TCDD.

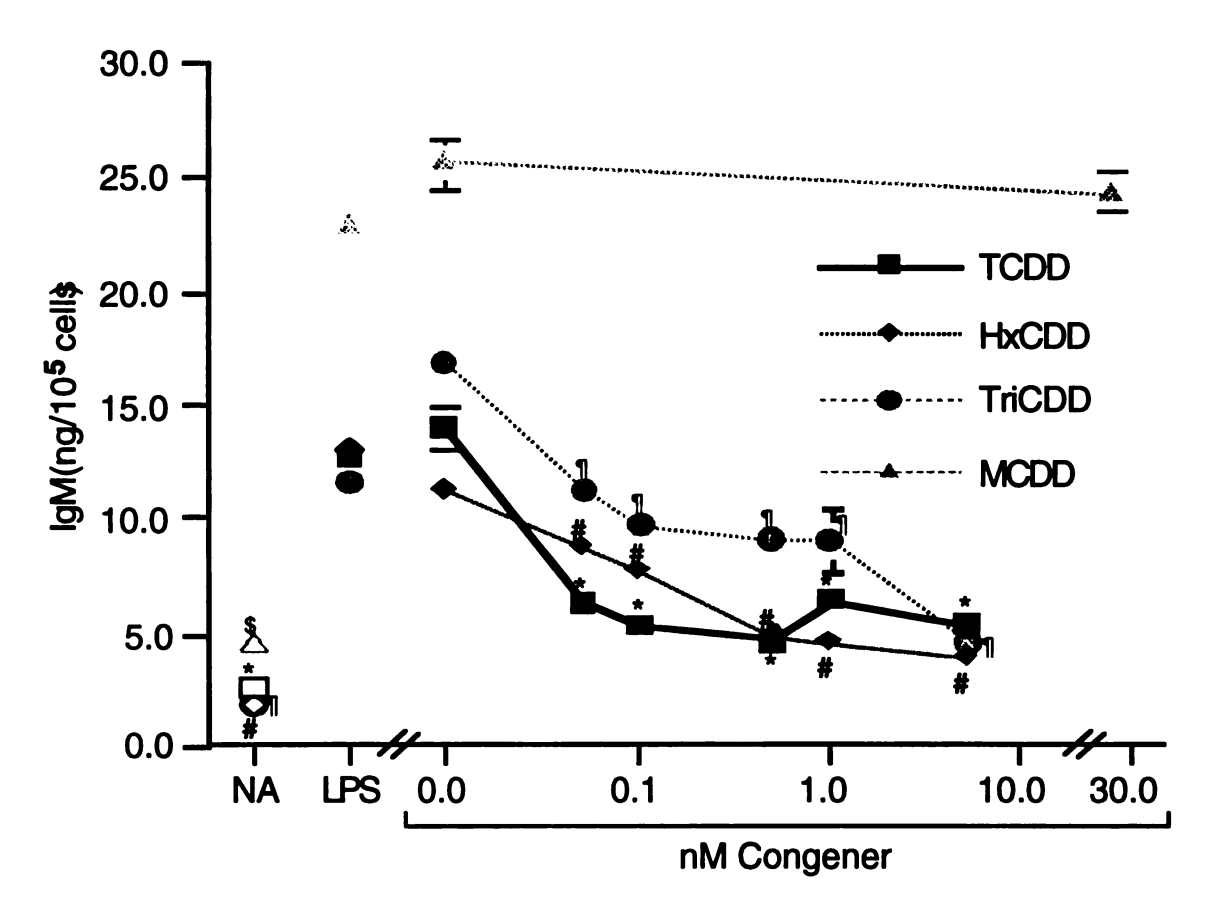


Figure 23. Concentration-dependent effect of selected chlorinated dibenzo-p-dioxin congeners on LPS-induced IgM secretion from CH12.LX cells. CH12.LX cells ( $1x10^4$  cells/ml) were treated with 3  $\mu$ g/ml LPS (filled symbols) and selected concentrations of TCDD, HxCDD, TriCDD or MCDD. The vehicle control (0.0 nM congener) was 0.01% DMSO. Supernatants were harvested at 72 hr and analyzed for IgM by sandwich ELISA. IgM is represented on the y-axis as ng/ $10^5$  cells. Symbol, mean  $\pm$  standard error for triplicate determinations (n=3). These results were analyzed for statistical significance using Dunnett's two-tailed t-test. \*, #, ¶, and \$, values that are significantly different from the VH control within the TCDD, HxCDD, TriCDD and MCDD experiments, respectively, at P<0.05. The results are representative of more than three separate experiments.

# B. Specific PCDD congeners have no affect on *Cyp1a1* expression or LPS-induced IgM secretion from the AhR-deficient BCL-1 B-cells

In agreement with a lack of AhR expression, TCDD, HxCDD, TriCDD and MCDD had no affect on *Cyp1a1* expression in BCL-1 cells as determined by qualitative RT-PCR (Figure 24). To confirm the AhR-dependency of congener-induced inhibition of IgM secretion, the effect of specific PCDD congeners on LPS-induced IgM secretion from the AhR-deficient BCL-1 cell line was evaluated by ELISA. As expected, TCDD, HxCDD, TriCDD and MCDD had no affect on IgM secretion (Figure 25).

# C. LPS-induced $\mu$ expression in CH12.LX cells is inhibited by PCDD congeners and follows an SAR for AhR binding

Since IgM is composed of two heavy chains and two light chains, the genes encoding these proteins are potential transcriptional targets modulated by TCDD. To determine if transcriptional regulation of the μ gene underlies the inhibition of IgM secretion by TCDD, expression of the μ gene in LPS-stimulated CH12.LX cells was analyzed by quantitative RT-PCR analysis following a 24 hr treatment with TCDD, HxCDD and TriCDD at various concentrations. Although TCDD and HxCDD inhibited μ gene expression in a concentration-dependent manner with TCDD being more potent than HxCDD, TriCDD which induces *Cyp1a1* and inhibits IgM secretion did not affect μ gene expression (Figure 26, Table 2). In addition the effect of HxCDD exhibited a rather flat concentration-response which is in contrast with its effect on *Cyp1a1* induction (compare Figure 22 and Figure 26). The lack of effect by TriCDD and the blunted response of HxCDD may be due to slower kinetics of AhR activation by lower affinity AhR ligands. This potential effect on kinetics might be more pronounced in the shorter, 24 hr μ assay as opposed to the longer, 72 hr IgM protein secretion assay. In contrast to μ expression, *Cyp1a1* induction,

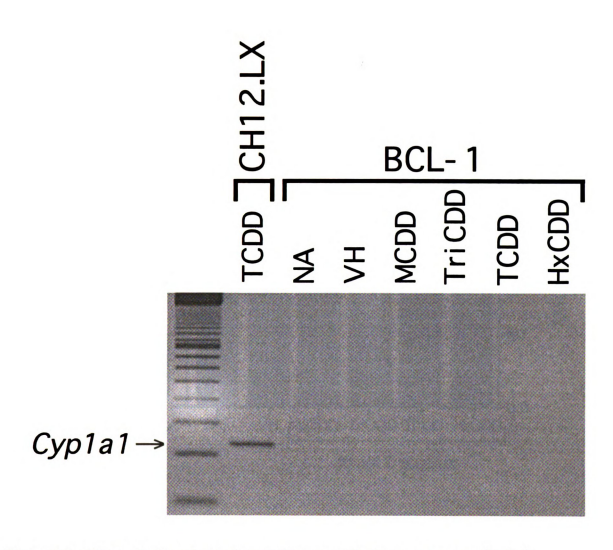


Figure 24. Effect of selected chlorinated dibenzo-p-dioxin congeners on Cyp1a1 expression in BCL-1 cells. BCL-1 cells (3x10<sup>5</sup> cells/ml) were treated with TCDD, HxCDD, TriCDD or MCDD at 30 nM. CH12.LX cells (1x10<sup>5</sup> cells/ml) served as a positive control and were treated with 3.0 nM TCDD. The vehicle (VH) control was 0.01% DMSO. Qualitative RT-PCR analysis for Cyp1a1 was performed on RNA extracted at 48 hr from each treatment group. Results are representative of more than two separate experiments.

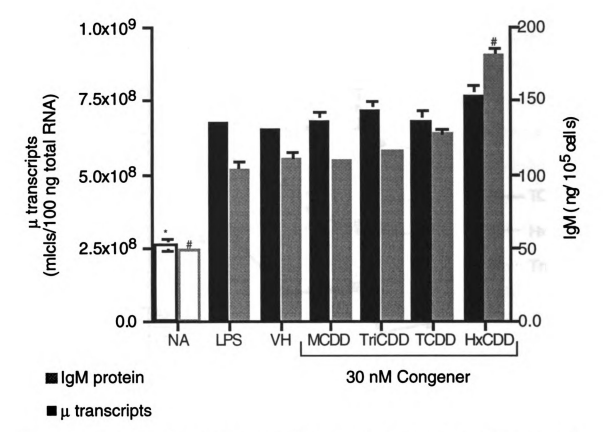


Figure 25. Effect of selected chlorinated dibenzo-p-dioxin congeners on LPS-induced μ expression and IgM secretion in BCL-1 cells. For analysis of μ RNA expression, BCL-1 cells (31.05 cells/ml) were treated with 30 μg/ml LPS (filled bars) and TCDD, HxCDD, TriCDD or MCDD at 30 nM. Quantitative RT-PCR analysis for μ was performed on RNA extracted at 48 hr from each treatment group. Transcripts for μ are identified on the left y-axis as molecules (mlcls)/100 ng RNA. Bar, mean ± standard error for three separate RNA isolations (n=3). For analysis of IgM secretion, BCL-1 cells (2x10<sup>5</sup> cells/ml) were treated with 30 μg/ml LPS (filled bars) and TCDD, HxCDD, TriCDD or MCDD at 30 nM. Supermatants were harvested at 72 hr and analyzed for IgM by sandwich ELISA. IgM is represented on the right y-axis as ng/10<sup>5</sup> cells. Bar, mean ± standard error for triplicate determinations (n=3). These results were analyzed for statistical significance using Dunnett's two-tailed-rest. \*and #, values that are significantly different, at P<0.05, from the vehicle (VH; 0.01% DMSO) controls for the μ expression and IgM secretion experiments, respectively. The results are representative of more than two separate experiments.

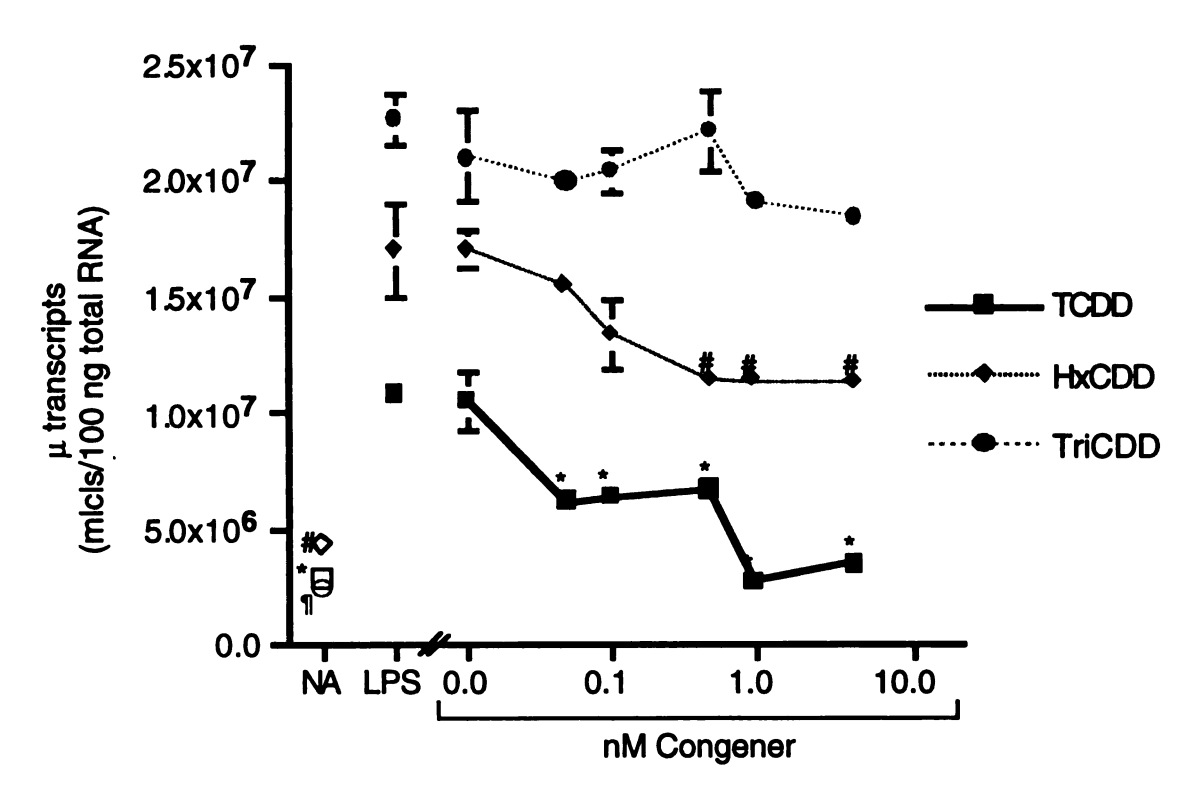


Figure 26. Concentration-dependent effect of a 24 hr incubation with selected chlorinated dibenzo-p-dioxin congeners on  $\mu$  expression in CH12.LX cells. CH12.LX cells (1x10<sup>5</sup> cells/ml) were treated with  $3\mu g/ml$  of LPS (filled symbols) and TCDD, HxCDD or TriCDD at various concentrations. The vehicle control (0.0 nM congener) was 0.01% DMSO. Quantitative RT-PCR analysis for  $\mu$  expression was performed on RNA extracted at 24 hr from each treatment group. Transcripts for  $\mu$  are identified on the y-axis as molecules/100 ng RNA. Symbol, mean  $\pm$  standard error for three separate RNA isolations (n=3). These results were analyzed for statistical significance using Dunnett's two-tailed t-test. \*, # and ¶, values that are significantly different from the VH control within the TCDD, HxCDD and TriCDD experiments, respectively, at P<0.05. The results are representative of more than two separate experiments.

in a 24 hr assay, is extremely sensitive to TCDD, HxCDD and TriCDD (Figure 22). This sensitivity is likely due to the presence of six DREs in the *Cyp1a1* promoter; five of which are capable of positively regulating transcription as demonstrated by reporter gene assays (172). Furthermore, the presence and functionality of DREs within critical regulatory regions of  $\mu$  is unclear. To explore the possibility of slower kinetics for the effects of TriCDD and HxCDD on  $\mu$  expression, LPS-stimulated CH12.LX cells were incubated with the PCDD congeners for 48 hr followed by RT-PCR analysis. In contrast to the 24 hr results,  $\mu$  expression was inhibited in a concentration-dependent manner by TriCDD and the concentration-response for HxCDD was sigmoidal (Figure 27). The rank order potency was TCDD > HxCDD > TriCDD >> MCDD; MCDD had no affect on  $\mu$  expression (Table 2, Figure 27). The effect of the PCDD congeners on LPS-induced  $\mu$  expression in the AhR-deficient BCL-1 cells was also analyzed at 48 hr by quantitative RT-PCR. All of the congeners had no effect on  $\mu$  gene expression from the BCL-1 cells (Figure 25).

# D. Inhibition of IgM protein secretion and $\mu$ expression is AhR dependent

IC<sub>50</sub> and EC<sub>50</sub> values were generated from extensive concentration response curves (i.e., at least nine concentrations per congener) for each congener (Table 2). An abbreviated version of these curves is represented in Figures 22-27. For a given congener, statistical comparisons of the IC<sub>50</sub>s for  $\mu$  expression (48 h) and IgM protein secretion and the EC<sub>50</sub> for induction of *Cyp1a1* expression were not significantly different with the exception of a slight difference between *Cyp1a1* induction and  $\mu$  (48 h) inhibition with the TriCDD congener (Table 2). These results suggest a common mechanism of action and since induction of *Cyp1a1* is an established AhR-mediated event, these results continue to support AhR-mediated inhibition of  $\mu$  expression and IgM protein secretion. In addition, the IC<sub>50</sub>s and EC<sub>50</sub>s for a given endpoint among the PCDD congeners tended towards a

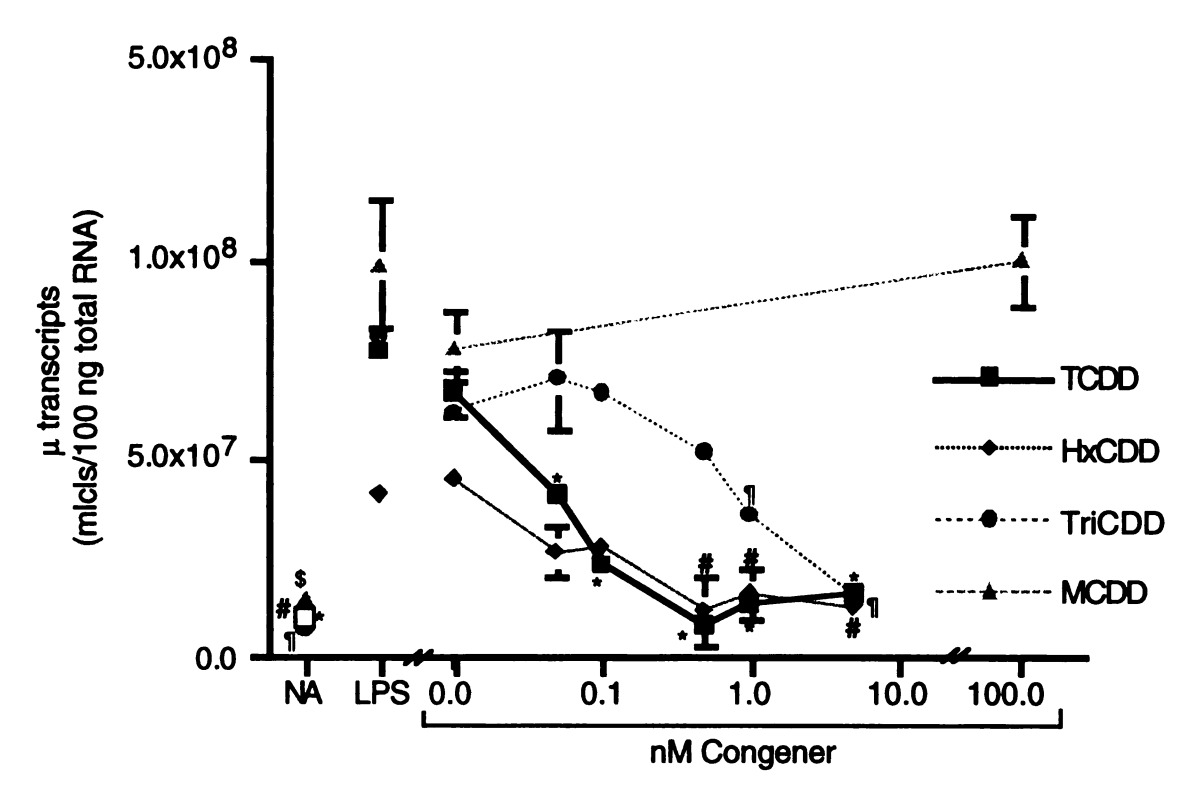


Figure 27. Concentration-dependent effect of a 48 hr incubation with selected chlorinated dibenzo-p-dioxin congeners on  $\mu$  expression in CH12.LX cells. CH12.LX cells (1x10<sup>5</sup> cells/ml) were treated with 3  $\mu$ g/ml LPS (filled symbols) and TCDD, HxCDD, TriCDD or MCDD at various concentrations. The vehicle control (0.0 nM congener) was 0.01% DMSO. Quantitative RT-PCR analysis for  $\mu$  expression was performed on RNA extracted at 48 hr from each treatment group. Transcripts for  $\mu$  are represented on the y-axis as molecules/100 ng RNA. Symbol, mean  $\pm$  standard error for three separate RNA isolations (n=3). These results were analyzed for statistical significance using Dunnett's two-tailed t-test. \*, #, ¶ and \$, values that are significantly different from the VH control within the TCDD, HxCDD, TriCDD and MCDD experiments, respectively, at P < 0.05. The results are representative of more than two separate experiments.

structure activity relationship which was concordant with the AhR binding affinity for the respective PCDD congeners, again supporting AhR-mediation of these three responses (Table 2).

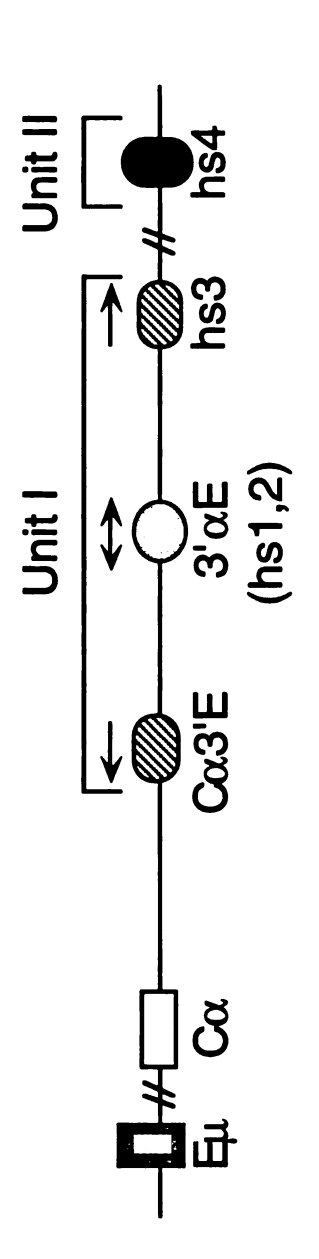
### IV. Alteration of protein binding at the $3'\alpha$ Ig heavy chain enhancer by TCDD

# A. TCDD induces binding to a DRE-like site located within the $3'\alpha E(hs1,2)$ and $3'\alpha$ -hs4 enhancers

heavy chain gene. Our studies focused on two of the DRE-like sites; one of which is

We have identified several DRE-like sequences in the  $3'\alpha$  enhancer of the mouse Ig

located in the 3' $\alpha$ E(hs1,2) enhancer and the other in the 3' $\alpha$ -hs4 enhancer (Figure 28). In the CH12.LX cells, EMSA analysis demonstrated TCDD-inducible binding, which migrated similarly to the DRE3 positive control, to both the  $3'\alpha E(hs1,2)$  and the  $3'\alpha$ -hs4 oligomers (Figs. 29A and 30A, lanes 2, 4 and 5). Binding to these oligomers was also reduced with the addition of unlabeled DRE3, though not as effectively as with the unlabeled oligomers themselves (Figure 29A and 30A, lanes 5-7). These results suggest that the AhR-nuclear complex binds to both DRE-like sites identified within the 3'αE(hs1,2) and 3'α-hs4 oligomers, which was confirmed by EMSA-Western analysis. Antibodies specific for the AhR and ARNT identified these proteins as components of the TCDD-inducible complex in both the 3'αE(hs1,2) and 3'α-hs4 oligomers, as well as in the DRE3 positive control (Figure 29B and C, lanes 2 and 4 and Figure 30B and C, lanes 2 and 4). The AhR and ARNT migrated identically among the oligomers in the EMSA-Western (Figs. 29 and 30, B and C, compare lanes 2 and 4), as well as with the TCDD-inducible protein complexes formed with both oligomers in the EMSA (Figs. 29 and 30, compare lane 2 and 5 of A to lanes 2 and 4 of B and C). However, it is notable that in the EMSA, the TCDD-inducible complex formed with the



 $3'\alpha E(hs1,2)$ 

TAGGGG TCTATTAAC ICACCACGCTA GGCCATCATGGAGAG partial KB

3'α-hs4

# AGCAGAGGGGGAC <u>TGGCGT **GGA<u>AA</u> GCCCC** ATTCACCCAT</u>

Ä

Figure 28. Oligomers derived from the 3' $\alpha$  enhancer used in the EMSA analysis. The 3' $\alpha$  enhancer is composed of two functional units. Unit I contains the C $\alpha$ 3'E, 3' $\alpha$ E(hs1,2) and hs3 enhancers. Unit II contains the 3' $\alpha$ -hs4 enhancer. A DRE-like site is located within the 3' $\alpha$ E(hs1,2) and 3' $\alpha$ -hs4 enhancers. Oligomers used in the EMSA studies are illustrated, including the DRE-like sites as well as a partial and full  $\kappa$ B site located in the 3' $\alpha$ E(hs1,2) and 3' $\alpha$ -hs4, respectively. Consensus DRE nucleotides are underlined.  $\kappa$ B sites

Figure 29. TCDD-induced binding to a DRE-like site within the 3'αE(hs1,2) enhancer. CH12.LX cells ( $5x10^5$  cells/ml) or BCL-1 cells ( $7.5x10^5$  C/ml)were treated with 30 nM TCDD [(A) lanes 2-7; and (B and C) lanes 2 and 4] or vehicle (VH; 0.01% DMSO) [(A) lanes 1; and (B and C) lanes 1, 3] for 1 hr followed by nuclear protein isolation. (A) Nuclear protein ( $10 \mu g$ ) and radiolabeled DRE3 or  $3'\alpha E(hs1,2)$  [hs1,2] oligomer (40,000 cpm) were loaded in each lane, resolved on a 4.0% nondenaturing PAGE gel, dried on 3mm filter paper and autoradiographed. Lane 0 is the radiolabeled probe without nuclear protein. Unlabeled competitor oligonucleotide (xDRE3 or xhs1,2) was added at an approximately 100-fold excess [(A) lanes 3, 6, and 7] to show specificity of protein-DNA binding. (B and C) Nuclear protein ( $10 \mu g$ ) and unlabeled DRE3 or hs1,2 oligomer ( $10 \mu g$ ) were loaded in each lane, resolved on a 4.0% nondenaturing PAGE gel, transferred to nitrocellulose and probed with 1  $\mu g/ml$  AhR (17-10B) antibody (B) or a 1:1000 dilution of the ARNT antibody (C). Arrows indicate specific binding of the AhR and ARNT to the 3'αE(hs1,2) oligomer. Results are representative of more than two separate experiments.

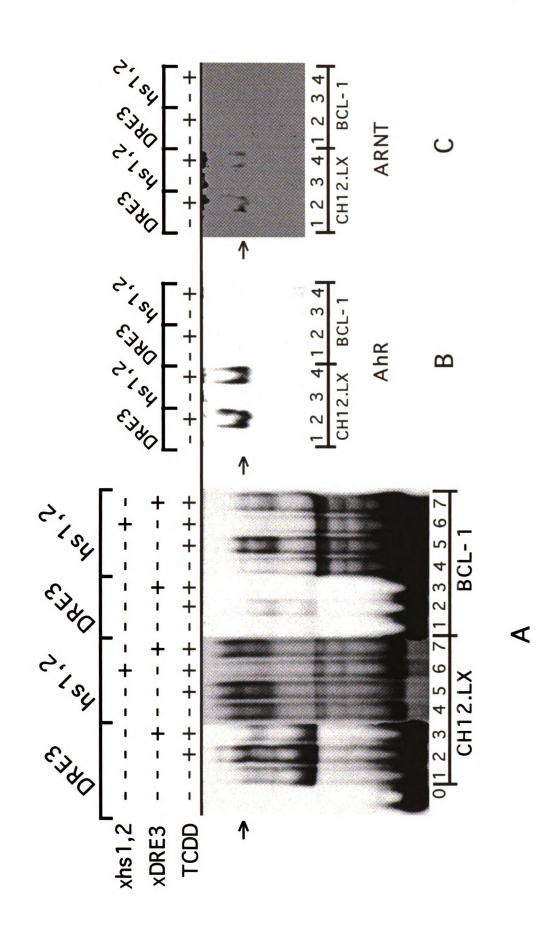


Figure 29. TCDD-induced binding to a DRE-like site within the 3'oE(hs1,2) enhancer.

Figure 30. TCDD-induced binding to a DRE-like site within the 3'α-hs4 enhancer. CH12.LX cells ( $5x10^5$  cells/ml) or BCL-1 cells ( $7.5x10^5$  C/ml) were treated with 30 nM TCDD [(A) lanes 2-7; and (B and C) lanes 2 and 4] or vehicle (VH; 0.01% DMSO) [(A) lane 1; and (B and C) lanes 1 and 3] for 1 hr followed by nuclear protein isolation. (A) Nuclear protein ( $10 \mu g$ ) and radiolabeled DRE3 or 3'α-hs4 (hs4) oligomer (40,000 cpm) were loaded in each lane, resolved on a 4.0% nondenaturing PAGE gel, dried on 3mm filter paper and autoradiographed. Lane 0 is the radiolabeled probe without nuclear protein. Unlabeled competitor oligonucleotide (xDRE3 or xhs4) was added at an approximately 100-fold excess [(A) lanes 3, 6, and 7] to show specificity of protein-DNA binding. (B and C) Nuclear protein ( $10 \mu g$ ) and unlabeled DRE3 or hs4 oligomer ( $10 \mu g$ ) and unlabeled DRE3 or hs4 oligomer ( $10 \mu g$ ) mol) were loaded in each lane, resolved on a 4.0% nondenaturing PAGE gel, transferred to nitrocellulose and probed with with 1 μg/ml AhR (17-10B) antibody (B) or a 1:1000 dilution of the ARNT antibody (C). Arrows indicate specific binding of the AhR and ARNT to the 3'α-hs4 oligomer. Results are representative of more than two separate experiments.

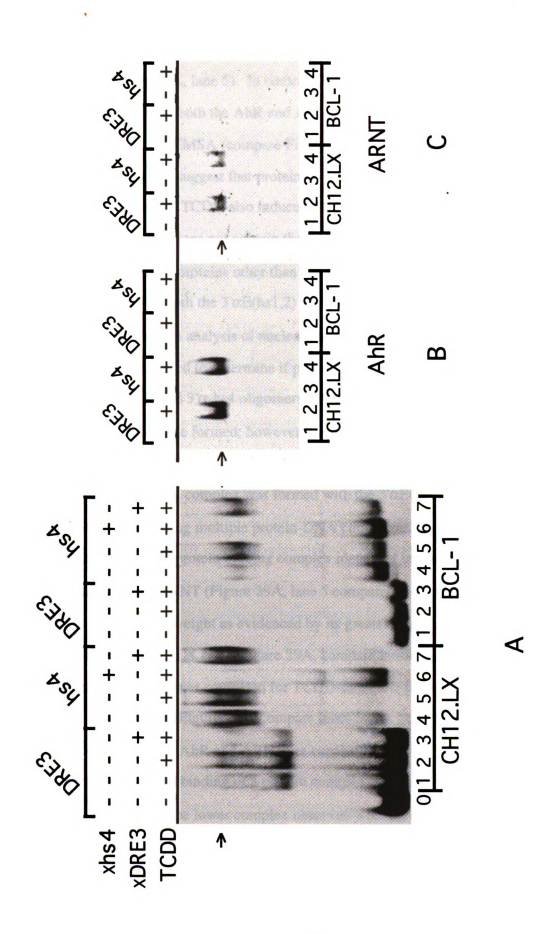


Figure 30. TCDD-induced binding to a DRE-like site within the 3'\alpha-hs4 enhancer.

3'αE(hs1,2) oligomer is rather broad and diffuse, suggesting multiple protein-DNA complexes (Figure 29A, lane 5). In contrast, the EMSA-Western analysis identified a sharp band containing both the AhR and ARNT which was part of the TCDD-inducible band identified in the EMSA (compare Figure 29A, lane 5 and Figure 29B and C, lane 4). These results strongly suggest that proteins other than the AhR are binding to the 3'αE(hs1,2) oligomer. TCDD also induced the binding of a second protein complex to the 3'α-hs4 oligomer that does not contain the AhR (compare Figure 30A, lane 5 and Figure 30B, lane 4). Nuclear proteins other than the AhR nuclear complex appear to be induced by TCDD to bind to both the 3'αE(hs1,2) and 3'α-hs4 oligomers.

EMSA-Western analysis of nuclear protein isolated from the AhR-deficient BCL-1 cells was also performed to determine if protein-DNA complexes are formed with the DRE3, 3'αE(hs1,2) and 3'α-hs4 oligomers. With the DRE3 oligomer, faint TCDDinducible complexes are formed; however these complexes do not contain the AhR or ARNT (Figs. 29 and 30, compare lane 2 of A, B and C). Similar to the CH12.LX cells, a broad TCDD-inducible complex was formed with the 3'αE(hs1,2) oligomer (Figure 29A, lane 5), again suggesting multiple protein-DNA complexes. In contrast, the TCDDinducible 3'αE(hs1,2) protein binding complex identified in the BCL-1 cells did not contain the AhR or ARNT (Figure 29A, lane 5 compared to Figure 29B and C, lane 4) and is of lower molecular weight as evidenced by its greater migration as compared to that observed in the CH12.LX cells (Figure 29A, compare lanes 5). Interestingly, the unlabeled DRE3 oligomer competed for TCDD-inducible binding to the labeled 3'αE(hs1,2) oligomer (Figure 29A, compare lanes 5 and 7); perhaps suggesting that proteins other than the AhR and ARNT are capable of binding to the DRE. TCDD treatment also induced binding of a protein complex to the 3'α-hs4 oligomer which migrated similarly to the lower complex observed with the CH12.LX cells (Figure 30A, compare lanes 4 and 5 of CH12.LX and BCL-1). Neither of these complexes contained the AhR or ARNT (Figure 30B and C, lanes 4). Collectively, these results suggest that

TCDD at concentrations that induce AhR activation also induce additional protein binding complexes that recognize both of these oligomers in an AhR-independent manner.

# B. TCDD induces binding to a $\kappa B$ site located within the 3' $\alpha$ -hs4 enhancer

Our EMSA-Western results suggest that nuclear proteins distinct from the AhR nuclear complex are induced by TCDD to bind the 3'αE(hs1,2) and 3'α-hs4 oligomers in both the CH12.LX and BCL-1 cells. Interestingly, the 3'α-hs4 oligomer possesses a full KB motif which overlaps the DRE site. The potential significance concerning the overlap of these two motifs is three-fold. First, it is well established that NF-κB/Rel proteins are important regulators of the 3'α enhancer (33, 34), suggesting that the NF-κB/Rel proteins are likely candidates for the additional TCDD-induced protein-3'α-hs4 complexes being observed. Second, an increase in KB binding following TCDD treatment has been recently demonstrated by EMSA (173, 174). Third, the AhR/ARNT complex may compete with NF-κB/Rel proteins for binding. Therefore, antibodies specific for the NF-κB/Rel family members, p65, p50, c-Rel and RelB were used to probe EMSA-Western blots for 3'α-hs4 in an attempt to identify the binding proteins induced by TCDD in the CH12.LX and BCL-1 cells. With the CH12.LX cells, analysis revealed TCDD-induced binding to the 3'α-hs4 oligomer of p65, RelB, p50 and c-Rel, all of which were identified in the lower protein-DNA complex (Figure 31, compare lanes 2 of A and E to lanes 2 of C,D,G and H). This complex does not contain the AhR or ARNT but may be composed of several protein-DNA complexes of various hetero- and homodimers of p65, RelB, p50 and c-Rel. For instance, there are slight differences in migration between the NF-kB/Rel proteins (i.e., p65 and RelB) and, in some instances, between vehicle and TCDD treatment (i.e., p65 and c-Rel); however all NF-κB/Rel proteins identified in the EMSA-Western migrate within the TCDD-inducible band identified in the EMSA (Figure 31, lane 2, compare A and E to C,

Figure 31. TCDD-induced binding of NF-κB/Rel proteins from CH12.LX cells to a κB binding site within the 3'α-hs4 enhancer. CH12.LX cells ( $5x10^5$  cells/ml) were treated with 30 nM TCDD [(A) lanes 2-5; (E) lanes 2-4; and (B-D and F-H) lane 2] or vehicle (VH; 0.01% DMSO) [(A-H) lane 1] for 1 hr followed by nuclear protein isolation. (A) Nuclear protein (10 μg) and radiolabeled 3'α-hs4 (hs4) oligomer (40,000 cpm) were loaded in each lane, resolved on a 4.0% nondenaturing PAGE gel, dried on 3mm filter paper and autoradiographed. Lane 0 is the radiolabeled probe without nuclear protein. Unlabeled competitor oligonucleotide (xhs4, xDRE3 or xhs4-κB) was added at an approximately 100-fold excess [(A) lanes 3-5; and (E) lanes 3 and 4] to show specificity of protein-DNA binding. (B-D and F-H) Nuclear protein (10 μg) and unlabeled hs4 oligomer (10 pmol) were loaded in each lane, resolved on a 4.0% nondenaturing PAGE gel, transferred to nitrocellulose and probed with 1 μg/ml anti-AhR (17-10B) (B and F), 0.4 μg/ml anti-p65 (C), 0.8 μg/ml anti-RelB (D), 1.6 μg/ml anti-p50 (G) or 0.8 μg/ml anti-c-Rel (H). Arrows indicate specific binding of the AhR or NF-κB/Rel proteins to the 3'α-hs4 oligomer. Results are representative of more than two separate experiments.

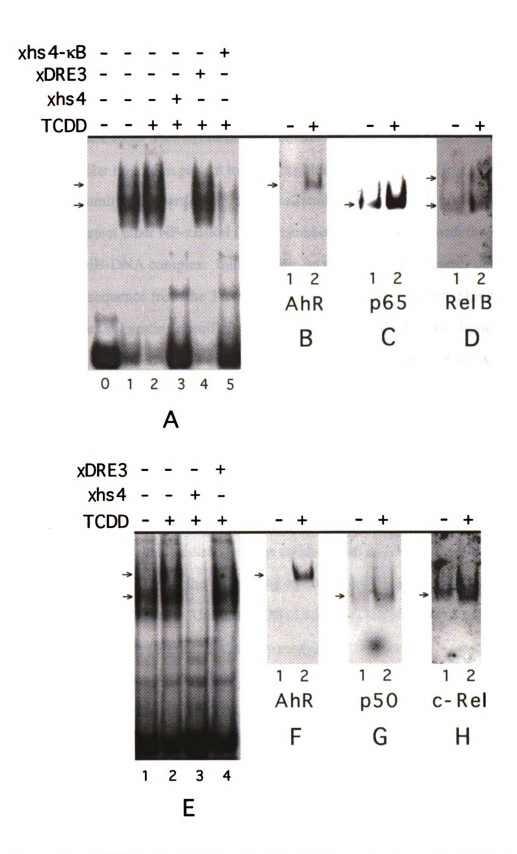


Figure 31. TCDD-induced binding of NF- $\kappa$ B/Rel proteins from CH12.LX cells to a  $\kappa$ B binding site within the 3' $\alpha$ -hs4 enhancer.

D, G, and H). Interestingly, a faint upper band was also identified with the Rel B antibody (Figure 31D, lanes 1 and 2) that migrated slightly higher than the AhR (Figs. 31, lane 2, compare B and D) and therefore, is not likely to be a component of the AhR/ARNT complex. Since RelB does not form homodimers and since none of the other kB proteins exhibit a similar migration pattern to RelB, its binding partner is unclear. It is notable that NF-κB/Rel family members can form "cross-family" dimers which might explain our inability to detect other NF-kB/Rel family members in association with the slower migrating RelB-DNA complex. Interestingly, an unlabeled KB oligomer containing the identical KB sequence from the  $3'\alpha$ -hs4 enhancer completely abrogated binding of the lower complex suggesting specificity of this sequence for kB binding (Figure 31, lane 5). Interestingly, unlabeled KB also decreased TCDD-induced binding of the AhR/ARNT complex though not completely. This effect may be related to the much stronger binding of the NF-kB/Rel proteins as well as the possibility that the excess unlabeled kB oligomer may nonspecifically affect DRE binding. Since the kB binding site overlaps the flanking region and one nucleotide of the core region of the DRE binding site and since the unlabeled kB oligomer does not contain the complete DRE site, it is unlikely that the AhR nuclear complex would bind directly to the unlabeled kB oligomer.

For the BCL-1 cells the κB binding to the 3'α-hs4 oligomer was slightly different than for the CH12.LX cells. Unlike the CH12.LX cells, there was relatively little basal κB binding in the EMSA (Figure 31A, lane 1 compared to Figure 32A, lane 1). The EMSA-Western indicated that c-Rel was the only NF-κB/Rel protein with detectable binding in the vehicle treatment group (Figure 32H, lane 1). TCDD treatment of the BCL-1 cells induced 3'α-hs4 binding of p65, RelB and c-Rel; these proteins migrated similarly to the single TCDD-inducible protein binding complex (Figure 32, lane 2, compare A and E to C, D and H). In contrast to the CH12.LX cells, p50 was not induced by TCDD (Figure 32G). Slight differences in migration between the NF-κB/Rel proteins (i.e., p65 and RelB) were identified (Figure 32) as demonstrated with the CH12.LX cells. Additionally, binding to

Figure 32. TCDD-induced binding of NF-κB/Rel proteins from BCL-1 cells to a κB binding site within the 3'α-hs4 enhancer. BCL-1 cells (7.5x10<sup>5</sup> cells/ml) were treated with 30 nM TCDD [(A) lanes 2-5; (E) lanes 2-4; and (B-D and F-H) lane 2] or vehicle (VH; 0.01% DMSO) [(A-H) lane 1] for 1 hr followed by nuclear protein isolation. (A) Nuclear protein (10 μg) and radiolabeled 3'α-hs4 (hs4) oligomer (40,000 cpm) were loaded in each lane, resolved on a 4.0% nondenaturing PAGE gel, dried on 3mm filter paper and autoradiographed. Lane 0 is the radiolabeled probe without nuclear protein. Unlabeled competitor oligonucleotide (xhs4, xDRE3 or xhs4-κB) was added at an approximately 100-fold excess [(A) lanes 3-5; and (E) lanes 3 and 4] to show specificity of protein-DNA binding. (B-D and F-H) Nuclear protein (10 μg) and unlabeled hs4 oligomer (10 pmol) were loaded in each lane, resolved on a 4.0% nondenaturing PAGE gel, transferred to nitrocellulose and probed with 1 μg/ml anti-AhR (17-10B) (B and F), 0.4 μg/ml anti-p65 (C), 0.8 μg/ml anti-RelB (D), 1.6 μg/ml anti-p50 (G) or 0.8 μg/ml anti-c-Rel (H) Arrows indicate specific binding of the AhR or NF-κB/Rel proteins to the 3'α-hs4 enhancer. Results are representative of more than two separate experiments.

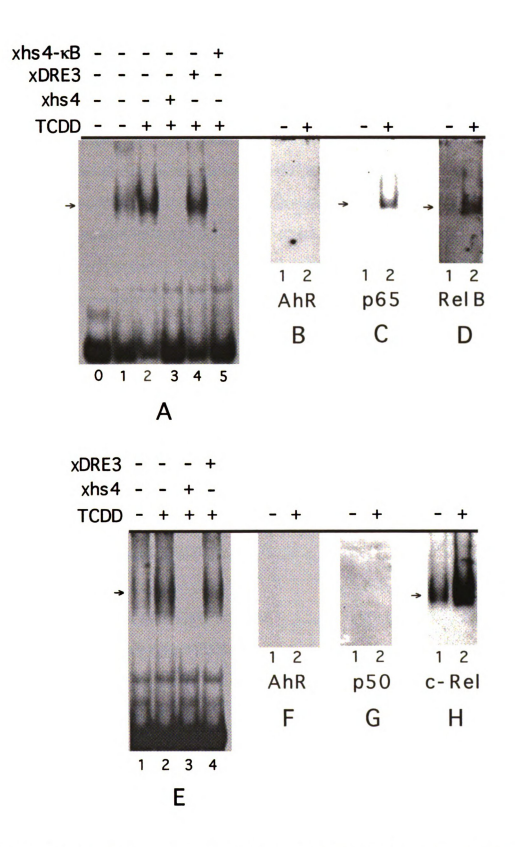


Figure 32. TCDD-induced binding of NF- $\kappa$ B/Rel proteins from BCL-1 cells to a  $\kappa$ B binding site within the 3' $\alpha$ -hs4 enhancer.

the 3' $\alpha$ -hs4 oligomer was also completely abrogated by the unlabeled  $\kappa B$  oligomer (Figure 32A, lane 5). Induction of DNA binding by NF- $\kappa B$ /Rel proteins after TCDD treatment in the AhR-deficient BCL-1 cells suggests an AhR-independent activation of p65, RelB and c-Rel.

### **DISCUSSION**

The toxicity of TCDD is thought to be mediated transcriptionally through an interaction of the AhR/ARNT nuclear complex with DREs in regulatory regions of TCDD sensitive genes. Putative DREs have been identified in regulatory regions of several non-metabolic genes supporting a potential for DRE-dependent transcriptional regulation (134); nevertheless, this type of regulation has been most extensively characterized for the induction of metabolic enzymes and has not been directly correlated with TCDD-induced toxicity, including immune suppression. However, considerable evidence does exist that supports an essential role for the AhR in TCDD-mediated immune suppression (1-3, 175). In addition, several laboratories have demonstrated novel protein-protein associations involving the AhR and several other proteins some of which are the NF-kB, Sp1, transcription factor IIB, retinoblastoma protein and the Src family kinase, c-src (109, 135-138). This suggests a possible interaction of the AhR with different signaling pathways and thus, a potential for DRE-independent mediation of some of TCDD's biological effects.

### I. Functional AhR and ARNT in murine splenocytes

At the onset of this investigation, no target genes in immunocompetent cells had been identified and the direct identification of the fundamental components of the AhR signaling cascade, specifically the AhR and ARNT protein, had not been convincingly demonstrated in immunocompetent cells. Lorenzen *et al.*, demonstrated specific and saturable binding of [<sup>3</sup>H]-TCDD in cellular cytosol from human tonsils suggesting the presence of cytosolic AhR. In these studies, the authors went on to identify the translocation of protein bound [<sup>3</sup>H]-TCDD to the nucleus by sucrose gradient centrifugation (147). Photoaffinity-labeled AhR has also been demonstrated in the cytosolic fraction of whole spleen from B6 mice (176), and transcripts for the AhR and

ARNT are present in whole tissue preparations from spleen and thymus in the rat (163). Although these findings are suggestive that immunocompetent cells possess the AhR and ARNT, it is unclear from the preparations used, whether the actual source of the AhR and ARNT is from the immunocompetent cells or the contaminating non-immunocompetent cells also present in the preparations. This possibility was of concern based on biodistribution studies by Neumann and coworkers (148) in which they treated mice with [<sup>3</sup>H]-TCDD and demonstrated a comparable amount of [<sup>3</sup>H]-TCDD in splenic capsule as that found associated with splenocytes. Further, these results are highly reminiscent of previous findings in which Greenlee and coworkers demonstrated that although the thymus possesses a significant amount of AhR, it is in fact primarily localized in thymic epithelium (89, 177).

To avoid the possibility of confounding results, splenocytes devoid of capsule and red blood cells were evaluated by Northern and Western blot analysis and by quantitative RT-PCR for both AhR and ARNT. Northern analysis of poly(A) RNA isolated from splenocytes revealed a single band, approximately 6.6 kb, to which the AhR cDNA probe hybridized (Figure 3B). As previously shown, B6C3F1 mice possess two forms of the AhR which are codominantly expressed and correspond to the  $Ah^{b-1}$  (C57BL/6J) and  $Ah^{b-2}$ (C3H) alleles (164). In agreement, we have identified two major AhR proteins of approximately 95 kDa and 104 kDa in splenocyte lysates by Western blot (Figure 4A). Northern analysis of mRNA isolated from spleen for ARNT revealed the presence of three mRNA transcripts of approximately 5.6 kb, 2.0 kb, and 1.1 kb (Figure 3C). An identical banding profile for ARNT was observed in RNA isolated from liver (Figure 3C). The presence of ARNT in mouse spleen was confirmed by Western blot analysis as an 87 kDa protein (Figure 4B). It should be emphasized that we have used splenocyte suspensions in our analyses, which would include both lymphocytes and macrophages. Although we cannot rule out a contribution by macrophages which have recently been shown to express high levels of AhR (178), we believe our results are most consistent with a profile of

activity in lymphocytes, primarily because macrophages constitute only about 5% of the splenocyte content from the B6C3F1 mouse (179, 180). In addition, recent results from this laboratory have identified both the AhR and ARNT in purified splenic B-cells from B6C3F1 mice (181).

Not surprisingly, because of the well-studied association of the AhR with the actions of TCDD in the liver, our quantitation of AhR by RT-PCR and slot blot analysis revealed greater amounts of message and protein for the receptor in liver than in splenocytes (Figure 5A and Table 1). However, it is quite intriguing that a greater amount of ARNT message and protein (approximately 3.2-fold and 2.4-fold, respectively) was present in splenocytes as compared to liver (Figure 5B and Table 1). Equally intriguing is the fact that more ARNT than AhR mRNA was expressed in the liver and splenocytes. A difference in the relative ratio of ARNT: AhR mRNA was also observed between the two preparations. These observations are in agreement with previous results by Carver and coworkers (163) in which they showed by RNase protection a trend towards greater expression of transcripts for ARNT as compared to AhR in rat spleen, thymus and placenta; however, it is notable that in these studies the authors did not consider this difference in expression to be significant in the lymphoid tissues (163). Carver and coworkers went on to speculate that the disparate levels of the AhR and ARNT may be indicative of other biological roles for ARNT (163). Interestingly, ARNT proteins can form homodimers and bind to the E-box DNA response element which is involved in many cellular processes such as mitogenesis, neurogenesis, sex determination and hematopoiesis (182, 183). In addition, a heterodimer of ARNT and HIF1α can activate, through HIF-1 DNA response elements, the transcription of several genes that mediate the cellular response to hypoxia (183). An alternative explanation for greater amounts of ARNT as compared to AhR in some tissues is that this skewed ratio would increase the likelihood that the ligand-bound receptor would find its necessary binding partner (i.e., the ARNT protein), especially in tissues where there are low amounts of AhR. In support of this

alternative possibility Li and co-workers (184) have demonstrated, in wild-type mouse hepatoma cells transfected with ARNT cDNA, an increase in magnitude, but not sensitivity, of the transcriptional response to TCDD. From this result they concluded that the intracellular concentration of ARNT influences the response of a target gene to TCDD (184).

The previous demonstration that protein bound [3H]-TCDD translocates from cytosol to the nucleus in human tonsillar cells (147) is especially significant since this was the first evidence suggesting that lymphoid cells may possess "functional" AhRs. However, the report by Lorenzen and Okey was inconsistent with results from studies by Denison and coworkers in which they were unable to demonstrate binding of the AhR/ARNT heterodimer to the DRE by EMSA using TCDD-treated splenic cytosol from a variety of animal species including rat, guinea pig and hamster (5). Taken together, these results indicate that it was not enough to demonstrate specific binding by radiolabeled TCDD, or even the presence of the AhR in lymphoid cells, without questioning whether the AhR is "functional" in lymphocytes. In splenocytes, we tested the functionality of the AhR/ARNT heterodimer by its ability to bind to the DRE following TCDD treatment. TCDD induced specific binding to the DRE motif as indicated by the ability of unlabeled DRE to compete with <sup>32</sup>P-labeled DRE for binding of the heterodimer (Figure 6). These results confirmed that the AhR and ARNT are in fact functional in B6C3F1-derived lymphocytes. We suspect that one reason this same result was not observed by Denison and coworkers may be due to the fact that the optimum conditions for AhR/ARNT binding to the DRE are modestly different for liver cytosolic preparations (a widely used comparative control) than that found in splenic preparations. In addition, we identified DRE binding in TCDD-treated splenocytes that resolved by EMSA as a rather broad band in comparison to DRE binding in TCDD-treated Hepa 1c1c7 cells (Figure 6, compare lanes 3 and 5). This was due to the formation of more than one TCDD-inducible protein-DNA complex in splenocytes as supported by: (a) the fact that B6C3F1 mice express two

different AhRs of approximately 95 kDa and 104 kDa; and (b) results by Bank *et al.* (185) demonstrating two distinct DRE binding complexes in hepatic cytosol from mouse and several other species.

While we have demonstrated that lymphocytes possess functional AhR and ARNT, these results do not necessarily confirm the role of an AhR-mediated mechanism for TCDD immunotoxicity. Several previously reported observations have challenged the exclusivity of this model, including: (a) the observation that B6C3F1 (high-responder) and DBA/2 (low-responder) mice, when treated subchronically with TCDD exhibit a comparable magnitude of immune suppression; and (b) that the low affinity AhR ligand, DCDD, and TCDD produce a comparable inhibition of the anti-sRBC IgM antibody forming cell response following subchronic treatment of mice *in vivo* and following direct addition to naive splenocytes *in vitro* (6). To address the involvement of the AhR signaling pathway in the effects of TCDD on B-cell function, we chose to develop a B-cell line model. In contrast to primary splenocytes, a B-cell line would offer a well characterized, homogeneous population of cells that rapidly proliferate. For experimental manipulation, especially with cell signaling studies, these characteristics offer an advantage over primary splenocytes.

### II. AhR-dependent suppression by TCDD of IgM secretion in activated B-cells

We have identified two B-cell lines that differ notably in their expression of the AhR as well as in their sensitivity to TCDD. The CH12.LX B-cell line markedly expresses both the AhR and ARNT protein as determined by Western and RT-PCR analysis; whereas, the BCL-1 B-cell line expresses only the ARNT protein and lacks expression of the AhR at the mRNA level (Figs. 7 and 8). Although a basis for the loss of Ahr expression in BCL-1 cells is unknown, it is noteworthy that the BCL-1 cell line is derived from an Ah high-responsive BALB/c mouse strain which has been characterized as

expressing an *Ahr* allele that encodes for an AhR with high affinity for TCDD (186). Further characterization of the AhR in the CH12.LX cells has verified a close similarity with the above results from studies conducted in primary lymphocytes. Specifically, the basal mRNA expression of *Ahr* and *Arnt* in primary lymphocytes was very similar to that detected in CH12.LX cells. In addition, both primary lymphocytes and CH12.LX cells exhibited a greater expression of *Arnt* transcripts as compared to *Ahr* transcripts (compare Table 1 with Figure 8B). As discussed earlier, this difference in expression has been detected in a variety of tissues and has led to the speculation that ARNT has other biological roles (163). As previously demonstrated in primary lymphocytes (187, 188 and Figure 6), the AhR and ARNT protein were shown to be "functional" in the CH12.LX cells by their ability to regulate *Cyp1a1* transcription (Figure 9).

As stated earlier, inhibition of IgM secretion from primary B-cells is a sensitive biological consequence of TCDD exposure (1, 91-94); however, the involvement of the AhR in mediating this effect is unclear. In addition to the previously mentioned studies involving acute DCDD treatment and subchronic TCDD treatment in which immunotoxicity did not segregate with the AhR (6, 7, 149), several other investigators have demonstrated TCDD-mediated events not dependent on a functional AhR. These include induction of junB and c-fos (132), induction of protein kinases (189, 190), phospholipase C (PLC) activation (191), and Ca<sup>2+</sup> influx (132). Induction of immediate early genes such as junB and c-fos are known to be involved in regulation of cellular proliferation and differentiation. In addition, increased protein phosphorylation that did not segregate with the AhR (99) and an increase in Ca<sup>2+</sup> influx (101, 102) have been identified in primary B-cells. The increase in Ca<sup>2+</sup> influx may also be AhR-independent as demonstrated by Puga *et al.* in hepatoma cells (132). Moreover, increased protein phosphorylation (99) and Ca<sup>2+</sup> influx (101, 102) were implicated in TCDD-induced suppression of the antibody response, further questioning the role of the AhR in suppression of antibody secretion.

Like primary B-cells, CH12.LX cells respond to an LPS differentiating signal with a significant increase in IgM secretion (Figure 11). Although lacking the AhR, BCL-1 cells are viable and are also capable of differentiating into antibody secreting cells (Figure 12). Therefore, BCL-1 cells respond similarly to an LPS differentiating signal as compared to CH12.LX cells which suggests that these cells have all of the necessary signaling components for B-cell activation. We have found that TCDD treatment of CH12.LX cells results in a sensitive and marked inhibition of IgM secretion similar to that seen in primary B-cells; however, LPS-induced IgM secretion from the AhR-deficient BCL-1 cells is not sensitive to inhibition by TCDD (Figs. 11 and 12). These results are the first to directly implicate a role for the AhR in mediating a TCDD-induced alteration of B-cell function. In addition, the CH12.LX and BCL-1 cell lines will offer a unique opportunity to study the TCDD-induced protein phosphorylation and Ca<sup>2+</sup> influx that appear to be AhR-independent but also appear to be involved in antibody suppression by TCDD.

A differential regulation of basal Ahr gene expression was demonstrated in cells of different lineages using deletion constructs of the Ahr 5' flanking region (192). The authors concluded that this variation in regulation of Ahr expression may provide the basis for differences in the sensitivity of various tissues to TCDD (192). Appearing to be in contrast with the above conclusion, leukocytes are very sensitive to TCDD, yet they express relatively low levels of AhR as compared to other target organs, such as the liver. However, an upregulation of AhR gene and protein expression was recently demonstrated in PMA/Io-stimulated primary leukocytes revealing a possible explanation for the sensitivity of these cells to TCDD (188). In agreement with these results, an upregulation of AhR gene and protein expression was detected in LPS-activated CH12.LX cells in the absence of TCDD (Figs. 13 and 15). This finding was recently verified in LPS-activated primary leukocytes and primary isolated B-cells (181). Interestingly, time of addition studies demonstrate that TCDD must be added within 24 hr of antigen addition to produce a significant and potent inhibition of the plaque forming cell response to sRBC (93); this

correlates well with the kinetics of AhR upregulation in differentiated B-cells. Taken together these results demonstrate an induction of the AhR upon lymphocyte activation and suggest a role for the AhR in cellular proliferation and/or differentiation. In addition to activated leukocytes, an upregulation of Ahr gene expression has also been observed during monocyte differentiation (178) and keratinocyte differentiation (193). The AhR has also been implicated in cell cycle regulation of Hepa 1c1c7 cells. Specifically, cells deficient in AhR have a longer doubling time then wild-type cells expressing the AhR. Introduction of antisense AhR cDNA into wild-type cells results in a longer doubling time resembling that of the AhR-deficient cells (194). An additional consequence of AhR upregulation may be an increased nuclear translocation and binding of ligand-activated AhR to DREs located in promoter regions of genes sensitive to TCDD. Masten and Shiverick (150) identified negative regulation by TCDD of a B-cell specific gene. They proposed that this effect was mediated by an AhR/DRE mechanism through a competition between BSAP and the AhR nuclear complex for binding to DNA that contained a DRE motif within the binding site for BSAP (150). Although this interaction between BSAP and the AhR is limited to the human CD19 promoter and to a moderate affinity BSAP site which may not play a prominent role in CD19 expression (43), it is possible that other genes involved in cellular proliferation and differentiation of B-cells may also contain DREs within their promoter regions. If so, the activated AhR nuclear complex may directly interfere with DNA binding of lineage specific transcription factors, such as BSAP, or simply modulate gene expression by binding DREs. In agreement with this model, TCDD-induced inhibition of estradiol-activated gene transcription involves, at least in part, an interference with the formation of estrogen receptor (ER)-Sp1 complexes by binding of the AhR to an imperfect DRE located between the ER and Sp1 binding sites (195).

To determine if an increase in AhR expression leads to an increase in sensitivity to TCDD, Cyplal expression in naive and LPS-stimulated CH12.LX was examined by RT-PCR for an alteration in the kinetics or magnitude of induction. Cotreatment or

pretreatment of LPS did not alter the kinetics or magnitude of TCDD-induced *Cyp1a1* expression (Figs. 19-21). These results do not support an increase in TCDD sensitivity with increasing AhR. However, the CH12.LX cell line may not be the most adequate model to study changes in sensitivity. Since basal and LPS-induced AhR expression appear to be much greater in these cells as compared to splenocytes, there may be sufficient levels of AhR to mediate the maximum possible response to TCDD within the kinetics of *Cyp1a1* induction. In addition, naive or LPS-induced *Ahr* expression was not affected by TCDD treatment (Figs. 17 and 18) which was of interest since the 5' untranslated region of the *Ahr* gene contains a consensus DRE (166).

## III. Transcriptional regulation of IgM expression by TCDD and the AhR/DRE signaling pathway

Further characterization of the CH12.LX cells has demonstrated an SAR between AhR binding affinity and three different endpoints: Cyp1a1 induction, IgM protein secretion and  $\mu$  gene expression (Figs. 22, 23, 26 and 27). In addition, the PCDD congeners had no effect on Cyp1a1 induction,  $\mu$  expression or IgM secretion in the AhR-deficient BCL-1 cells (Figs. 24 and 25). These results extend the above observation that the AhR is obligatory for the effects of TCDD on IgM secretion (Figs. 11 and 12) but more importantly, a comparison of the EC50 and IC50s of each congener for a particular biological response provides pharmacological evidence for or against a common receptor-mediated mechanism. Other than a modest difference between Cyp1a1 induction and inhibition of  $\mu$  expression with the TriCDD congener, the EC50 and IC50s for each endpoint were not significantly different for each congener suggesting that inhibition of IgM protein secretion is a result of an AhR-dependent mechanism which involves, at least in part, an inhibition of  $\mu$  expression (Table 2). It should be noted that studies with the CH12.LX/BCL-1 model were conducted to address the previously observed

immunotoxicity of the low affinity DCDD ligand (6, 149); however, consistent effects with this ligand on IgM secretion were not obtained.

Poland and Glover (197) discovered that the AhR binding affinity of TriCDD did not correlate with its biological potency. AhR binding (0.14 of TCDD) was much greater than the relative ability of TriCDD to induce hepatic hydroxylase activity in the chick embryo (0.0006 of TCDD). Poland and Glover (197) did not know the reason for this discrepancy but suggested a potential metabolic inactivation of TriCDD *in vivo*. This is in contrast to our results with the CH12.LX cells, in which the difference in potency between TCDD and TriCDD for *Cyp1a1* induction and inhibition of IgM secretion and μ expression was 0.07, 0.05 and 0.06, respectively (Table 2). This discrepancy between our results and those of Poland and Glover (197) may be due to differing kinetics of these responses as shown for μ expression, differences in the the experimental models and/or differences in metabolism, as suggested by Poland and Glover (197), which is consistent with the low drug metabolizing capability of lymphocytes. In any case, our results demonstrate a good correlation in the difference of potency between TCDD and TriCDD for each endpoint (Table 2).

The TEF, which is defined as the potency of an individual congener relative to TCDD, is 0.1 for the HxCDD congener (196). This is in general agreement with the difference in potency between TCDD and HxCDD for *Cyp1a1* induction (0.11) and inhibition of IgM secretion (0.19); however, the difference in potency for inhibition of  $\mu$  expression (0.4) is less than that for the other two responses (Table 2). Though the TEF is a rather fluid value, it may not account for differences across biological responses. For example, the AhR-nuclear complex may have differing affinities for DRE-like sites within various target genes; the number of DRE sites within a gene may also be an important factor in the magnitude of transcriptional regulation mediated through this response element. Additionally, AhR-mediated effects may occur independently of binding to the DRE, perhaps through an interaction with other cellular signaling pathways. In light of

these variables, a single TEF may not adequately reflect the toxicity of any given PCDD congener for all of its potential biological responses. This is underscored by the above discussion in which Poland and Glover (197) observed a low biological potency for the TriCDD congener relative to TCDD. These results do not correlate with the AhR binding affinity of TriCDD or with the much greater potency of this congener in the CH12.LX cells. Based on the Poland and Glover (197) results, a TEF value of 0 would be assigned to the TriCDD congener. However, the TEF value for this congener would be approximately 0.06 if based on the results from the CH12.LX cells. This suggests that multiple experimental models with several biological endpoints may be necessary to more adequately describe the biological potency of a particular AhR ligand.

The identification of several putative DREs within the  $3'\alpha$  enhancer of the mouse Ig heavy chain gene supports a potential role for DRE-dependent transcriptional regulation of the  $\mu$  gene (Figure 28). The 3' $\alpha$  enhancer is composed of four enhancer domains [C $\alpha$ 3'E,  $3'\alpha E(hs1,2)$ , hs3 and  $3'\alpha$ -hs4] which form a locus control region that appears to regulate high level Ig production and Ig heavy chain class switching (21, 22, 198). In addition, Dariavach and co-workers (20) demonstrated an approximately 2-fold increase in  $\mu$ expression, as measured by a ribonuclease protection assay, following transfection of a plasmacytoma with only the 3'αE(hs1,2) enhancer region. Addition of the other enhancer domains might result in a more profound effect on  $\mu$  expression which would be consistent with the results of Chauveau et al., (33) demonstrating the greatest transcriptional activity in a gene reporter assay with the entire 3'\alpha enhancer. We have identified a TCDDinducible protein-DNA complex by EMSA analysis with the 3'αE(hs1,2) and 3'α-hs4 Oligomers; each contain a DRE-like site (Figs. 29 and 30). Addition of unlabeled DRE3 competed for the TCDD-inducible complex suggesting that the protein complex is composed of AhR and ARNT. Further analysis by EMSA-Western demonstrated that the AhR and ARNT have affinity for the  $3'\alpha E(hs1,2)$  and  $3'\alpha$ -hs4 DREs and lends further

support for the premise of DRE-dependent regulation of  $\mu$  gene expression (Figs. 29 and 30).

Michaelson and coworkers (34) have demonstrated the regulation both the  $3'\alpha E(hs1,2)$  and  $3'\alpha$ -hs4 enhancers by  $\kappa B$  binding proteins. Interestingly, the  $3'\alpha$ -hs4 oligomer used in our studies contains a full kB binding site which overlaps the DRE binding motif (Figure 28). EMSA-Western analysis has identified TCDD-inducible protein binding, which does not include the AhR, to this KB site (Figure 31). Specifically, the second TCDD-inducible binding complex contained four NF-kB/Rel family members, p65, p50, c-Rel and RelB. Although the mechanism responsible for the TCDD-induced increase in kB binding is unknown, this increase is in general agreement with similar observations made by other laboratories (77, 173, 174, 199). The Puga laboratory has suggested that the increase in kB binding is due to TCDD-mediated oxidative stress which is a known inducer of NF-kB/Rel proteins (77, 173). Interestingly, kB binding was induced by TCDD with the AhR-deficient BCL-1 cells suggesting an AhR-independent induction of at least p65, RelB and c-Rel (Figure 32). Unlike the CH12.LX cells, p50 was not induced with the BCL-1 cells. Induction of NF-kB/Rel proteins by TCDD in the BCL-1 cells and normal LPS-induced IgM secretion in the presence of TCDD might suggest that activation of these proteins is not critical to the inhibition of IgM expression. However, the EMSA and EMSA-Western analyses were conducted using unstimulated cells and the effect of LPS-stimulation in the presence or absence of TCDD may be very similar to the TCDD effect seen in these BCL-1 experiments. In addition, the inhibition of IgM secretion by TCDD may require the induction of both DRE and kB binding. Since these sites overlap in the DRE flanking region, binding to either the DRE or kB motif may facilitate or stabilize binding to the other motif. Alternatively, there may be competition between the AhR/ARNT and NF-kB/Rel protein complexes for binding to these overlapping motifs which would not be ascertained in these experiments since the labeled oligomer is in excess to the nuclear protein. Furthermore, since NF-kB/Rel proteins bind DNA as dimers, they

are capable of complexing in a variety of combinations and each combination may have distinct transcriptional functions. TCDD may affect these dimerizations differently in the CH12.LX and BCL-1 cells (as seen with p50 and Rel B binding) perhaps resulting in an altered sensitivity of IgM expression between these cell lines. We have also identified a κB binding site within close proximity to the DRE site within the 3'αE(hs1,2) enhancer. However, the 3'αE(hs1,2) oligomer utilized in the present experiments only contains half of this κB motif (Figure 28). EMSA analysis did detect a rather diffuse TCDD-inducible band; although, the AhR was only present in a discrete region of this band. Therefore, it is presently unclear if this banding pattern is a result of NF-κB/Rel proteins binding to the κB half site or due to the binding of other proteins to other regions of the 3'αE(hs1,2) oligomer. Future studies utilizing an oligomer containing the entire κB response element will be required in order to adequately characterize whether NF-κB proteins are a component of these TCDD-inducible protein-DNA complexes.

The present studies demonstrate an essential role by the AhR in the inhibition of IgM secretion by PCDDs. However, more importantly, my results demonstrate TCDD-inducible binding of the AhR and  $\kappa B$  proteins to sites within the 3' $\alpha E$  enhancer, thus providing the first direct, putative link between TCDD-mediated transcriptional regulation and TCDD-induced inhibition of  $\mu$  gene expression. In addition, the magnitude of inhibition for  $\mu$  expression (from 70-80%) is concordant with the magnitude of inhibition for IgM protein secretion (approximately 60-70%). It will be interesting to characterize the interaction of TCDD-induced DRE and  $\kappa B$  binding and to determine their effect on transcriptional regulation of the 3' $\alpha$  enhancer, especially since the induction of  $\kappa B$  binding by TCDD appears to be AhR-independent. Interestingly, Harper and coworkers (200) have shown a significant decrease and delay in the IgG response to TNP-LPS in TCDD-treated mice. Analysis of two specific IgG isotypes demonstrate a significant decrease in the IgG2a response to interferon- $\gamma$  (IFN- $\gamma$ ) but no effect on the IgG1 response to IL-4 in P815 tumor challenged mice (201). These results are similar to the effects seen in

3'αE(hs1,2) knockout mice where LPS or LPS plus IL-4 induced class switch to IgG3, IgG2a and IgG2b was impaired, while class switch to IgG1 following LPS plus IL-4 treatment was normal (22). Taken together, these results indirectly support an effect of TCDD on the 3'αE(hs1,2) enhancer.

Until now, we have lacked an appropriate model to study, at a molecular level, the mechanisms involved in one of the most sensitive effects of TCDD exposure, alteration of B-cell function. A majority of the studies which have lead to the identification and characterization of the AhR have been performed using the hepatic cell line model, Hepa 1c1c7, and various clones derived from this cell line that are deficient, or express, a mutant form of the AhR or ARNT protein (202-204). However, B-cells are unique among the cellular targets of TCDD in that these cells require cellular activation prior to mediating their effector functions. Since the AhR may have a significant role in cellular proliferation and/or differentiation as discussed earlier, the B-cell may represent an important model for studying the role of the AhR in these processes. Development of the CH12.LX/BCL-1 cell line model has in this investigation provided considerable insight into the mechanism of TCDD-induced alteration of B-cell function and studies with this model have supported my hypothesis that an AhR/ARNT-DRE mechanism mediates, at least partly, TCDD-induced inhibition of Ig secretion. The induction of  $\kappa B$  binding in the 3' $\alpha$  enhancer appears to be AhR-independent and may imply that  $\kappa B$  binding is not critical to the inhibition of  $\mu$ expression by TCDD. However, an induction of kB binding may have profound effects on the vast number of genes that are regulated by NF-kB/Rel proteins. Further studies with this model should prove useful in elucidating other molecular events induced by TCDD in B-cells, such as increased Ca<sup>2+</sup> influx and protein phosphorylation as well as potential interactions with other signaling pathways (i.e., c-src, NF-κB, Sp1, and retinoblastoma protein).

LITERATURE CITED

## LITERATURE CITED

- 1. Vecchi, A., M. Sironi, M. Canegrati, M. Recchia, and S. Garattini. Immunosuppressive effects of 2,3,7,8-tetrachlorodibenzo-p-dioxin in strains of mice with different susceptibility to induction of aryl hydrocarbon hydroxylase. *Toxicol. Appl. Pharmacol.* **68**:434-441 (1983).
- 2. Kerkvliet, N. I., L. B. Steppan, J. A. Brauner, J. A. Deyo, M. C. Henderson, R. S. Tomar, and D. R. Buhler. Influence of the Ah locus on the humoral immunotoxicity of 2,3,7,8-tetrachlorodibenzo-p-dioxin: Evidence for Ah-receptor-dependent and Ah-receptor-independent mechanisms of immunosuppression. *Toxicol. Appl. Pharmacol.* 105:26-36 (1990).
- 3. Davis, D., and S. Safe. Immunosuppressive activities of polychlorinated dibenzofuran congeners: quantitative structure activity relationships and interactive effects. *Toxicol. Appl. Pharmacol.* **94:**141-149 (1988).
- 4. Harper, N., M. Steinberg, J. Thomsen, and S. Safe. Halogenated aromatic hydrocarbon-induced suppression of the plaque-forming cell response in B6C3F1 splenocytes cultured with allogenic mouse serum: Ah receptor structure activity relationships. *Toxicol.* 99:199-206 (1995).
- 5. Denison, M. S., C.L. Phelps, J. Dehoog, H.J. Kim, P.A. Bank, E.F. Yao, and P.A. Harper. Species variation in Ah receptor transformation and DNA binding. Banbury Report 35: Biological Basis for Risk Assessment of Dioxins and Related Compounds (1991).
- 6. Holsapple, M. P., J. A. McCay, and D. W. Barnes. Immunosuppression without liver induction by subchronic exposure to 2,7-dichlorodibenzo-p-dioxin in adult female B6C3F1 mice. *Toxicol. Appl. Pharmacol.* 83:445-455 (1986).
- 7. Morris, D. L., N. K. Snyder, R. E. Gokani, R. E. Blair, and M. P. Holsapple. Enhanced suppression of humoral immunity in DBA/2 mice following subchronic exposure to 2,3,7,8-tetrachlorodibenzo-p-dioxin (TCDD). *Toxicol. Appl. Pharmacol.* 112:128-132 (1992).
- 8. DeFranco, A. L. B-lymphocyte activation, in *Fundamental immunology* (W. E. Paul, ed.). Lippincott-Raven, Philadelphia, 225-261 (1999).
- 9. Fish, S., E. Zenowich, M. Fleming, and T. Manser. Molecular analysis of original antigenic sin. I. Clonal selection, somatic mutation and isotype switching during a memory B cell response. J. Exp. Med. 170:1191-1209 (1989).
- 10. Ulevitch, R. J., and P. S. Tobias. Receptor-dependent mechanisms of cell stimulation by bacterial endotoxin. *Ann. Rev. Immunol.* 13:437-457 (1995).
- 11. Chen, J., F. Young, A. Bottaro, V. Stewart, R. K. Smith, and F. W. Alt. *EMBO J.* 12:4635-4645 (1993).

- 12. Serwe, M., and F. Sablitzky. V(D)J recombination in B cells is impaired but not blocked by targeted deletion of the immunoglobulin heavy chain intron enhancer. *EMBO J.* 12:2321-2327 (1993).
- 13. Arulampalam, M., P. A. Grant, A. Samuelsson, U. Lendahl, and S. Pettersson. Lipopolysaccharide-dependent transactivation of the temporally regulated immunoglobulin heavy chain 3' enhancer. Eur. J. Immunol. 24:1671-1677 (1994).
- 14. Stall, A. M., F. G. M. Kroese, F. T. Gadus, D. G. Sieckmann, L. A. Herzenberg, and L. A. Herzenberg. Rearrangement and expression of endogenous immunoglobulin genes occur in many murine B cells expressing transgenic membrane IgM. *Proc. Natl. Acad. Sci. USA* 85:3546-3550 (1988).
- 15. Neuberger, M. S., H. M. Caskey, S. Pettersson, and G. T. S. Williams M. A. Isotype exclusion and transgene down-regulation in immunoglobulin-lambda transgenic mice. *Nature* 338:350-352 (1989).
- 16. Klein, S., F. Sablitsky, and A. Radbruch. Deletion of the IgH enhancer does not reduce immunoglobulin heavy chain production of a hybridoma IgD class switch variant. *EMBO J.* 3:2473-2476 (1984).
- 17. Wabl, M. R., and P. D. Burrows. Expression of immunoglobulin heavy chain at a high level in the absence of a proposed immunoglobulin enhancer element in cis. *Proc. Natl. Acad. Sci. USA* 81:2452-2455 (1984).
- 18. Aguilera, R. J., T. J. Hope, and H. Sakano. Characterization of immunoglobulin enhancer deletions in murine plasmacytomas. *EMBO J.* 4:3689-3693 (1985).
- 19. Eckhardt, L. A., and B. K. Birshtein. Independent immunoglobulin class-switch events occurring in a single myeloma cell line. *Mol. Cell. Biol.* 5:856-868 (1985).
- 20. Dariavach, P., G. T. Williams, K. Campbell, S. Pettersson, and M. S. Neuberger. The mouse IgH 3'-enhancer. *Eur. J. Immunol.* 21:1499-1504 (1991).
- 21. Lieberson, R., J. Ong, X. Shi, and L. A. Eckhardt. Immunoglobulin gene transcription ceases upon deletion of a distant enhancer. *EMBO* 14:6229-6238 (1995).
- 22. Cogne, M., R. Lansford, A. Bottaro, J. Zhang, J. Gorman, F. Young, H. Cheng, and F. W. Alt. A class switch control region at the 3' end of the immunoglobulin heavy chain locus. *Cell* 77:737-747 (1994).
- 23. Matthias, P., and D. Baltimore. The immunoglobulin heavy chain locus contains another B-cell specific 3' enhancer close to the α constant region. *Mol. Cell. Biol.* 13:1547-1553 (1993).
- 24. Michaelson, J. S., S. L. Giannini, and B. K. Birshtein. Identification of 3'α-hs4, a novel Ig heavy chain enhancer element regulated at multiple stages of B cell differentiation. *Nucleic Acids Res.* 23:975-981 (1995).

- 25. Madisen, L., and M. Groudine. Identification of a locus control region in the immunoglobulin heavy-chain locus that deregulates c-myc expression in plasmacytoma and Burkitt's lymphoma cells. *Genes Dev.* 8:2212-2226 (1994).
- 26. Saleque, S., M. Singh, R. D. Little, S. L. Giannini, J. S. Michaelson, and B. K. Birshtein. Dyad symmetry within the 3' IgH regulatory region includes two virtually identical enhancers (Cα3'E and hs3). *J. Immunol.* **158:**4780-4787 (1997).
- 27. Chaveau, C., and M. Cogne. Palindromic structure of the IgH 3' locus control region. *Nature Genet.* 14:15-16 (1996).
- 28. Giannini, S. L., M. Singh, C.-F. Calvo, G. Ding, and B. K. Birshtein. DNA regions flanking the mouse Ig 3'α enhancer are differentially methylated and DNase I hypersensitive during B cell differentiation. *J. Immunol.* **150**:1772-1780 (1993).
- 29. Lieberson, R., S. L. Giannini, B. K. Birshtein, and L. A. Eckhardt. An enhancer at the 3' end of the mouse immunoglobulin heavy chain locus. *Nucl. Acids Res.* 19:933-937 (1991).
- 30. Grant, P. A., V. Arulampalam, L. Ahrlund-Richter, and S. Petterson. Identification of ets-like lymphoid specific elements within the immunoglobulin heavy chain 3' enhancer. *Nucl. Acids Res.* 20:4401-4408 (1992).
- 31. Neurath, M. F., W. Strober, and Y. Wakatsuki. The murine Ig 3'α enhancer is a target site with repressor function for the B cell lneage-specific transcription factor BSAP (NF-HB, Sα-BP). J. Immunol. 153:730-742 (1994).
- 32. Singh, M., and B. K. Birshtein. NF-HB (BSAP) is a repressor of the murine immunoglobulin heavy-chain 3'α enhancer at early stages of B cell differentiation. *Mol. Cell. Biol.* 13:3611 (1993).
- 33. Chauveau, C., E. Pinaud, and M. Cogne. Synergies between regulatory elements of the immunoglobulin heavy chain locus and its palindromic 3' locus control region. *Eur. J. Immunol.* 28:3048-3056 (1998).
- 34. Michaelson, J. S., M. Singh, C. M. Snapper, D. B. Sha, and K. Birshtein. Regulation of 3' IgH enhancers by a common set of factors including κB-binding proteins. J. Immunol. 156:2828-2839 (1996).
- 35. Birshtein, B. K., C. Chen, S. Saleque, J. S. Michaelson, M. Singh, and R. D. Little. *Murine and human 3' IgH regulatory sequences*. Springer-Verlag, Berlin Heidelberg (1997).
- 36. Gregor, P. D., and S. L. Morrison. Myeloma mutant with a novel 3' flanking region: loss of normal sequence and insertion of repetitive elements leads to decreased transcription but normal processing of the alpha heavy-chain gene products. *Mol. Cell. Biol.* 6:1903-1916 (1986).

- 37. Lieberson, R., J. Ong, X. Shi, and L. A. Eckhardt. Transcription of an immunoglobulin γ2a gene ceases upon deletion of an enhancer region over 70 kilobases away. *EMBO J.* **14**:6229-6238 (1995).
- 38. Neurath, M. F., E. E. Max, and W. Strober. Pax5 (BSAP) regulates the murine immunoglobulin 3'α enhancer by suppressing binding of NF-αP, a protein that controls heavy chain transcription. *Proc. Natl. Acad. Sci. USA* 92:5336-5340 (1995).
- 39. Singh, M., and B. K. Birshtein. Concerted repression of an immunoglobulin heavy chain 3'α enhancer (3'αΕ). *Proc. Natl. Acad. Sci. USA* 93:4392-4397 (1996).
- 40. Snapper, C. M., and F. D. Finkelman. Immunoglobulin class switching, in Fundamental immunology (W. E. Paul, ed.). Lippincott-Raven, Philadelphia, 831-861 (1999).
- 41. Adams, B., P. Dorfler, A. Aguzzi, Z. Kozmik, P. Urbanek, I. Maurer-Fogy, and M. Busslinger. Pax-5 encodes the transcription factor BSAP and is expressed in B lymphocytes, the developing CNS, and adult testis. *Genes Dev.* 6:1589 (1992).
- 42. Barberis, A., K. Widenhorn, L. Vitelli, and M. Busslinger. A novel B-cell lineage-specific transcription factor present at early but not late stages of differentiation. *Genes Dev.* 4:849 (1990).
- 43. Kozmik, Z., S. Wang, B. Dorfler, B. Adams, and M. Busslinger. The promoter of the CD19 gene is a target for the B-cell-specific transcription factor BSAP. *Mol. Cell. Biol.* 12(2662) (1992).
- Zwollo, P., and S. Desiderio. Specific recognition of the blk promoter by the B-lymphoid transcription factor B-cell-specific activator protein. J. Biol. Chem.
   269(21):15310-15317 (1994).
- Okabe, T., T. Watanabe, and A. Kudo. A pre-B- and B cell-specific DNA-binding protein, EBB-1, which binds to the promoter of the V<sub>preB1</sub> gene. Eur. J. Immunol.
   22:37-43 (1992).
- 46. Urbanek, P., Z. Wand, I. Fetka, E. F. Wagner, and M. Busslinger. Complete block of early B cell differentiation and altered patterning of the posterior midbrain in mice lacking Pax5/BSAP. Cell 79:901-912 (1994).
- 47. Liao, F., S. L. Giannini, and B. K. Birshetein. A nuclear DNA-binding protein expressed during early stages of B cell differentiation interacts with diverse segments within and 3' of the Ig H chain gene cluster. *J. Immunol.* 148:2909 (1992).
- 48. Rothman, P., S. C. Li, B. Gorham, L. Glimcher, F. Alt, and M. Boothby. Identification of a conserved lipopolysaccharide-plus-interleukin-4-responsive element located at the promoter of germline ε transcripts. *Mol. Cell. Biol.* 11:5551 (1991).

- 49. Waters, S. H., K. U. Saikh, and J. Stavnezer. A B-cell-specific nuclear protein that binds to DNA sites 5' to immunoglobulin Sα tandem repeats is regulated during differentiation. *Mol. Cell. Biol.* 9(12):5594-5601 (1989).
- 50. Wakatsuki, Y., M. F. Neurath, E. E. Max, and W. Strober. The B cell-specific transcription factor BSAP regulates B cell proliferation. *J. Exp. Med.* 179:1099-1108 (1994).
- 51. Baeuerle, P. A., and T. Henkel. Function and activation of NF-κB in the immune system. *Annu. Rev. Immunol.* 12:141-179 (1994).
- 52. Siebenlist, U., G. Franzoso, and K. Brown. Structure, regulation and function of NF-κB. Annu. Rev. Cell Biol. 10:405-455 (1994).
- 53. Thanos, D., and T. Maniatis. NF-κB: A lession in family values. Cell 80:529-532 (1995).
- 54. Stancovski, I., and D. Baltimore. NF-kB activation: The IkB kinase revealed? *Cell* 91:299-302 (1997).
- 55. Beg, A. A., and A. S. Baldwin. The I kappa B proteins: multifunctional regulators of Rel/NF-kappa B transcription factors. *Genes Dev.* 7(2064-2070) (1993).
- 56. Mellits, K. H., R. T. Hay, and S. Goodbourn. Proteolytic degradation of MAD3 (I kappa B alpha) and enhanced processing of the NF-kappa B precursor p105 are obligatory steps in the activation of NF-kappa B. *Nucl. Acids Res.* 21:5059-5066 (1993).
- 57. Naumann, M., and C. Scheidereit. Activation of NF-kappa B in vivo is regulated by multiple phosphorylations. *EMBO J.* 13:4597-4607 (1994).
- 58. May, M. J., and S. Ghosh. IkB kinases: Kinsmen with different crafts. *Science* **284:**271-273 (1999).
- 59. Baldwin, A. S. The NF-κB and IκB proteins: New discoveries and insights. Ann. Rev. Immunol. 14:649-681 (1996).
- 60. Baeuerle, P. A., and D. Baltimore. NF-kappa B: ten years after. Cell 87:13-20 (1996).
- 61. Sen, R., and D. Baltimore. Inducibility of kappa immunoglobulin enhancer-binding protein N F-kappa B by a posttranslational mechanism. *Cell* 47:921-928 (1986).
- 62. Liou, H. C., W. Sha, M. Scott, and D. Baltimore. Sequential induction of NF-κB/Rel family proteins during B-cell terminal differentiation. *Mol. Cell. Biol.* 14:5349-5359 (1994).

- 63. Miyamoto, S., P. Chiao, and I. Verma. Enhanced IκBα degradation is responsible for constitutive NF-κB activity in mature B-cell lines. *Mol. Cell. Biol.* 14:3276-3282 (1994).
- 64. Sha, W., H. C. Liou, E. Tuomanen, and D. Baltimore. Targeted disruption of the p50 subunit of NF-κB leads to multifocal defects in immune responses. *Cell* 80:321-330 (1995).
- Delphin, S., and J. Stavnezer. Characterization of an IL-4 responsive region in the Ig heavy chain ε germline promoter: regulation by NF-IL4, a C/EBP family member and NFκ-B p50. J. Exp. Med. 181:181-192 (1995).
- 66. Kontgen, F., R. Grumont, A. Strasser, D. Metcalf, R. Li, D. Tarlinton, and S. Gerondakis. Mice lacking the c-Rel proto-oncogene exhibit defects in lymphocyte proliferation, humoral immunity, and IL-2 expression. *Genes Dev.* 9:1965-1977 (1995).
- Weih, F., D. Carrasco, S. Durham, D. Barton, C. Rizzo, R. P. Ryseck, S. Lira, and R. Bravo. Multiorgan inflammation and hematopoietic abnormalities in mice with a targeted disruption of RelB, a member of the NF-κB/Rel family. *Cell* 80:331-340 (1995).
- 68. Burkly, L., C. Hession, L. Ogata, C. Reilly, L. Marconi, D. Olson, R. Tizard, R. Cate, and D. Lo. Expression of relB is required for the development of thymic medulla and dendritic cells. *Nature* 373:531-536 (1995).
- 69. Beg, A., W. Sha, R. Bronson, S. Ghosh, and D. Baltimore. Embryonic lethality and liver degeneration in mice lacking the RelA component of NF-κB. *Nature* 376(167-170) (1995).
- 70. Veterans and Agent Orange: Health effects of herbicides used in Vietnam. Institute of Medicine. National Academy Press, Washington DC (1994).
- 71. Knutson, A. P. Immunologic effects of TCDD exposure in humans. *Bull. Environ. Contam. Toxicol.* 33:673 (1984).
- 72. Webb, K., R. G. Evans, P. Stehr, and S. M. Ayres. Pilot study on health effects of environmental 2,3,7,8-TCDD in Missouri. *Arch. Environ. Health* 41:16 (1987).
- 73. Pocchiari, F., V. Silano, and A. Zampieri. Human health effects from accidental release of tetrachlorodibenzo-p-dioxin. *Ann. N. Y. Acad. Sci.* **320:**311 (1979).
- 74. Tognoni, G., and A. Bonaccorsi. Epidemiological problems with TCDD. *Drug Metab. Rev.* 13(3):447 (1982).
- 75. Poland, A., and J. C. Knutson. 2,3,7,8-tetrachlorodibenzo-p-dioxin and related aromatic hydrocarbons: examination of the mechanism of toxicity. *Annu. Rev. Pharmacol. Toxicol.* 22:517-554 (1982).

- 76. Whitlock, J. P., Jr. Genetic and molecular aspects of 2,3,7,8-tetrachlorodibenzo-p-dioxin action. *Annu. Rev. Pharmacol. Toxicol.* **30:**251-277 (1990).
- 77. Yao, Y., A. Hoffer, C. Chang, and A. Puga. Dioxin activates HIV-1 gene expression by an oxidative stress pathway requiring a functional cytochrome P450 CYP1A1 enzyme. *Environ. Health Perspect.* 103:366-371 (1995).
- 78. Shertter. Dioxin causes a sustained oxidative stress response in the mouse. *Biochem. Biophys. Res. Commun.* 253:44-48 (1998).
- 79. Safe, S. H. Modulation of gene expression and endocrine response pathways by 2,3,7,8-tetrachlorodibenzo-p-dioxin and related compounds. *Pharmac. Ther.* 67(2):247-281 (1995).
- 80. Whitlock, J. P., Jr. The regulation of gene expression by 2,3,7,8-tetrachlorodibenzo-p-dioxin. *Pharmacological Reviews* 39(2):147-161 (1987).
- 81. Matsumura, F. How important is the protein phosphorylation pathway in the toxic expression of dioxin-type chemicals? *Biochem. Pharmacol.* 48(2):215-224 (1994).
- 82. Poland, A., and E. Glover. Comparison of 2,3,7,8-tetrachlorodibenzo-p-dioxin, a potent inducer of aryl hydrocarbon hydroxylase, with 3-methylcholanthrene. *Mol. Pharmacol.* 10:349-359 (1974).
- 83. Thomas, P. E., R. E. Kouri, and J. J. Hutton. The genetics of aryl hydrocarbon hydroxylase induction in mice: a single gene difference between C57BL/6J and DBA/2J. *Biochem. Genet.* 6:157-168 (1972).
- 84. Schmid, F. A., I. Elmer, and G. S. Tarnowski. Genetic determination of differential inflammatory reactivity and subcutaneous tumor susceptibility of AKR/J and C57BL/6J mice to 7,12-dimethylbenz(a)anthracene. *Cancer Res.* 29:1585-1589 (1969).
- 85. Poland, A., and E. Glover. Genetic expression of aryl hydrocarbon hydroxylase by 2,3,7,8-tetrachlorodibenzo-p-dioxin: evidence for a receptor mutation in genetically non-responsive mice. *Mol. Pharmacol.* 11:389-398 (1975).
- 86. Holsapple, M. P., N.K. Synder, S.C. Wood, and D.L. Morris. A review of 2,3,7,8-tetrachlorodibenzo-p-dioxin-induced changes in immunocompetence: 1991 update. *Toxicol.* **69:**219-255 (1991).
- 87. Vos, J. G., and J. A. Moore. Suppression of cellular immunity in rats and mice by maternal treatment with 2,3,7,8-tetrachlorodibenzo. *Int. Arch. Allergy* 47:777 (1974).
- 88. Kociba, R. J., P. A. Keeler, C. N. Park, and P. J. Gehring. 2,3,7,8-tetrachlorodibenzo-p-dioxin (TCDD): Results of a 13-week oral toxicity study in rats. *Toxicol. Appl. Pharmacol.* 35:553 (1976).
- 89. Greenlee, W. F., K. M. Dold, R. D. Irons, and R. Osborne. Evidence for direct action of 2,3,7,8-tetrachlorodibenzo-p-dioxin (TCDD) on thymic epithelium. *Toxiol. Appl. Pharmacol.* **79:**112-120 (1985).

- 90. Staples, J. E., F. G. Murante, N. C. Fiore, T. A. Gasiewicz, and A. E. Silverstone. Thymic alterations induced by 3,4,7,8-tetrachlorodibenzo-p-dioxin are strictly dependent on aryl hydrocarbon receptor activation in hemopoietic cells. *J. Immunol.* 160:3844-3854 (1998).
- 91. Dean, J. H., and L. D. Lauer. Immunological effects following exposure to 2,3,7,8-tetrachlorodibenzo-p-dioxin: a review, in *Public Health Risk of the Dioxins* (W. W. Lowrance, ed.). William Kaufmann, Los Altos, CA, 275 (1984).
- 92. Luster, M. I., A. N. Tucker, L. Hong, G. A. Boorman, and R. Patterson. In vivo and in vitro effects of TCDD on stem cell and B cell differentiation, in *Banbury Report 18: Biological Mechanisms of Dioxin Action* (R. D. Kimbrough, ed.). Cold Spring Harbor Laboratory, 401 (1984).
- 93. Tucker, A. N., S. J. Vore, and M. I. Luster. Suppression of B cell differentiation by 2,3,7,8-tetrachlorodibenzo-p-dioxin. *Mol. Pharmacol.* **29:**372-377 (1986).
- 94. Vecchi, A., M. Mantovani, M. Sironi, W. Luini, M. Cairo, and S. Garattini. Effect of acute exposure to 2,3,7,8-tetrachlorodibenzo-p-dioxin on humoral antibody production in mice. *Chem. Biol. Interact.* 30:337-342 (1980).
- 95. Kerkvliet, N. I., L. Baecher-Steppan, B. B. Smith, J. A. Youngberg, M. C. Henderson, and D. R. Buhler. Role of the Ah locus in suppression of cytotoxic T lymphocyte activity by halogenated aromatic hydrocarbons (PCBs and TCDD): Structure-activity relationships and effects in C57Bl/6 mice congenic at the Ah locus. (1990).
- 96. Chastain, J. E., Jr., and T. L. Pazdernik. 2,3,7,8-tetrachlorodibenzo-p-dioxin (TCDD)-induced immunotoxicity. *Int. J. Immunopharmacol.* 7(6):849-856 (1985).
- 97. Dooley, R. K., and M. P. Holsapple. Elucidation of the cellular targets responsible for 2,3,7,8-tetrachlorodibenzo-p-dioxin (TCDD)-induced suppression of the antibody response: I. The role of the B lymphocyte. *Immunopharmacol.* 16:167-180 (1988).
- 98. Dooley, R. K., D. L. Morris, and M. P. Holsapple. Elucidation of cellular targets responsible for 2,3,7,8-tetrachlorodibenzo-p-dioxin (TCDD)-induced suppression of antibody responses: II. The role of the T lymphocytes. *Immunopharmacology* 19:47-58 (1990).
- 99. Snyder, N., C. Kramer, R. Dooley, and M. Holsapple. Characterization of protein phosphorylation by 2,3,7,8-tetrachlorodibenzo-p-dioxin in murine lymphocytes: indirect evidence for a role in the suppression of humoral immunity. *Drug Chem. Toxicol.* 16(2):135-163 (1993).
- 100. Clark, G. C., J. A. Blank, D. R. Germolec, and M. I. Luster. 2,3,7,8-Tetrachlorodibenzo-p-dioxin stimulation of tyrosine phosphorylation in B lymphocytes: Potential role in immunosuppression. *Mol. Pharmacol.* 39:495-501 (1991).

- 101. Karras, J., and M. Holsapple. Inhibition of calcium-dependent B cell activation by 2,3,7,8-tetrachlorodibenzo-p-dioxin. *Toxicol. Appl. Pharmacol.* 125:264-270 (1994).
- 102. Karras, J., D. Morris, R. Matulka, C. Kramer, and M. Holsapple. 2,3,7,8-Tetrachlorodibenzo-p-dioxin (TCDD) elevates basal B-cell intracellular calcium concentration and suppresses surface Ig- but not CD40-induced antibody secretion. *Toxicol. Appl. Pharmacol.* 137:275-284 (1996).
- 103. Shepherd, D. M., and N. I. Kerkvliet. The effects of TCDD on the activation of OVA-specific DO11.10 transgenic T cells in adoptively-transferred mice. *Toxicologist* **48:**306 (1999).
- 104. Lawrence, B. P., M. Leid, and N. I. Kerkvliet. Distribution and behavior of the Ah receptor in murine T lymphocytes. *Toxicol. Appl. Pharmacol.* 138:275-284 (1996).
- 105. Ema, M., K. Sogawa, N. Watanabe, Y. Cujoh, N. Matsushita, O. Gotoh, Y. Funae, and Y. Fujii-Kuriyama. cDNA cloning and structure of mouse putative Ah receptor. *Biochem. Biophys. Res. Commun.* 184:246-253 (1992).
- 106. Burbach, C. M., A. Poland, and C. A. Bradfield. Cloning of the Ah-receptor cDNA reveals a distinctive ligand-activated transcription factor. *Proc. Natl. Acad. Sci. USA* 89:8185-8189 (1992).
- 107. Harper, P. A., R. D. Prokipcak, L. E. Bush, C. L. Golas, and A. B. Okey. Detection and characterization of the Ah receptor for 2,3,7,8-tetrachlorodibenzo-p-dioxin in human colon adenocarcinoma cell line LS180. *Arch. Biochem. Biophys.* 290:27-36 (1991).
- 108. Rowlands, J. C., and J. Gustafsson. Aryl hydrocarbon receptor-mediated signal transduction. *Crit. Rev. Toxicol.* 27:109-134 (1997).
- 109. Enan, E., and F. Matsumura. Identification of c-Src as the integral component of the cytosolic Ah receptor complex, transducing the signal of 2,3,7,8-tetrachlorodibenzo-p-dioxin (TCDD) through the protein phosphorylation pathway. *Biochem. Pharm.* 52:1599-1612 (1996).
- 110. Ma, Q., and J. P. Whitlock Jr. A novel cytoplasmic protein that interacts with the Ah receptor, contains tetratricopeptide repeat motifs, and augments the transcriptional response to 2,3,7,8-tetrachlorodibenzo-p-dioxin. J. Biol. Chem. 272:8878-8884 (1997).
- 111. Pollenz, R. S., C. A. Sattler, and A. Poland. The Aryl Hydrocarbon Receptor and Aryl Hydrocarbon Receptor Nuclear Translocator Protein Show Distinct Subcellular Localizations in Hepa 1c1c7 Cells by Immunfluorescence Microscopy. *Mol. Pharmacol.* 45:428-438 (1994).
- 112. Carver, L. A., J. J. LaPres, S. Jain, E. E. Dunham, and C. A. Bradfield. Characterization of the Ah receptor-associated protein, ARA9. *J. Biol. Chem.* 273:33580-33587 (1998).

- 113. Reyes, H., S. Reisz-Porszasz, and O. Hankinson. Identification of the Ah Receptor Nuclear Translocator Protein (ARNT) as a Component of the DNA Binding Form of the Ah Receptor. *Science* **256**:1193-1195 (1992).
- 114. Perdew, G. H. Association of the Ah receptor with the 90-kDa heat shock protein. J. Biol. Chem. 263(27):13802-13805 (1988).
- 115. Denis, M., S. Cuthill, A. C. Wikstroem, L. Poellinger, and J. A. Gustafsson. Association of the dioxin receptor with the Mr 90,000 heat shock protein. *Biochem. Biophys. Res. Commun.* 155:801-807 (1988).
- 116. Pongratz, I. G., G. F. Masson, and L. Poellinger. Dual roles of the 90-kDa heat shock protein hsp90 in modulating functional activities of the dioxin receptor. *J. Biol. Chem.* 267:13728-13734 (1992).
- 117. Okey, A. B., G. P. Bondy, M. Mason, D. W. Nebert, C. J. Forester-Gibson, J. Muncan, and M. J. Dufresne. Temperature-dependent cytosol-to-nuclear translocation of the Ah receptor for 2,3,7,8-tetrachlorodibenzo-p-dioxin in continuous cell culture lines. J. Biol. Chem. 255:11415-11422 (1980).
- 118. Cuthill, S., L. Poellinger, and J. A. Gustafsson. The receptor for 2,3,7,8-tetrachlorodibenzo-p-dioxin in the mouse hepatoma cell line Hepa 1c1c7. *J. Biol. Chem.* 262:3477-3481 (1987).
- 119. Probst, M. P., S. Reisz-Porszasz, R. V. Agbunag, M. S. Ong, and O. Hankinson. Role of the Aryl Hydrocarbon Receptor Nuclear Translocator Protein in Aryl Hydrocarbon (Dioxin) Receptor Action. *Mol. Pharmacol.* 44:511-518 (1993).
- 120. Ma, X., and J. G. Babish. 2,3,7,8-Tetrachlorodibenzo-p-dioxin increases tyrosine phosphorylation of murine hepatic p34 (cdc2) kinase *in vivo* and *in vitro*. *Toxicologist* 13(1112) (1993).
- 121. Ma, X., N. A. Mufti, and B. J. G. Protein tyrosine phosphorylation as an indicator of 2,3,7,8-tetrachlorodibenzo-p-dioxin exposure in vivo and in vitro. Biophys. Res. Commun. 189:59-65 (1992).
- 122. Hoffman, E. C., H. Reyes, F. F. Chu, F. Sander, L. H. Conley, B. A. Brooks, and O. Hankinson. Cloning of a factor required for activity of the Ah (dioxin) receptor. *Science (Washington D.C.)* 252:954-958 (1991).
- 123. Fujisawa-Sehara, A., K. Sogawa, M. Yamane, and Y. Fujii-Kuriyama. Characterization of xenobiotic responsive elements upstream from the drug metabolizing cytochrome P450c gene: a similarity to glucocorticoid response elements. *Nucleic Acids Res.* 15:4179-4191 (1987).
- 124. Elferink, C. J., T. A. Gasiewicz, and J. P. Whitlock. Protein-DNA interactions at a dioxin-responsive enhancer. *J. Biol. Chem.* 265:20708-20712 (1990).
- 125. Sutter, T. R., and W. F. Greenlee. Classification of members of the Ah gene battery. *Chemosphere* 25:223-226 (1992).

- 126. Watson, A. J., and O. Hankinson. Dioxin and Ah receptor-dependent protein binding to xenobiotic responsive elements and G-rich DNA studied by in vivo footprinting. J. Biol. Chem. 266:6874-6878 (1992).
- 127. Hakansson, H., L. Johansson, E. Manzoor, and U. G. Ahlborg. Effect of 2,3,7,8-tetrachlorodibenzo-p-dioxin on the hepatic 7-ethoxyresorufin 0-deethylase activity in four rodent species. *Eur. J. Pharmacol.* 270:279-284 (1994).
- 128. Sutter, T. R., K. Guzman, K. M. Dold, and W. F. Greenlee. Targets for dioxingenes for plasminogen activator inhibitor-2 and interleukin-1β. *Science* **254**:415-418 (1991).
- 129. Gaido, K. W., S. C. Maness, L. S. Leonard, and W. F. Greenlee. 2,3,7,8-Tetrachlorodibenzo-p-dioxin-dependent regulation of transforming growth factors- $\alpha$  and  $\beta_2$  expression in a human keratinocyte cell line involves both transcriptional and post-transcriptional control. *J. Biol. Chem.* 267(34):24591-24595 (1992).
- 130. Astroff, B., C. Rowlands, R. Dickerson, and S. Safe. 2,3,7,8-Tetrachlorodibenzo-p-dioxin inhibition of 17 beta-estradiol-induced increases in rat uterine epidermal growth factor receptor binding activity and gene expression. *Mol. Cell. endocrinol.* 72:247-252 (1990).
- 131. Lu, Y., X. Wang, and S. Safe. Interaction of 2,3,7,8-tetrachlorodibenzo-p-dioxin and retinoic acid in MCF-7 human breast cancer cells. *Toxicol. Appl. Pharmacol.* 127:1-8 (1994).
- 132. Puga, A., D. Nebert, and F. Carrier. Dioxin induces expression of c-fos and c-jun proto-oncogenes and a large increase in transcription factor AP-1. *DNA Cell Biol.* 11(4):269-281 (1992).
- 133. Silverstone, A. E., D. E. Frazier, N. C. Fiore, J. A. Soults, and T. A. Gasiewicz. Dexamethasone, beta-estradiol, and 2,3,7,8-tetrachlorodibenzo-p-dioxin elicit thymic atrophy through different cellular targets. *Toxicol. Appl. Pharmacol.* 126:248-259 (1994).
- 134. Lai, Z., T. Pineau, and C. Esser. Identification of dioxin-responsive elements (DREs) in the 5' regions of putative dioxin-inducible genes. *Chemico-Biological Interactions* 100:97-112 (1996).
- 135. Tian, Y., S. Ke, M. S. Denison, A. B. Rabson, and M. A. Gallo. Ah receptor and NF-kB interactions, a potential mechanism for dioxin toxicity. *J. Biol. Chem.* 274:510-515 (1999).
- 136. Kobayashi, A., S. Kazuhiro, and Y. Fujji-Kuriyama. Cooperative interaction between AhR•ARNT and Sp1 for the drug-inducible expression of Cyp1a1 gene. *J. Biol. Chem.* 271:12310-12316 (1996).
- 137. Swanson, H. I., and J. Yang. The aryl hydrocarbon receptor interacts with transcription factor IIB. *Mol. Pharmacol.* **54:**671-677 (1998).

- 138. Ge, N., and C. J. Elferink. A direct interaction between the aryl hydrocarbon receptor and retinoblastoma protein. J. Biol. Chem. 273:22708-22713 (1998).
- 139. Poland, A., D. Palen, and E. Glover. Analysis of the four alleles of the murine aryl hydrocarbon receptor. *Mol. Pharmacol.* **46:**915-921 (1994).
- 140. Sinal, C. J., and J. R. Bend. Aryl hydrocarbon receptor-dependent induction of Cyp1a1 by bilirubin in mouse hepatoma Hepa 1c1c7 cells. *Mol. Pharmacol.* 52:590-599 (1997).
- 141. Dzeletovic, N., J. McGuire, M. Daujat, J. Tholander, M. Ema, Y. Fujii-Kuriyama, J. Bergman, P. Maurel, and L. Poellinger. Regulation of dioxin receptor function by omeprazole. *J. Biol. Chem.* 272:12705-12713 (1997).
- 142. Kleman, M. I., L. Poellinger, and J. Gustafsson. Regulation of human dioxin receptor function by indolocarbazoles, receptor ligands of dietary origin. *J. Biol. Chem.* **269:**5137-5144 (1994).
- 143. Heath-Pagliuso, S., W. J. Rogers, K. Tullis, S. D. Seidel, P. H. Cenijn, A. Brouwer, and M. S. Denison. Activation of the Ah receptor by tryptophan and tryptophan metabolites. *Biochem.* 37:11508-11515 (1998).
- 144. Safe, S. H. Comparative toxicology and mechanism of action of polychlorinated dibenzo-p-dioxins and dibenzofurans. *Ann. Rev. Pharmacol. Toxicol.* **26:371** (1986).
- 145. Goldstein, J. A., and S. Safe. Mechanism of action and structure-activity relationship for the chlorinated dibenzo-p-dioxins and related compounds, in *In: Halogenated Biphenyls, Terphenyls, Naphthlaenes, Dibenzodioxins and Related Products* (R. D. Kimbrough and A. A. Jensen, ed.). Elsevier Science Publishers B.V. (Biomedical Division), Amsterdam, 239 (1989).
- 146. Sharma, R. P., and P. J. Gehring. Effects of 2,3,7,8-tetrachlorodibenzo-p-dioxin (TCDD) on splenic lymphocyte transformation in mice after a single and repeated exposure. *Ann. N.Y. Acad. Sci.* 320:487-497 (1979).
- 147. Lorenzen, A., and A.B. Okey. Detection and characterization of Ah receptor in tissue and cells from human tonsils. *Toxicol. Appl. Pharmacol.* 107:203-214 (1991).
- 148. Neumann, C. M., L. B. Steppan, and N. I. Kerkvliet. Distribution of 2,3,7,8-tetrachlorodibenzo-p-dioxin in splenic tissue of C57BL/6J mice. *Drug Metab. Dispos.* 20:467-469 (1992).
- 149. Holsapple, M. P., R. K. Dooley, P. J. McNerney, and J. A. McCay. Direct suppression of antibody responses by chlorinated dibenzodioxins in cultured spleen cells from (C57BL/6 x C3H)F1 and DBA/2 mice. *Immunopharmacol.* 12:175-186 (1986).
- 150. Masten, S. A., and K. T. Shiverick. The Ah receptor recognizes DNA binding sites for the B cell transcription factor, BSAP: a possible mechanism for dioxin-mediated

- alteration of CD19 gene expression in human B lymphocytes. *Biochem. Biophys. Res. Comm.* 212(1):27-34 (1995).
- 151. Tedder, T. F., L. J. Zhou, and P. Engel. The CD19/CD21 signal transduction complex of B lymphocytes. *Immunol. Today* 15:437-442 (1994).
- 152. Bishop, G. A., and G. Haughton. Induced differentiation of a transformed clone of Ly-1+ B cells by clonal T cells and antigen. *Proc. Natl. Acad. Sci. USA* 83:7410-7414 (1986).
- 153. Slavin, S., and S. Strober. Spontaneous murine B-cell leukaemia. *Nature* 272(13):624-626 (1978).
- 154. Gronowicz, E., C. Doss, F. Howard, D. Morrison, and S. Strober. An in vitro line of the B cell tumor BCL<sub>1</sub> can be activated by LPS to secrete IgM. *J. Immunol.* 125(3):976-980 (1980).
- 155. Chomczynski, P., and N. Sacchi. Single-Step Method of RNA Isolation by Acid Guanidium Thiocyanate-Phenol-Chloroform Extraction. *Anal. Biochem.* 162:156-159 (1987).
- 156. Chomczynski, P. A reagent for the single-step simultaneous isolation of RNA, DNA and proteins from cell and tissue samples. *Biotechniques* 15:532-537 (1993).
- 157. Chomczynski, P., and K. Mackey. Substitution of chloroform with bromochloroproane in the single-stip method of RNA isolation. *Anal Biochem* **225**:163-164 (1995).
- 158. Gilliland, G., S. Perrin, and H. Bunn. Competitive PCR for quantitation of mRNA. *In: Innis, M.A. et al. (eds), PCR Protocols: A Guide to Methods and Applications*. San Deigo, CA: Academic Press, Inc., 60-66 (1990).
- 159. Gilliland, G., K. Perrin, K. Blanchard, and H. Bunn. Analysis of cytokine mRNA and DNA: detection and quantitation by competitive polymerase chain reaction. *Proc. Natl. Acad. Sci., USA* 87:2725-2729 (1990).
- Vanden Heuvel, J., F. Tyson, and D. Bell. Construction of Recombinant RNA Templates for Use as Internal Standards in Quantitative RT-PCR. *BioTechniques* 14:395-398 (1993).
- 161. Kaminski, N. E., W. S. Koh, K. H. Yang, M. Lee, and F. K. Kessler.
  Suppression Of The Humoral Immune Response By Cannabinoids Is Partially
  Mediated Through Inhibition Of Adenylate Cyclase By A Pertussis Toxin-Sensitive
  G-Protein Coupled Mechanism. *Biochem. Pharm.* 48(10):1899-1908 (1994).
- 162. Denison, M. S., and E. F. Yao. Characterization of the Interaction of Transformed Rat Hepatic Cytosolic Ah Receptor with a Dioxin Responsive Transcriptional Enhancer. *Arch. Biochem. Biophys.* 284(1):158-166 (1991).
- 163. Carver, L. A., J. B. Hogenesch, and C. A. Bradfield. Tissue specific expression of the rat Ah-receptor and ARNT mRNAs. *Nucleic Acids Res.* 22(15):3038-3044 (1994).

- 164. Poland, A., E. Glover, and B. A. Taylor. The murine Ah locus: a new allele and mapping to chromosome 12. *Mol. Pharmacol.* 32:471-478 (1987).
- 165. Poland, A., and E. Glover. Ca<sup>2+</sup>-Dependent Proteolysis of the Ah Receptor. Arch. Biochem. Biophys. 261:103-111 (1988).
- 166. Garrison, P. M., and M. S. Denison. Characterization of the promoter and 5' flanking region of the murine Ah receptor gene. *Toxicologist* 30:1683 (1996).
- 167. Jones, P. B. C., D. R. Galeazzi, J. M. Fisher, and J. P. Whitlock Jr. Control of cytochrome P<sub>1</sub>-450 gene expression by dioxin. *Science* 227:1499-1502 (1985).
- 168. Jones, P. B. C., D. L.K., D. R. Galeazzi, and J. P. Whitlock Jr. Control of cytochrome P<sub>1</sub>-450 gene expression: analysis of a dioxin-responsive enhancer system. *Proc. Natl. Acad. Sci. USA* 83:2802-2806 (1986).
- Jones, P. B. C., L. K. Durrin, J. M. Fisher, and J. P. Whitlock Jr. Control of gene expression by 2,3,7,8-tetrachlorodibenzo-p-dioxin: multiple dioxin-responsive domains 5'-ward of the cytochrome P1-450 gene. J. Biol. Chem. 261:6647-6650 (1986).
- 170. Poland, A., W. F. Greenlee, and A. S. Kende. Studies on the mechanism of action of the chlorinated dibenzo-p-dioxins and related compounds. *Ann. N. Y. Acad. Sci.* 320:214-230 (1979).
- 171. Poland, A., and E. Glover. Chlorinated dibenzo-p-dioxins: Potent inducers of δ-aminolevulinic acid synthetase and aryl hydrocarbon hydroxylase. *Mol. Pharmacol.* 9:736-747 (1973).
- 172. Lusska, A., E. Shen, and J. P. Whitlock Jr. Protein-DNA interactions at a dioxin-responsive enhancer. J. Biol. Chem. 268:6575-6580 (1993).
- 173. Ashida, H., and F. Matsumura. Effect of in vivo administered 2,3,7,8-tetrachlorodibenzo-p-dioxin on DNA-binding activitites of nuclear transcription factors in liver of guinea pigs. J. Biochem. Mol. Toxicol. 12:191-204 (1998).
- 174. Barnes, S. J., C. Y. Chang, H. Zhu, K. P. Nephew, S. A. Khan, H. G. Shertzer, and A. Puga. Activation of redox-controlled transcription factors by TCDD. *Toxicologist* 48(1-S):297 (1999).
- 175. Sulentic, C. E. W., N. E. Kaminski, and M. P. Holsapple. Aryl hydrocarbon receptor-dependent suppression by 2,3,7,8-tetrachlorodibenzo-p-dioxin of IgM secretion in activated B cells. *Mol. Pharmacol.* 53:623-629 (1998).
- Poland, A., E. Glover, and C. Bradfield. Characterization of polyclonal antibodies to the Ah receptor prepared by immunization with a synthetic peptide hapten. *Mol. Pharmacol.* 39:20-26 (1991).

- 177. Cook, J. C., and W. F. Greenlee. Characterization of a specific binding protein for 2,3,7,8-tetrachloridibenzo-p-dioxin in human thymic epithelial cells. *Mol. Pharmacol.* 35:713-719 (1989).
- 178. Hayashi, S., J. Okabe-Kado, Y. Honma, and K. Kawajiri. Expression of Ah receptor (TCDD receptor) during human monocytic differentiation. *Carcinogenesis* **16**(6):1403-1409 (1995).
- 179. Delaney, B., and N. E. Kaminski. Induction of Serum Borne Immunomodulatory Factors in B6C3F1 Mice by Carbon Tetrachloride. *Toxicology* 88:201-212 (1994).
- 180. Holsapple, M. P. The Plaque-Forming Cell (PFC) Response in Immunotoxicology: An Approach to Monitoring the Primary Effector Function of B Lymphocytes., in *Methods in Immunotoxicology* (G. R. Burleson, J. H. Dean and A. E. Munson, ed.). Wiley-Liss, Inc., New York, 71-108 (1995).
- 181. Marcus, R. S., M. P. Holsapple, and N. E. Kaminski. Lipopolysaccharide activation of murine splenocytes and splenic B cells increased the expression of aryl hydrocarbon receptor and aryl hydrocarbon receptor nuclear translocator. *J. Pharmacol. Exper. Therap.* 287:1113-1118 (1998).
- 182. Swanson, H. I., W. K. Chan, and C. A. Bradfield. DNA binding specificities and pairing rules of the Ah receptor, ARNT, and SIM proteins. *J. Biol. Chem.* 270:26292-26302 (1995).
- 183. Rolands, J. C., and J. Gustafsson. Aryl hydrocarbon receptor-mediated signal transduction. *Crit. Rev. Toxicol.* 27:109-134 (1997).
- 184. Li, H., L. Dong, and J. J. Whitlock. Transcriptional Activation Function of the Mouse Ah Receptor Nuclear Translocator. *J. Biol. Chem.* **269**(45):28098-28105 (1994).
- 185. Bank, P., E. Yao, H. Swanson, K. Tullis, and M. Denison. DNA Binding of the Transformed Guinea Pig Hepatic Ah Receptor Complex: Identification and Partial Characterization of Two High-Affinity DNA-Binding Forms. *Arch. Biochem. and Biophys.* 317(2):439-448 (1995).
- 186. Poland, A., and E. Glover. Characterization and strain distribution pattern of the murine Ah receptor specified by the Ah<sup>d</sup> and Ah<sup>b-3</sup> alleles. *Mol. Pharm.* 38:306-312 (1990).
- 187. Vanden Heuvel, J., G. Clark, M. Kohn, A. Tritscher, W. Greenlee, G. Lucier, and D. Bell. Dioxin-responsive Genes: Examination of Dose-Response Relationships Using Quantitative Reverse Transcriptase-Polymerase Chain Reaction. *Cancer Res.* 54:62-68 (1994).
- 188. Crawford, R. B., M. P. Holsapple, and N. E. Kaminski. Leukocyte activation induces aryl hydrocarbon receptor up-regulation, DNA binding and increased Cyp IA1 expression in the absence of exogenous ligand. *Mol. Pharm.* 52:921-927 (1997).

- 189. Bombick, D., J. Jankun, K. Tullis, and F. Matsumura. TCDD (2,3,7,8-tetrachlorodibenzo-p-dioxin) causes increases in protein kinases particularly protein kinase C in the hepatic plasma membrane of the rat and the guinea pig. *Biochem. Biophys. Res. Comm.* 127:296-302 (1985).
- 190. Bombick, D., J. Jankun, K. Tullis, and F. Matsumura. 2,3,7,8-Tetrachlorodibenzo-p-dioxin causes increases in expression of c-erb-A and levels of protein-tyrosine kinases in selected tissues of responsive mouse strains. *Proc.* Natl. Acad. Sci. USA 85:4128-4132 (1988).
- 191. Beebe, L., S. Park, and L. Anderson. Differential enzyme induction of mouse liver and lung following a single low or high dose of 2,3,7,8-tetrachlorodibenzo-p-dioxin (TCDD). J. Biochem. Toxicol. 5:211-219 (1990).
- 192. FitzGerald, C., P. Fernandez-Salguero, F. Gonzalez, D. Nebert, and A. Puga. Differential regulation of mouse Ah receptor gene expression in cell lines of different tissue origin. *Arch. Biochem. Biophys.* 333(1):170-178 (1996).
- 193. Wanner, R., S. Brommer, B. Czarnetzki, and T. Rosenbach. The differentiation-related upregulation of aryl hydrocarbon receptor transcript levels is suppressed by retinoic acid. *Biochem. Biophys. Res. Commun.* 209(2):706-711 (1995).
- 194. Ma, Q., and J. Whitlock Jr. The aromatic hydrocarbon receptor modulates the hepa 1c1c7 cell cycle and differentiated state independently of dioxin. *Mol. Cell. Biol.* 16(5):2144-2150 (1996).
- 195. Krishnan, B., W. Porter, M. Santostefano, X. H. Wang, and S. Safe. Molecular mechanism of inhibition of estrogen-induced cathepsin D gene expression by 2,3,7,8-tetrachlorodibenzo-p-dioxin (TCDD) in MCF-7 cells. *Mol. Cell. Biol.* 15:6710- (1995).
- 196. Safe, S. H. Development validation and problems with the toxic equivalency factors: Approach for risk assessment of dioxins and related compounds. *J. Anim. Sci.* 76:134-141 (1998).
- 197. Poland, A., and E. Glover. Stereospecific, high affinity binding of 2,3,7,8-tetrachlorodibenzo-p-dioxin by hepatic cytosol. *J. Biol. Chem.* **251**:4936-4946 (1976).
- 198. Pettersson, S., V. Arulampalam, and M. Neurath. Temporal control of IgH gene expression in developing B cells by the 3' locus control region. *Immunobiol*. **198:**236-248 (1997).
- Gollapudi, S., C. H. Kim, A. Patel, R. Sindhu, and S. Gupta. Dioxin activates human immunodeficiency virus-1 expression in chronically infected promonocytic U1 cells by enhancing NF-κB activity and production of tumor necrosis factor-α. Biochem. Biophys. Res. Commun. 226:889-894 (1996).
- 200. Harper, N., K. Conner, M. Steinberg, and S. Safe. An enzyme-linked immunosorbant assay (ELISA) specific for antibodies to TNP-LPS detects alterations in serum immunoglobulins and isotype switching in C57BL/6 and

- DBA/2 mice exposed to 2,3,7,8-tetrachlorodibenzo-p-dioxin and related compounds. *Toxicol.* 92:155-167 (1994).
- 201. Kerkvliet, N. I., L. Baecher-Steppan, D. M. Shepherd, J. A. Oughton, B. A. Vorderstrasse, and G. K. DeKrey. Inhibition of TC-1 cytokine production, effector cytotoxic T lymphocyte development and alloantibody production by 2,3,7,8-tetrachlorodibenzo-p-dioxin. *J. Immunol.* 157:2310-2319 (1996).
- 202. Miller, A., D. Israel, and J. Whitlock Jr. Biochemical and genetic analysis of variant mouse hepatoma cells defective in the induction of benzo(a)pyrenemetabolizing enzyme activity. *J. Biol. Chem.* 258:3523-3527 (1983).
- 203. Hankinson, O. The aryl hydrocarbon receptor complex. *Annu. Rev. Pharmacol. Toxicol.* **35:**307-340 (1995).
- 204. Whitlock, J., Jr. Mechanistic aspects of dioxin action. *Chem. Res. Toxicol.* **6:**754-763 (1993).

